



THE UNIVERSITY OF  
**WAIKATO**  
*Te Whare Wānanga o Waikato*

Research Commons

<http://researchcommons.waikato.ac.nz/>

## Research Commons at the University of Waikato

### Copyright Statement:

The digital copy of this thesis is protected by the Copyright Act 1994 (New Zealand).

The thesis may be consulted by you, provided you comply with the provisions of the Act and the following conditions of use:

- Any use you make of these documents or images must be for research or private study purposes only, and you may not make them available to any other person.
- Authors control the copyright of their thesis. You will recognise the author's right to be identified as the author of the thesis, and due acknowledgement will be made to the author where appropriate.
- You will obtain the author's permission before publishing any material from the thesis.

# **Morphology of the Te Tumu Cut Under the Potential Re-diversion of the Kaituna River**

A thesis submitted in partial fulfilment  
of the requirements for the degree

of

**Master of Science  
in Earth and Ocean Sciences**

at

**The University of Waikato**

By

**Joshua Carl Mawer**

---

The University of Waikato

2012



THE UNIVERSITY OF  
**WAIKATO**  
*Te Whare Wānanga o Waikato*



# Abstract

---

Following the diversion of the Kaituna River from Maketū Estuary, out to sea at Te Tumu in 1956, the local community has continually voiced concerns over the estuary's increased sedimentation rates and decreasing ecological health. These concerns led to the partial re-opening of Fords Cut in 1996. However, this has only resulted in a slight improvement in water quality, and no measurable reduction in sedimentation. The Bay of Plenty Regional Council is currently investigating a number of different re-diversion options to partially or fully restore the flow of the Kaituna River into Maketū Estuary, with the aim of restoring the estuary's health. However, a consequence of re-diversion is the possible reduction in discharge through the inlet at Te Tumu. Significantly reducing the discharge would likely cause a large amount of sedimentation in, and around the cut, which could ultimately lead to the closure of the channel.

In order to predict the geomorphic response to the proposed options of lowering the Ford's Cut Culverts to RL -1.6 m (Option J), or reopening Papahikahawai Channel (Option N) a coupled 2-dimensional, wave, hydrodynamic and sediment transport model was developed. Despite being unable to calibrate the hydrodynamic model due to the highly variable nature of the ADCP data collected, the coupled model was entirely calibrated through the sediment transport model. Comparisons between five transects extracted from a survey conducted in 2008 and from the model results of a simulation run over the same time period, showed predicted bed levels to match on average within 0.35 m. Bed levels inside the river were predicted almost exactly, however, the error increased over the ebb delta, although, the same overall shape was still recreated.

Through simulations of average and low river flows, and average and twice the average wave height conditions the morphological response of the Te Tumu Cut to various potential re-diversion options were found. Simulations of Option J showed that the majority of increased water entering the estuary through Ford's Cut occurred during the incoming tide. This therefore increased the flood tidal volume and sediment transport capacity entering the cut, and caused the ebb channel to become shorter by approximately 20 metres. Similarly, reopening Papahikahawai Channel with one-way flapgated culverts caused an increase in the flood tidal volume entering the Cut. However, unlike Option J there was no corresponding increase in sedimentation around the river mouth. This was attributed to dredging required to install the flapgates, resulting in a loss of sediment from the system and the inlet not yet reaching a new equilibrium. When Papahikahawai Channel is reopened without flapgated culverts both the peak flood tidal discharge and peak ebb discharge increased. The increased ebb flows resulted in a small increase in size of the ebb channel through the delta, with the increase in size varying between the different river flow and wave condition simulations.

The effect of adding parallel twin jetty structures to the Te Tumu Cut was also assessed at a preliminary level. Model simulations showed jetties spaced either 45 or 35 metres apart would aid in increasing the navigability through the river mouth. The 35 metre spaced jetties produced a more uniform and deeper channel

compared to the 45 metre spaced option. However, further investigation is required to determine the ideal jetty configuration and long term effects on the surrounding coastlines.

# *Acknowledgements*

---

I wish to thank my supervisor Dr. Willem de Lange for his support, help and guidance throughout the duration of this thesis.

Thank you to DHI NZ for providing me with a copy of the MIKE modelling package, that without, this thesis would not have been possible. More specifically, thank you to Graham Macky and Ben Tuckey for your assistance.

Thank you to Daniel Bates from the Bay of Plenty Regional Council for providing the idea for this project, explaining the background behind it, providing all of the data required and answering any questions that I had.

I wish to thank Dirk Immenga for his assistance in the field and his wealth of experience and knowledge in helping ensure my fieldwork ran smoothly without any problems.

I would like to extend a big thank you to Bryna Flaim for her help with my many modelling questions, processing of ADCP data and for being so friendly all of the time.

Thanks to Simon, Mike, Karl, Sean, Megan, Anna, Kirsty and all of the other students at Waikato University for your support, help and good times throughout the duration of this thesis. You all made the long hours in the offices a much brighter and enjoyable time.

Finally I would like to extend massive thank you to my friends and family. Thanks for your help and support.



# Table of Contents

---

<b>Abstract</b> .....	iii
<b>Acknowledgements</b> .....	v
<b>Table of Contents</b> .....	vii
<b>List of Figures</b> .....	xi
<b>List of Tables</b> .....	xv
<b>Chapter One – Introduction</b>	
1.1 Introduction .....	1
1.2 Nature of the Problem .....	1
1.3 Description of the Study Area .....	4
1.3.1 Te Tumu Cut – The Present River Mouth.....	5
1.3.2 Maketū Estuary .....	5
1.3.3 Climate and River Flow Conditions.....	5
1.3.4 Wave Climate and Tides .....	6
1.3.5 Littoral Drift and Sediment Transport .....	7
1.4 Aims and Objectives .....	10
1.5 Thesis Outline.....	11
<b>Chapter Two – History of the Lower Kaituna River &amp; Te Tumu Cut</b>	
2.1 Natural Variation Before Diversion .....	13
2.2 Engineering Works.....	14
2.2.1 Effects of the Diversion .....	18
2.3 Present State .....	19
2.4 Potential Re-diversion Options .....	19
2.5 Summary .....	22

## **Chapter Three – Literature Review**

3.1	Introduction.....	23
3.2	Inlet Classification .....	23
3.2.1	Estuary Inlet Classification.....	24
3.2.2	Coastal Lagoons .....	26
3.2.3	Inlet Features .....	28
3.3	Inlet Stability.....	30
3.3.1	Bruun Ratio .....	30
3.3.2	Cross-sectional Stability of the Inlet .....	33
3.3.3	Ebb Delta Stability .....	35
3.4	Mechanisms of Inlet Closure .....	37
3.5	Engineering Structures to Maintain Inlet Stability .....	40
3.5.1	Single Structure Jetties .....	40
3.5.2	Twin Structure Jetties .....	43
3.5.3	Opotiki Harbour Example .....	44
3.6	Summary.....	46

## **Chapter Four – Field Data & Bathymetry Measurements**

4.1	Introduction.....	47
4.2	RTK GPS Set Up .....	47
4.3	Land Based Survey .....	48
4.4	Single Beam Survey.....	50
4.4.1	Post Processing.....	51
4.5	Digitised Hydrographic Chart.....	52
4.6	Maketū Estuary Bathymetry Data.....	53
4.7	ADCP Measurements .....	54
4.8	Sediment Samples.....	55
4.9	Summary.....	56

## Chapter Five – Numerical Modelling

5.1	Introduction .....	57
5.2	Time Series Data Used to Force the Models .....	57
5.3	River Flow Model .....	59
5.3.1	Boundary Conditions .....	60
5.4	Flexible Mesh Generation .....	62
5.5	Simulation Time Scales .....	66
5.6	Spectral Wave Modelling .....	67
5.6.1	Wave Model Resolution .....	67
5.6.2	Wave Model Parameters .....	67
5.6.3	Wave Model Validation .....	70
5.6.4	Local Scale Spectral Wave Model .....	72
5.6.5	Spectral Wave Model Limitation .....	72
5.7	Hydrodynamic Modelling .....	73
5.7.1	HD Boundary Conditions and Model Parameters .....	73
5.7.2	Hydrodynamic Model Calibration .....	74
5.7.3	Bed Resistance Values .....	77
5.8	Sediment Transport Modelling .....	79
5.8.1	Model Parameters & Forcing .....	79
5.8.2	Sediment Transport Model Calibration .....	80
5.8.3	Sediment Transport Model Limitation .....	85
5.9	Modelled Scenarios .....	86
5.9.1	Calibration Time .....	88
5.9.2	Average Wave & River Flow Conditions .....	88
5.9.3	7-Day Annual Low Flow & Average Wave Conditions .....	88
5.9.4	2 x Average Height & Average River Flow Conditions .....	89
5.10	Summary .....	90

## **Chapter Six – Results**

6.1	Introduction.....	91
6.2	Sediment Sample Analysis .....	91
6.3	Morphological Modelling Results .....	93
6.3.1	Calibration Time – Varying Conditions .....	93
6.3.2	Constant Average Wave & River Flow Conditions .....	95
6.3.3	Constant Average Wave & Average 7 Day Low River Flows.....	97
6.3.4	2x Average Wave & Average River Flow Conditions .....	99
6.3.5	Decreased River Flows Compared to Average Conditions .....	101
6.3.6	Increased Wave Heights Compared to Average Conditions .....	101
6.3.7	Addition of Twin Training Walls .....	102

## **Chapter Seven – Discussion**

7.1	Introduction.....	105
7.2	Analysis of Model Results .....	106
7.2.1	Option J .....	106
7.2.2	Option N – With Flapgated Culverts .....	110
7.2.3	Option N – Without Flapgated Culverts.....	112
7.2.4	Decreased River Flow Conditions .....	114
7.2.5	Increased Wave Height Conditions .....	115
7.2.6	Twin Jetty Structures .....	119
7.3	Summary & Conclusions .....	121
7.4	Recommendations for Further Research.....	124
	<b>References.....</b>	<b>125</b>
	<b>Appendix 1 – Sediment Sample Laser Sizer Results .....</b>	<b>133</b>
	<b>Appendix 2 – ADCP and Modelled Current Vector Plots.....</b>	<b>139</b>
	<b>Appendix 3 – Q3D Sediment Transport Table Parameters .....</b>	<b>141</b>

# List of Figures

---

<b>Figure 1.1:</b>	Aerial photograph of the Te Tumu Cut in its current configuration...	1
<b>Figure 1.2:</b>	Location of the Kaituna River and Maketū Estuary .....	4
<b>Figure 1.3:</b>	Mean annual suspended sediment discharge at Te Matai.....	8
<b>Figure 2.1:</b>	Location of the Kaituna River Outlet between 1907 and 1978 .....	14
<b>Figure 2.2:</b>	Historic aerial photographs of the Lower Kaituna River.....	15
<b>Figure 2.3:</b>	Schematic showing the straightening, stopbanks and canal development on the lower Kaituna River .....	17
<b>Figure 2.4:</b>	The five most likely re-diversion options outlined by the BOPRC..	21
<b>Figure 3.1:</b>	Typical features of an ebb delta on an open sandy coast.....	28
<b>Figure 3.2:</b>	Ebb delta features of the Te Tumu Cut.....	29
<b>Figure 3.3:</b>	Inlet cross-section area vs tidal prism relationships plot from from Hume & Herdendorf (1992) .....	33
<b>Figure 3.4:</b>	Relationship between spring tidal prism and ebb delta volume for 17 North Island inlets.....	35
<b>Figure 3.5:</b>	Location of the ebb delta between 2003 – 2011 .....	36
<b>Figure 3.6:</b>	Schematic depiction of inlet closure by longshore and cross-shore processes .....	37
<b>Figure 3.7:</b>	Historic images from Google Earth showing spit growth across the river mouth.....	38
<b>Figure 3.8:</b>	Range of river mouth lagoon states and state changes from Hart, (2009).....	39
<b>Figure 3.9:</b>	Current flow paths around a single updrift jetty structure .....	40
<b>Figure 3.10:</b>	Schematic of a weir section in a jetty system .....	42

<b>Figure 3.11:</b> Schematic of a Haupt jetty system.....	42
<b>Figure 3.12:</b> Schematic of a twin jetty system .....	43
<b>Figure 3.13:</b> Aerial photograph showing the recommended twin jetty structure for the Opotiki Entrance.....	45
<b>Figure 4.1:</b> Location of the benchmarks used for the RTK GPS system.....	48
<b>Figure 4.2:</b> Map depicting the location of where the various bathymetry survey methods were used .....	49
<b>Figure 4.3:</b> Comparison between the Ford's Cut tide gauge readings and the tide level obtained from the RTK GPS system .....	51
<b>Figure 4.4:</b> LINZ Chart NZ5413 – Approaches to Tauranga .....	52
<b>Figure 4.5:</b> Tidal elevation plot from the 19 <sup>th</sup> of May 2011, indicating the duration of the ADCP survey .....	54
<b>Figure 4.6:</b> Locations of the sediment samples collected .....	55
<b>Figure 5.1:</b> Map showing the locations of where the various time series were obtained .....	58
<b>Figure 5.2:</b> Annotated screenshot from the Mike 11 network editor showing the extent of the model, and the location of the different boundaries....	59
<b>Figure 5.3:</b> 15 minute discharge readings from the Te Matai and Raparapahoe flow gauges .....	60
<b>Figure 5.4:</b> Interpolated mesh showing the bathymetry used for the regional scale spectral wave simulations.....	63
<b>Figure 5.5:</b> Interpolated mesh showing the bathymetry and mesh elements used for the coupled local Hydrodynamic, Spectral Wave and Sediment Transport modelling of the Status Quo and Option J scenarios.....	63
<b>Figure 5.6:</b> Interpolated mesh showing the bathymetry used for the coupled local HD, SW and ST modelling of Option N .....	64

<b>Figure 5.7:</b> Time and spatial scale compatability for nearshore morphodynamic modelling .....	66
<b>Figure 5.8:</b> Rose plot of Significant Wave Heights from the BOPRC wave buoy 2006 – 2011. ....	68
<b>Figure 5.9:</b> Modelled and observed significant wave height and average wave period, at the location of the BOPRC wave buoy over 21 days in February 2008 .....	71
<b>Figure 5.10:</b> A subset of the vector diagrams from the ADCP transects, compared to the current vectors predicated by the Hydrodynamic model .....	75
<b>Figure 5.11:</b> Map showing the Manning Numbers used in the Mike 11, Kaituna River flow model .....	78
<b>Figure 5.12:</b> Location of the 5 transects used to compare the Sediment Transport Model results against the 2008 DML survey .....	81
<b>Figure 5.13:</b> Transects within the Kaituna River comparing the Sediment Transport Model results against the 2008 DML survey .....	82
<b>Figure 5.14:</b> Transects outside the Kaituna River over the ebb delta comparing the Sediment Transport Model results against the 2008 DML survey ...	83
<b>Figure 5.15:</b> Tidal curve used during the model simulations .....	86
<b>Figure 6.1:</b> Sediment particle size distributions for the collected sediment samples.....	92
<b>Figure 6.2:</b> Predicted bed levels after a 14 day simulation run over the same time in which the sediment transport model was calibrated .....	94
<b>Figure 6.3:</b> Predicted bed levels after a 14 day simulation of constant average river flow and wave conditions.....	96
<b>Figure 6.4:</b> Predicted bed levels after a 14 day simulation of constant 7 day low river flow and average wave conditions .....	98

<b>Figure 6.5:</b> Predicted bed levels after a 14 day simulation of constant average river flow and 2x wave conditions. ....	100
<b>Figure 6.6:</b> Predicted bed levels after a 14 day simulation with the addition of training walls placed 35 and 45 metres apart .....	103
<b>Figure 7.1:</b> Discharge time series from the Mike 11 model used to force the model boundaries for the coupled Mike 21 model for the Status Quo and Option J scenarios.....	107
<b>Figure 7.2:</b> Map showing the two transects where discharge values were extracted from the model results for Option J and Option N.....	108
<b>Figure 7.3:</b> Predicted increase in discharge through Ford’s Cut under the diversion Option J compared to the current inflows .....	108
<b>Figure 7.4:</b> Comparison of discharge values taken from the average river flow and wave condition simulations for the Status Quo and the Option N - with flapgates scenarios .....	110
<b>Figure 7.5:</b> Comparison of discharge values taken from the average river flow and wave condition simulations for the Status Quo and the Option N - without flapgates scenarios .....	112
<b>Figure 7.6:</b> Inlet throat cross-section comparison between Status Quo and Option N –without flapgated culverts .....	113
<b>Figure 7.7:</b> Comparison of discharge values taken from the 7 day lowriver flow and average average river flow simulations for the Status Quo and the Option N - without flapgates scenarios .....	115
<b>Figure 7.8:</b> Deans criterion for onshore – offshore sediment transport .....	117
<b>Figure 7.9:</b> Schematic of the ebb tidal delta breaching process of inlet sediment bypassing from FitzGerald <i>et al.</i> (2000) .....	118
<b>Figure 7.10:</b> Estimated scour depth of the Kaituna River mouth using the USACE formula for annual average flow conditions with varying training wall spacing.....	119

# *List of Tables*

---

<b>Table 1.1:</b>	Flow Statistics for the Kaituna River at Te Matai .....	6
<b>Table 3.1:</b>	Classification of New Zealand estuaries after Hume & Herdendorf, 1988. ....	25
<b>Table 3.2:</b>	Classification of inlets based on tidal prism to littoral drift ( $\Omega/M_{tot}$ ) ratios.....	31
<b>Table 5.1:</b>	Parameters used for the Mike 21 Spectral Wave Model .....	69
<b>Table 5.2:</b>	Parameters used for the Mike 21 Hydrodynamic model .....	74
<b>Table 5.3:</b>	Parameters used for the Mike 21 Sediment Transport model.....	80
<b>Table 5.4:</b>	Error statistics comparing the bed level from the model results against the 2008 survey along five transects .....	84
<b>Table 6.1:</b>	Sediment sample statistics .....	92



# Chapter 1

## Introduction

---

### 1.1 Introduction

This thesis describes the creation and application of a 2-dimensional spectral wave, hydrodynamic and sediment transport model of the Te Tumu Cut, Bay of Plenty, New Zealand. This model was used to investigate the morphological response of the Te Tumu Cut, to various potential re-diversion options for the lower Kaituna River, which have been proposed by the Bay of Plenty Regional Council.



**Figure 1.1:** Aerial Photograph of the Te Tumu Cut in its current configuration (EBoP, 2010).

### 1.2 Nature of the Problem

The Kaituna River naturally discharged to the sea through Papahikahawai Channel, and into the Maketū Estuary. However, over the past six decades, the lower Kaituna River has undergone extensive changes. As a result of frequent

flooding of the surrounding plains, which at the time were predominantly used for agriculture, various engineering works have been undertaken on the lower river. The most significant of these was the construction of a large rock causeway in 1956 – 1957, which blocked off Ford's Cut and Papahikahawai Channel (Figure 1.1), permanently diverting the river straight out to sea.

Following the diversion of the Kaituna River from Maketū Estuary, the local community has continually voiced concerns over the estuary's deteriorating health. A major concern has been the increased sedimentation, which in turn is associated with ecological impacts such as the smothering of shellfish beds. A secondary concern has been the change in water quality associated with the reduced freshwater inflow to the estuary (EBoP, 2009). These concerns led to a partial re-opening of Fords Cut in 1996. At present approximately 4% of the average Kaituna River flow is diverted back into the Maketū Estuary. However, this has only resulted in a slight improvement in water quality and shellfish population health (Bates, July 2010, Memorandum to C. Meadowcroft; Goodhue, 2007).

The Bay of Plenty Regional Council is currently investigating a number of potential re-diversion options to partially or fully restore the flow of the Kaituna River into Maketū Estuary, in order to restore the estuary's health (EBoP, 2008). However, a consequence of such re-diversion is the possible reduction in the discharge through the inlet at Te Tumu. Significantly reducing the discharge through the inlet is likely to cause a large amount of sedimentation in and around the cut, which could ultimately lead to the closure of the inlet channel. However, loss of access through Te Tumu Cut is undesirable.

The main opposing parties to any diversion option that would result in the loss of the inlet are the Te Tumu Land Owners Group and local recreational boat users. In the rivers present configuration the Te Tumu Cut is a commonly used access point to the sea for many local boat owners. Removing this access point would also remove a key selling point of the land to the west of the river, which has been identified as an area for significant growth in the near future (SmartGrowth, 2008). Although restoring the ecological health of the Maketū Estuary is the primary goal of the proposed diversion options, full closure of the Te Tumu Cut could also possibly have a negative impact on some of the surrounding wildlife. The Maketū

barrier sand dunes to the east of the Cut are an important nesting and breeding ground for the New Zealand Dotterel and many other birds. Closure of the Te Tumu inlet would increase the ease of access to this area, which at the moment is fairly limited.

### 1.3 Description of the Study Area

The Kaituna River is located in the central Bay of Plenty region. The rivers headwaters begin at the Okere arm of Lake Rotoiti, from which it runs 53 km to the sea, at Te Tumu (Figure 1.2). The river can be classified into two distinct sections based on its gradient. The first 25 km of the river are fast flowing with several waterfalls, and drops approximately 260 m below its start point. The remaining 28 km meander across the Te Puke Lowlands and drop a further 20 m to reach sea level (Park, 2007). The total catchment area of the river, including the lakes is approximately 1,218 km<sup>2</sup>. Of the total catchment approximately 48% feeds directly into the Kaituna River, and these are known as the lower Kaituna sub-catchments (Park, 2007).

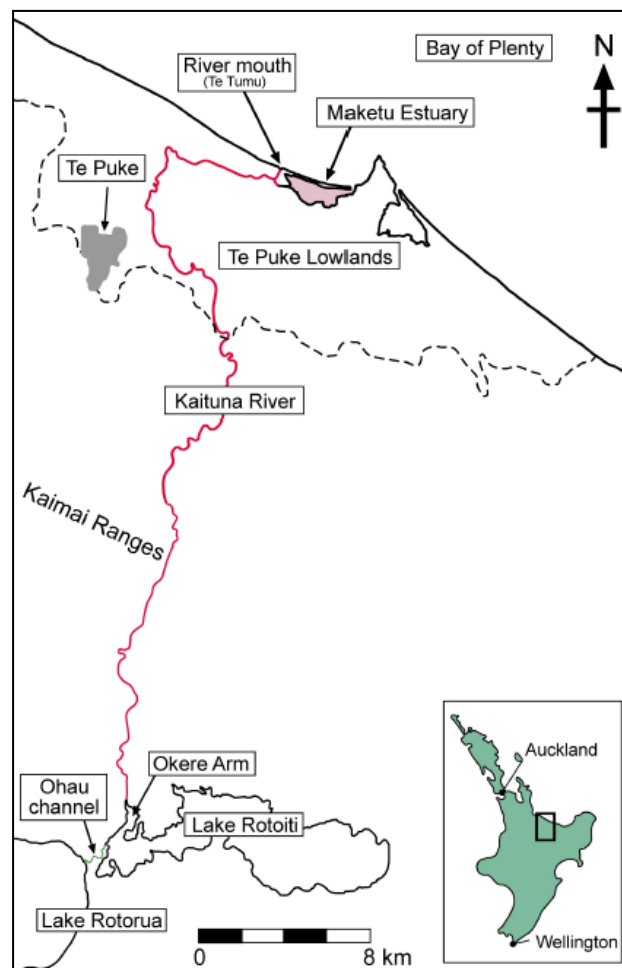


**Figure 1.2:** Location of the Kaituna River and Maketū Estuary (From Goodhue, 2007).

### **1.3.1 Te Tumu Cut – The Present River Mouth**

At present the Kaituna River discharges into the sea at Te Tumu (Figure 1.1). However, it has only discharged at this location since 1957, when the Te Tumu Cut was created, and a concrete training wall put in place to stabilise the mouth's position. The complete history of the river mouth is further discussed in Chapter 2.

The Te Tumu Cut is located on the western side of the Maketū Estuary and is a “cut” through very low and fragile sand dunes that have been subjected to several natural breaches throughout history. The Te Tumu area consists of a wide zone of Holocene sandy progradation, formed from the influx of inner shelf sediments during the post glacial marine transgression. The resulting dune belt is approximately 1,300 m wide at Papamoa beach and narrows towards Maketū, where the belt forms the barrier spit enclosing Maketū Estuary (Wigley, 1990; Healy *et al.*, 1997).

### **1.3.2 Maketū Estuary**

Maketū Estuary is 1.5 km<sup>2</sup> in size and is classified as a micro-tidal lagoon. It formed following the inundation of the Kaituna River basin, as a result of Holocene sea level transgression. Since its formation, and following sea level becoming stable (*c.* 7200 yrs. B.P.), the estuary has continually been subjected to infilling with sediment from numerous sources, such as: fluvially-transported, volcanogenic sediments derived from the Okatina and Taupo Volcanic Centres, erosion of fan deposits from the Town Point headland, marine sands from spit erosion and sediment within the littoral drift system (Burton & Healy, 1985; Wigley, 1990). However, the rate of infilling has increased as a result of human modification, through the addition of engineering structures on the lower Kaituna River over the last 60 years.

### **1.3.3 Climate and River Flow Conditions**

The Te Puke lowlands receive on average 1500 – 1700 mm yr<sup>-1</sup> of rainfall. However, in the upper catchment the Kaimai Ranges receive an average of 2500 –

2600 mm yr<sup>-1</sup> (Quayle, 1984). The base flow of the Kaituna River is primarily from Lakes Rotorua and Rotoiti with small inputs from several tributaries, leading to a mean flow at Te Matai of 39.5 m<sup>3</sup>/s. Conversely the majority of the flood flows come from the tributaries downstream of the lakes such as: the Mangorewa River, the Waiari, Ohineangaanga, Raparapahoe and the Kopuaroa streams (BOPRC, 2011). Based on recordings from 1968 – 2005 peak flows of 170, 230 and 405 m<sup>3</sup>/s have been assessed for 5, 10 and 50 year return periods respectively (EBOP, 2007).

**Table 1.1:** Flow Statistics for the Kaituna River at Te Matai (EBoP, 2007).

<b>Kaituna River at Te Matai</b>	
Flow (m <sup>3</sup> /s)	
<b>Minimum Flow</b>	20.6
<b>Mean Annual Minimum Flow</b>	29.2
<b>Mean Flow</b>	39.5
<b>Median Flow</b>	37.6
<b>Mean Specific Flow (/km<sup>2</sup>)</b>	0.04

#### 1.3.4 Wave Climate and Tides

Due to the sheltering of waves from the East Cape and northern part of the North Island, waves are limited to directions from the north through to the east for the Bay of Plenty Region (Pickrill & Mitchell, 1979). The wave climate ranges in height ( $H_s$ ) from 0.5 – 1.5 m with periods ( $T_s$ ) of 5 – 9 s for typical conditions. Storm conditions can reach up to 2 – 5 m with periods of 7 – 9 s (Foster *et al.*, 1994).

Based on analysis of a three year long time series (1991 – 1993) from a wave buoy in 34 m water depth, offshore of the Katikati inlet, Macky *et al.* (1995) calculated a mean significant wave height of 0.8 m, and a maximum of 4.3 m, with wave heights less than 1 m occurring 70% of the time. The peak spectral density of wave energy occurred at 10 – 11 s and the wave steepness indicated that majority of the waves originated close to the wave buoy. However, the data was collected during an El Nino phase, which typically produces fewer storms and therefore, may not be an accurate analysis of the long-term wave climate.

On the east coast of New Zealand the tides are predominantly semidiurnal with a small diurnal component, with a spring and neap tidal range of 1.62 m and 1.27 m respectively for the Bay of Plenty Region (Bell & Goring, 1998).

### **1.3.5 Littoral Drift and Sediment Transport**

The combination of waves and currents in the nearshore zone act to produce a transport of beach sediment, with the mass movement of sediment in a single direction known as littoral drift. There have been no direct measurements of the littoral drift in the Bay of Plenty region. Several estimates have been determined, although, there is considerable variation between them. However, it is agreed the net littoral drift occurs in a north-west to south-east direction.

Burton & Healy (1985) estimated the littoral drift along the Maketū coastline to be approximately 40,000 m<sup>3</sup>/year. This was based on Wallingford's (1969) estimate of 102,510 m<sup>3</sup>/year and Healy's (1980) estimate of 70,000 m<sup>3</sup>/year ±20,000 along the Bay of Plenty coastline, and reduced to allow for a decrease in the littoral drift rates further along the coast, at Maketū. Hicks & Hume (1996) estimated an annual littoral drift of 70,000 m<sup>3</sup>/year, at the Ohiwa, and Tauranga Harbours, which are located 65 and 25 km east, and west respectively of the Te Tumu Cut. Although, it was not mentioned how this was derived. The net littoral drift at Pukehina Beach (~10 km east of Te Tumu) was estimated at 22,000 m<sup>3</sup>/year by Easton (2002) through numerical modelling. This is likely smaller than Burton & Healy's (1985) estimate due to Maketū Town Point partially impeding the littoral drift system to Pukehina.

The other main source of sediment for the Kaituna region is from the Kaituna River itself. It has been estimated the River provides approximately 4.07 x 10<sup>5</sup> tonnes of suspended sediment to the surrounding ocean annually (Griffiths & Glasby, 1985). Assuming this material is predominately quartz and feldspar with an average density of 2650 kg/m<sup>3</sup>, this is the equivalent to approximately 150,000 m<sup>3</sup> of sediment per year. However more recent estimations from NIWA's (2011) WRENZ GIS based web application suggest sediment additions of 68.1

kilotonnes of suspended sediment per year. Following the same assumptions as above, this is equivalent to 25,698 m<sup>3</sup> per year.

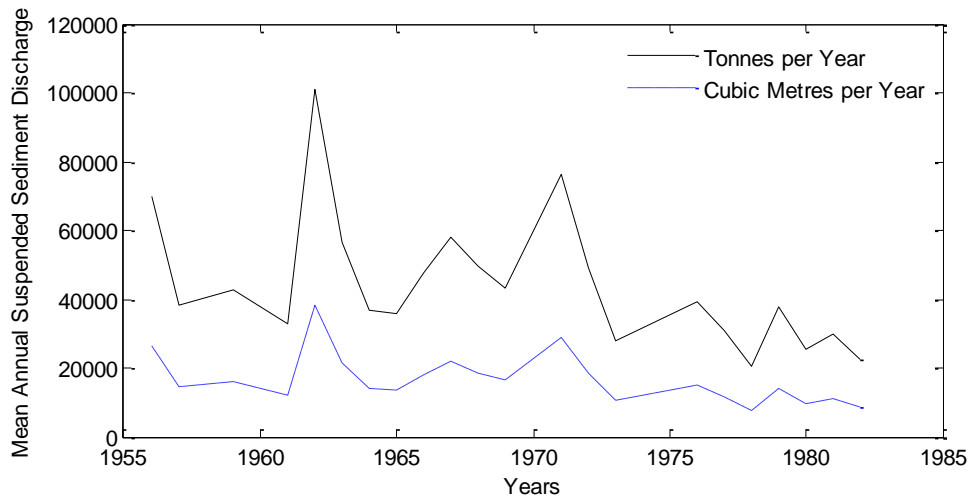


**Figure 1.3:** Mean annual suspended sediment discharge at Te Matai in Tonnes/Year (Recreated from Easton (2002). Data originally provided by NIWA) and annual volume estimated from the assumption that all of the material is quartz and feldspar with a density of 2650 kg/m<sup>3</sup>.

Figure 1.3 shows that the suspended sediment data from 1955 – 1982 recorded at Te Matai is considerably lower than the estimates from Griffiths & Glasby (1985) and NIWA’s WRENZ web based GIS tool. However, Easton (2002) suggested that sediment discharged from the Kaituna River may be higher than Figure 1.3 shows, due to sediment abrasion. Easton (2002) also suggested that the high suspended sediment discharges in 1962 and 1971 could possibly be linked to the large scale afforestation of *Pinus radiata* in 1962 by Tasman Forestry, primarily in the Tarawera catchment, but also in part of the Kaituna catchment. The heaviest planting occurred in 1969 and 1975 and the use of heavy machinery may have led to the increased sediment discharges during these periods.

There is considerable variation and uncertainty between the two estimates of suspended sediment yields, with Griffiths & Glasby’s estimate an order of magnitude larger than NIWA’s WRENZ estimate, and the Te Matai data. However, it is thought that the majority of the suspended sediment discharged would be fine particles, which would be transported as wash load out to sea, and

therefore not affect the Te Tumu inlet (Tuckey, pers. Comm, 2011). This is also consistent with data from numerous South Island rivers, with Kirk (1991) stating that for rivers he investigated, the majority of the sediment load delivered to the ocean was fine sand and silt which was lost out to the continental shelf.

## **1.4 Aims and Objectives**

This thesis addresses the main aim of modelling the morphological response of the Te Tumu Cut to the various potential Kaituna River re-diversion options, and to evaluate whether river training structures could be used to stabilise the channel.

To achieve this aim the project was broken down into three smaller objectives:

1. To conduct a single beam survey of the lower Kaituna river bed and ebb delta area surrounding the Te Tumu inlet.
2. To create a MIKE 21 model using the bathymetry collected from the single beam survey and from data supplied by the Bay of Plenty Regional Council of the lower Kaituna River and coastal area seaward of the inlet.
3. To use the model created in Objective 2 to assess the morphological response of the inlet to the different re-diversion options and to assess at a preliminary stage the potential for river training structures.

## 1.5 Thesis Outline

Following this introductory chapter, the historic natural variation in the Kaituna River mouth's position, and subsequent engineering works undertaken in order to fix the mouths location are described, along with the proposed re-diversion options for the Kaituna River and Maketū Estuary in **Chapter Two**.

**Chapter Three** summarises the literature surrounding inlet classification, stability, mechanisms of closure and the main types of engineering structures used to keep inlets open.

Bathymetry data were collected inside the river and over the delta using a single beam echosounder, over the intertidal zone with an RTK GPS and collated from multiple studies for inside Maketū Estuary. Current velocities and sediment samples were also collected using an ADCP and drop sampler respectively. The full methodology used, and the locations where data were collected are described in **Chapter Four**.

**Chapter Five** describes the setup and application of a Mike 11 1-dimensional hydrodynamic river flow model and the 2-dimensional Mike 21 FM spectral wave, hydrodynamic and sediment transport models used to simulate the various scenarios, which are also outlined within Chapter Five.

The results from the various simulations are presented in **Chapter Six** by comparing simulations of the various diversion options against simulations of the existing river configuration.

**Chapter Seven** expands on the results from Chapter Six and presents explanations as to why the resulting bed level changes occurred. Following this, a summary of the conclusions drawn from this project and recommendations for further research are given.



# Chapter 2

## *History of the Lower Kaituna River & Te Tumu Cut*

---

### **2.1 Natural Variation Before Diversion**

According to the document titled “Maketū Estuary Environmental Issues and Environment” prepared by the Commission for the Environment in 1984, the Upper Kaituna Catchment has remained stable in its present configuration over the last 9,000 years. However, throughout the literature it is apparent that the river mouth has experienced considerable variation as to where it enters the sea. This has been a result of repeated cycles of spit breach near Te Tumu, followed by gradual migration eastwards towards Okurei (Town) Point, due to the predominantly easterly littoral drift (KRTA, 1986).

Historic recounts by Wi Matene te Hukai to the Maori Land Court report that the Maori canoe, Te Arawa, landed at the Kaituna River mouth at Te Awahou, near Te Tumu (Stafford, 1967). Although this is only anecdotal evidence it suggests that c.600 years ago during the arrival of the Arawa Canoe the Kaituna River was located near Te Tumu.

As time has progressed the location of the Kaituna River mouth has become documented in increasing detail. The first detailed account dates back to 1907 when it is known a large flood broke through the sand dunes at Te Tumu, allowing the Kaituna River to discharge directly out to sea. The gradual eastward migration following the spit breach in 1907 is illustrated in Figure 2.1, with the successive eastward movements of location indicated in 1907, 1908 and 1912. By 1920 - 1924 the river mouth had entered into the Maketū Estuary through Papahikahawai Channel and migrated approximately halfway to the Maketū Estuary inlet. By 1939 the river mouth reached its former location again, at the eastern inlet of the Maketū Estuary.

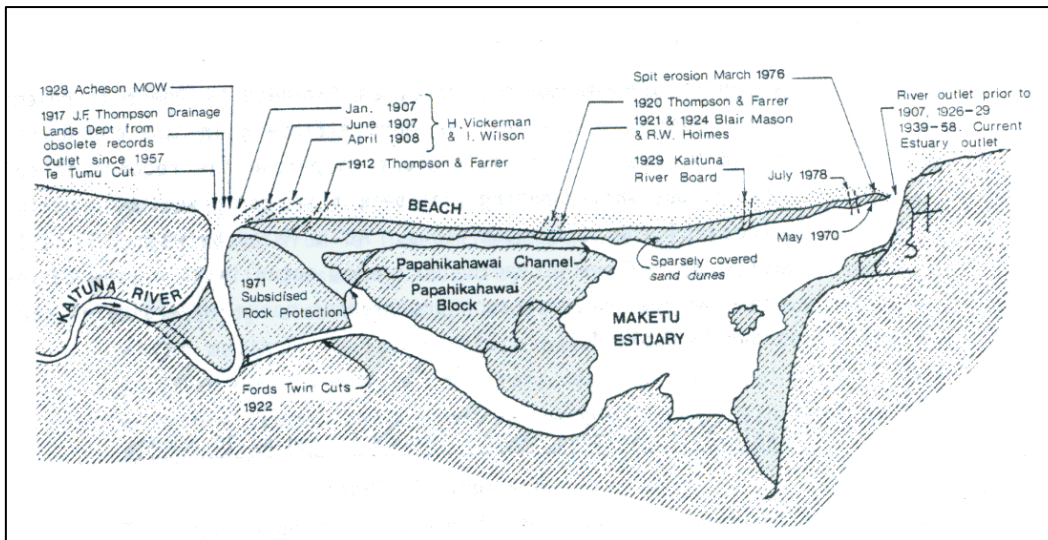


**Figure 2.1:** Locations of the Kaituna River Outlet between 1907 and 1978, from KRTA (1986).

## 2.2 Engineering Works

The first major engineering work undertaken on the lower Kaituna River was the excavation of Ford's Cut, as a result of the breach at Te Tumu in 1907. It was hoped this would divert part of the Kaituna River into Maketū Estuary before Papahikahawai Channel to prevent further breaching of Maketū Spit. Due to the limited reach of the excavation machinery used, Ford's Cut consisted of two channels due to being excavated from both sides. It was thought that once the cut was open, the water flowing through would scour out the middle ridge. However, this was unsuccessful and it appears that over the following years the mouth migrated back eastward into Papahikahawai Channel. At present, Ford's Cut still remains as a pair of channels, leading to it also being known as Ford's Twin Cut.

The exact date in which Ford's Cut was excavated is unknown, with some reports stating 1922 (Wildland Consultants, 2007 & Titchmarsh, 1998). However, a hand drawn map by Stokes (1980, as cited in KRTA, 1986) showing the lower Kaituna River in 1925 does not include Ford's Cut, while Oliver Bain was quoted as saying the Cut was made in 1928 (Bay of Plenty Times, 1 July 1978, as cited in KRTA, 1986).



**Figure 2.2:** Historic aerial photographs of the lower Kaituna River from Wallace *et al.* (2008).

Between 1926 and 1927 a number of engineering works were completed near the mouth of the Kaituna River. This included the closing of the Te Tumu mouth, returning the flow to the Maketū Estuary Mouth, through which flow had not occurred since 1907. However, shortly after in March 1928 the Te Tumu Mouth opened again and the Maketū Outlet closed during a storm by natural processes (Acheson, 1953, as cited in KRTA, 1986).

In the following years, flooding of the surrounding hinterland frequently occurred. As a result the Kaituna River Board employed consultants to advise on a solution to the flooding problem. After much debate, the Soil Conservation and Rivers Control Council approved a scheme to divert the Kaituna River out of Maketū

Estuary in 1954, against the recommendation of an engineering report by A. Murray (1951, as cited in KRTA, 1986). However, government approval was not gained. As a result, it was suggested a cut at Te Tumu would provide immediate relief and lower river levels up stream at an acceptable price, allowing time to investigate alternatives to the problem properly (KRTA, 1986; Wallace *et al.*, 2008)

In February 1957 the diversion works were completed by the Kaituna River Board with the establishment of a new outlet at Te Tumu. This outlet was fixed by a solid rock barrier on the eastern side to prevent further eastward migration, as had occurred in the past under natural conditions (KRTA, 1986). As a result of the diversion in 1957 the Kaituna River no longer discharged into the Maketū Estuary. This led to deterioration of the estuary's health, and is further explained in Section 2.2.1.

In 1973 the Kaituna Catchment control scheme was devised with the aims to straighten, widen, and deepen the lower Kaituna River. It was hoped that this would ease the flow to the sea, allowing the river to handle 100 year flood events. The majority of the work for this scheme was undertaken between 1981 and 1985 and included 67 km of stopbanking (Figure 2.3), 88 km of canals, construction of the rock rubble groyne at Te Tumu, 7 pump stations and 5 flood gate structures.

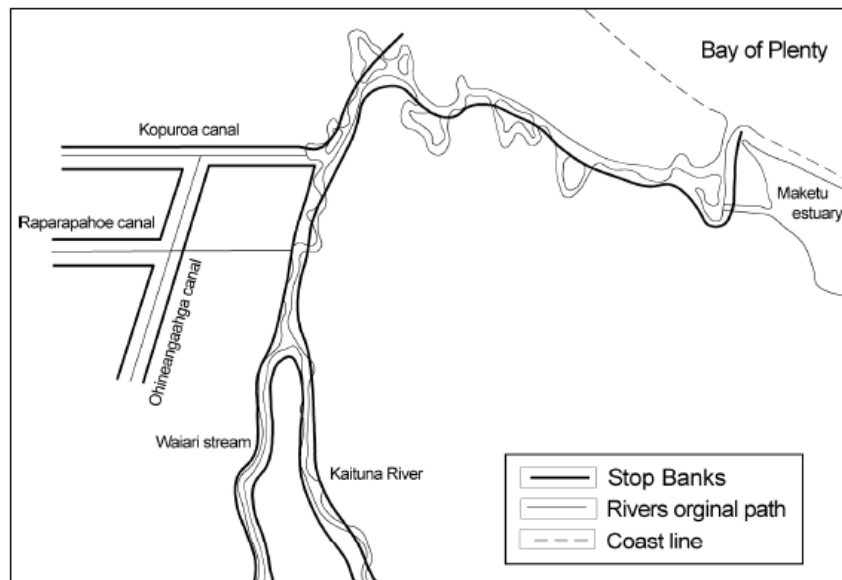


**Figure 2.3:** Schematic showing the straightening, stopbank and canal development on the lower Kaituna River (Goodhue, 2007).

Following concerns over Maketū Estuary’s deteriorating health as a result of the diversion, the Department of Conservation applied for resource consent to divert flow through culverts at Ford’s Cut. Consent was granted by Environment Bay of Plenty, although, this decision was appealed following a Planning Tribunal hearing in 1993. Consent was finally granted in 1994 and four flapgate culverts were installed in 1995. However, as a result of legal action by the Bain family the gates remained closed until February 1996, when they were opened illegally by a member of the public. The High Court then ruled against the Bain Family and the gates have remained open since (Wallace, *et al.*, 2008).

### **2.2.1 Effects of the Diversion**

Increased sedimentation within Maketū Estuary has continually been outlined as one of the most significant concerns of local residents. Historic accounts and reports suggest that in the past that the estuary channels were significantly deeper, with residents estimating that depths had decreased by about 5 metres in parts. Reports also mention boats as large as 60 tonnes with one metre drafts entering the estuary, suggesting the channels must have been much deeper in the past (Domijan, 2007).

It has been estimated that between 1985 and 1996 the inter-tidal storage volume of the estuary decreased by  $0.15 \times 10^6 \text{ m}^3$  (17.3%). This was attributed to sedimentation at a rate of  $13,640 \text{ m}^3$  per year by Domijan (2007). There is a possibility that similar sedimentation rates were also occurring prior to the diversion, with reports of blasting to deepen the entrance as early as 1926 (Murray, 1978). However, it is generally agreed that the diversion has played a part in increasing the sedimentation rate.

The other main concern of local residents is the effect the diversion has had on shellfish populations. Shellfish populations, especially the Pipi, have decreased due to a combination of smothering due to increased sedimentation, changing salinities from reduced freshwater inflows and eutrophication of the estuary water (Richmond & Forbes, 1990; Park, 2003). In the absence of quantitative data on the ecology of the estuary prior to the diversion, there is no direct measurement of the effect the diversion has had on the shellfish populations. However, it is agreed that shellfish populations have declined.

## 2.3 Present State

At present the lower Kaituna River is in the configuration shown in Figure 1.1. The original pathway of the river through Papahikahawai Channel (Figure 2.2, top) is completely blocked off by a causeway and several earthen blocks. Ford's Cut is controlled by gated one way culverts. The current consent and flapgate structures allow for 100,000 m<sup>3</sup> of net inflow into the estuary per tidal cycle. At present the net inflow through Ford's Cut is approximately 4% of average river flow (40 m<sup>3</sup>/s). With the net inflow of freshwater into the estuary varying between 100,000 – 115,000 m<sup>3</sup>, the percentage of freshwater within the estuary ranges from 6-10% (Bates, 2010 Memorandum to C. Meadowcroft).

## 2.4 Potential Re-diversion Options

At present (2011) five different re-diversion options have been identified as the most likely options from which the final option will be chosen. These five options were chosen based on four preliminary criteria of: (1) volume of water added to Maketū Estuary, (2) effects on local drainage and flooding, (3) cost and (4) flexibility (EBoP, 2008). These five options are outlined below and shown in Figure 2.4.

### Option H – Complete Make Over:

This option is for the complete makeover from the present configuration. It includes blocking the Te Tumu Cut, removing the culverts and causeway that currently block the river from entering the estuary, removal of the block in the old river channel which is upstream of Te Tumu and reopening Papahikahawai Channel allowing the river to flow into the estuary. Numerical Modelling has shown this would increase the net inflow volume in to Maketū Estuary from the present 105,000m<sup>3</sup> to 2,887,000 m<sup>3</sup> per tidal cycle.

#### Option N – Increased flow through Papahikahawai Channel:

Option N includes creating an opening in the causeway, the removal of the blocks in Papahikahawai Channel and the subsequent addition of two large one-way flood gated culverts to allow flood relief, but prevent backflow into the river. Numerical modelling has shown this would increase the net inflow volume to 449,000 m<sup>3</sup>.

#### Option J – Alteration of Ford's Cut (A):

Lower the height of the culverts to -1.6 m RL so they are submerged at mid-tide to allow increased river flow into the estuary. Numerical modelling has shown this would increase the net inflow volume to approximately 200,000 m<sup>3</sup>.

#### Option L – Alteration of Ford's Cut (B):

Option L includes the removal of the Ford's Cut culverts and causeway between the river and the estuary, and the subsequent construction of an opening between the cut and estuary controlled by a flood gate culvert to prevent backflow into the river. Numerical modelling has shown this would increase the net inflow volume to 383,000 m<sup>3</sup>.

#### Option R – Change Ford's Cut and Te Tumu Cut:

Option R is to insert control gates at both the Te Tumu Cut and Ford's Cut with the control gates at Te Tumu open and Ford's Cut closed during flood events, and the opposite during normal conditions. Numerical modelling has shown this would increase the net inflow volume to 2,856,000 m<sup>3</sup>.

Options H and R are the most effective options in terms of restoring flow into the Maketū Estuary as they re-divert all normal flow into the estuary. However, both of these options will increase the adverse effects of river flood levels, drainage and sedimentation within the Te Tumu Cut. Mitigation of such effects would likely be costly, but essential to protect the surrounding landowners. In terms of flood relief and drainage Option N is the best as it would increase the inflow volume to the estuary by four-fold. Option N is also favoured as it offers

flexibility to later be transformed into H, J, L or R if required (EBoP, 2008; Wallace *et al*, 2008).

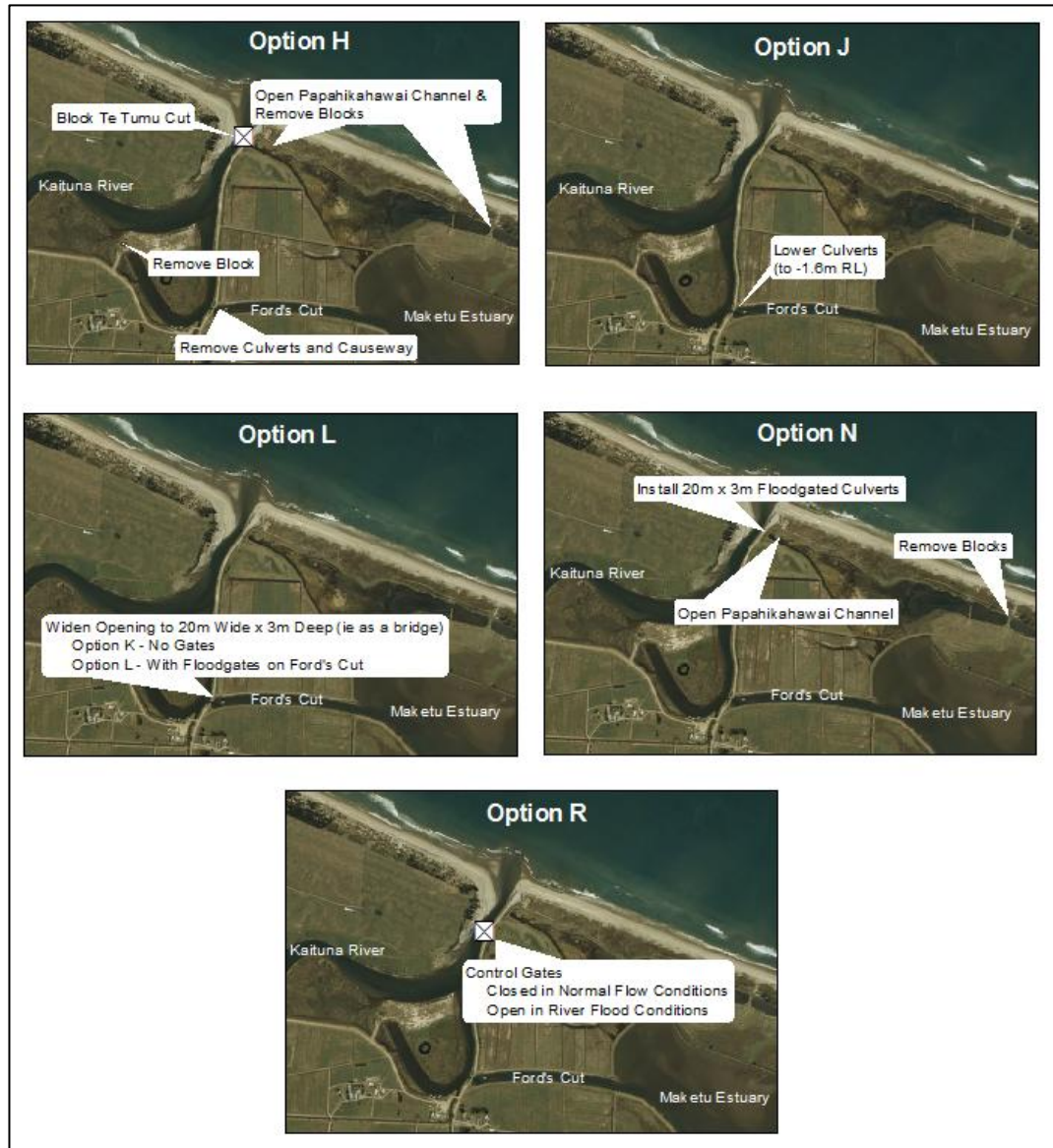


**Figure 2.4:** The five most likely re-diversion options outlined by the BOPRC (modified from EBoP, 2008).

## **2.5 Summary**

The Kaituna River historically discharged into Maketū Estuary through Papahikahawai Channel. However, it also spent considerable amounts of time discharging straight out to sea at Te Tumu, as a result breaching of Maketū spit during times of large storm and flood events. In response to a large breaching event in 1907, an artificial channel known as Ford's Cut was created with the aim of diverting part of the river into the estuary earlier to prevent further breaching. Ford's Cut was later reclosed in 1956, by the construction of a rock causeway. This permanently diverted the Kaituna River straight out to sea at Te Tumu, away from Maketū Estuary, with the aim of alleviating the flood susceptibility of the surrounding farmland. In response to concerns over the estuary's health Ford's Cut was reopened with a series of one way flapgates in 1996. However, this had little effect in remediating the estuary, and as a result the Bay of Plenty Regional Council is currently investigating a number of potential options to partially or fully restore flow of the Kaituna River, back into Maketū Estuary.

# Chapter 3

## *Literature Review*

---

### **3.1 Introduction**

The majority of research on inlet stability, especially in New Zealand, has primarily focused on tidal inlets in the form of harbours and estuaries, rather than river mouths. However, many of the principles applied to estuary and harbour inlets can be applied to the Kaituna River mouth, as the inlet is also influenced by tidal flow, in addition to river discharge.

In regards to the influence of reduced river flow on inlets, research has predominantly focused on the seasonal closure of inlets in response to periods of low river flow, and the effect various wave conditions have on inlet closure times. Examples of such situations include the Wilson Inlet in Western Australia (Ranasinghe & Pattiaratchi, 1999, 2003), the Narrabeen, Wamberal and Wollumboola Lagoons in New South Wales, Australia (Gordon, 1990) and the Hue Inlets on the Central Coast Vietnam (Lam *et al.*, 2007). In New Zealand research has primarily focused on South Island rivers, such as the work of Kirk (1991); Kirk & Lauder (2000) and Hart (2009).

### **3.2 Inlet Classification**

The morphology and sediment depositional patterns at river mouths and inlets are some of the most varied of all coastal depositional forms in the world (Wright, 1977; Siegle, *et al.*, 2004). Therefore, there is not one sole classification system applicable to all inlets. This has led to a wide variety of classification schemes based on factors such as the inlets oceanography (wave height, period, tidal range etc.), processes that formed the inlet and descriptions of the inlet's features. The two most commonly used classification schemes in New Zealand are the Hayes

(1979) classification based on tidal range and wave height, and the Hume & Herdendorf (1988) classification schemes. However, the use of estuary type classification schemes for river mouths is disputed by Kirk (1991), who suggests they are better described as coastal lagoons.

### 3.2.1 Estuary Inlet Classifications

Hayes (1979) proposed a classification scheme which divides inlets into five classes, based on their mean tidal range as follows:

<b>Class</b>	<b>Mean Tidal Range</b>
• Microtidal	< 1.0 m
• Low Mesotidal	1.0 – 2.0 m
• High Mesotidal	2.0 – 3.5 m
• Low Macrotidal	3.5 – 5.5 m
• High Macrotidal	> 5.5 m

Hayes (1979) also defined a classification based on the mean annual wave height ( $H_m$ ), with the following three classes:

<b>Class</b>	<b>Mean Wave Height</b>
• Low Wave Energy	< 0.6 m
• Medium Wave Energy	0.6 – 1.5 m
• High Wave Energy	> 1.5 m

Based on an average tidal range of 1.45 m and a mean annual wave height of 0.8 m (Section 1.3.4) the Te Tumu Cut can be classified according to the Hayes (1979) scheme as a low mesotidal, medium wave energy inlet.

Another way of classifying inlets is by the primary processes that shaped the deposition basin. This method was applied by Hume & Herdendorf (1988) for New Zealand estuaries (Table 3.1). This classification scheme divides inlets into five primary modes of origin, and then further subdivides them into 16 categories based on geomorphic and oceanographic characteristics. Based on this classification the Te Tumu Inlet is categorised as a Type 8 Straight Banked, River Mouth. These types of inlets are typically characterised by parallel or funnel shaped entrances and a marked salinity structure (Hume & Herdendorf, 1988). However, prior to the Kaituna River mouth being fixed at Te Tumu in 1956 the river would have been classified as a Type 9 or 10 Spit-lagoon River Mouth.

**Table 3.1:** Classification of New Zealand estuaries (after Hume & Herdendorf, 1988b), recreated from Hume & Herdendorf (1993).

Primary Mode of Origin of Depositional Basin	Estuary Type	
Fluvial erosion	Funnel-shaped (Type 1)	
	Headland enclosed (Type 2)	
	Barrier enclosed	Double-spit (Type 3)
		Single-spit (Type 4)
		Tomobolo (Type 5)
		Island (Type 6)
		Beach (Type 7)
	River mouth	Straight-banked (Type 8)
		Spit-lagoon (Type 9)
		Spit-lagoon (Type 10)
		Deltaic (Type 11)
Marine/fluvial	Coastal embayment (Type 12)	
	Fault defined embayment (Type 13)	
Tectonism	Diastrophic embayment (Type 14)	
Volcanism		
Glaciation	Volcanic embayment (Type 15)	
	Glacial embayment (Type 16)	

Hume *et al.* (2007) developed an estuary environment classification (EEC) based on a graded class of physical factors that largely influence estuary environments. The classification was based on a range of indices such as the estuaries total volume, tidal prism, estuary elongation and a shoreline complexity index, and calculated for a range of estuaries in New Zealand using a Geographic Information System (GIS) application. Although information was not available to calculate all of the indices used for the classification of Hume *et al.* (2007) the Te Tumu Cut closely matches the description of a Level 2, Category B estuary. These

types of estuaries are characterised by simple shaped, elongated basins with a predominantly subtidal estuarine area, with freshwater inflows accounting for a significant proportion of the basins volume.

### **3.2.2 Coastal Lagoons**

Kirk (1991) debates the classifications of river mouths as a type of estuary by Hume & Herdendorf (1988), on the basis that river mouths are primarily dominated by freshwater outflow rather than tidal flows. Therefore unlike estuaries, river mouths are inadequately explained by tidal hydraulics as suggest by Hume & Herdendorf (1988 & 1993). It is also suggested that the term ‘outlet’ is better suited than ‘inlet’ to describe river mouths (Kirk, 1991). However, both terms are used interchangeably within this thesis.

The term ‘coastal lagoon’ was described by Kjerfve (1994, pp. 2-3) as:

*“... an inland body of water, usually oriented parallel to the coast, separated from the ocean by a barrier, connected to the ocean by one or more restricted inlets, and having depths which seldom exceed a couple of meters. A lagoon may or may not be subject to tidal mixing, and salinity can vary from that of a coastal freshwater lake to a hypersaline lagoon, depending on the hydrologic balance. Lagoons formed as a result of rising sea level during the Holocene or Pleistocene and the building of coastal barriers by marine processes.”*

With the added restriction, that the tidal force is not the dominant process Kirk & Lauder (2000) further subdivided this definition in to two lagoon types which are common in the South Island of New Zealand: Coastal Lakes and River Mouth Lagoons.

Coastal Lakes have small or infrequent exchanges of water with the ocean and thus predominantly have fresh or brackish waters. They are also commonly closed from the sea, leading to the name ‘choked lagoons’. However, periodically they may burst their barrier to become open to the sea. Examples of coastal lakes in New Zealand are Waihora/Lake Ellesmere and Waituna in the South Island.

River Mouth Lagoons, also often referred to by their Maori name of Hapua, are generally shore-parallel bodies of freshwater separated from the ocean by a narrow spit, that formed by the offsetting of the river mouth from longshore drift. Examples of Hapua from the South Island, New Zealand include the Hurunui, Rakaia, Ashburton, Opihi and Waitaki Rivers.

As described in Section 2.1 and Figure 2.1, prior to the Kaituna River mouth becoming fixed at Te Tumu in 1976, the river flowed eastward parallel to the coast, separated from the ocean by a spit, until it discharged out to sea through an area of spit breach. This fits the description of a River Mouth Lagoon described above. However, following the construction of the Te Tumu Cut and causeway to fix the Kaituna River mouth at Te Tumu, the river could no longer flow parallel to the coast before discharging out to sea.

### 3.2.3 Inlet Features

Figure 3.1 depicts the typical features of an idealised ebb delta on an open sandy coast system, such as the Te Tumu area. The main ebb channel is the deepest part of the delta and extends out to the end of the delta. At the end of the main channel is the terminal lobe, which is a steep sloping, compared to the other features, lobe of sand that indicates the seaward edge of the delta. Flanking either side of the ebb channel are the marginal flood channels, which are created by the inflow of the flood tide into the inlet. The relatively flat area between the ebb channel, terminal lobe and flood channel is known as a swash platform and often includes swash bars, created by the swash action of waves (Hayes, 1980).

The cross-sectional area of the ebb channel and volume of sediment within the ebb delta show a strong relationship to the inlets tidal prism. These relationships are further explained in Sections 3.3.2 and 3.3.3 respectively.

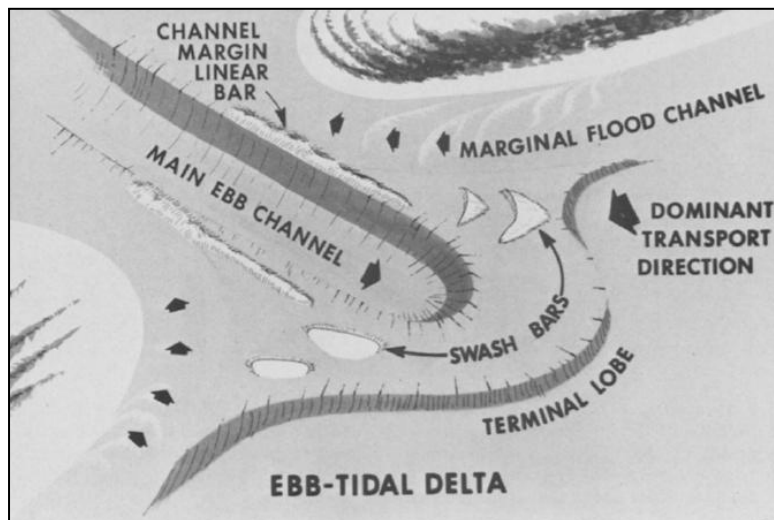


**Figure 3.1:** Typical features of an ebb delta on an open sandy beach system (Hayes, 1980).

Figure 3.2 shows the Te Tumu Cut ebb delta in March 2008. During this time there was well defined ebb channel, which formed along the path of the river discharge axis, and ends at the terminal lobe. Flanking either side of the ebb channel is two large swash platforms. Swash bars exist on both swash platforms, with the western swash bar being much larger due to its location on the updrift

side of the predominant littoral drift direction. Inside the swash bar on the western side is a marginal flood channel, and it appears there is also a much smaller marginal flood channel inside the eastern swash bar.



**Figure 3.2:** Aerial photograph showing the main features of the Te Tumu Cut ebb delta, in March 2008.

### 3.3 Inlet Stability

Inlet stability was defined by Bruun *et al.* (1978 p. 245) as “a dynamic stability by which elements involved attempt to maintain a situation characterized by relatively small changes in inlet geometry including, location, planform and cross sectional areas and shape.”

The stability of an inlet is controlled by a number of factors such as the tidal prism, littoral drift, wave climate, freshwater discharge, sediment grain size, and the time period over which stability is being considered (Hubbard *et al.*, 1979; Hayes, 1980; Hume & Herdendorf, 1992, 1993; FitzGerald *et al.*, 2000).

Tidal inlet stability has been the subject of numerous studies since the 1930s following O’Brien’s (1931) discovery that there is a relationship between the inlet channel area and the tidal prism. This relationship has since been further applied around the world and shown to hold true for many inlets (Section 3.3.2). Another simple, yet commonly used empirical relationship is that of Bruun & Gerritsen (1960) who proposed the ratio between the local longshore sediment transport volume and tidal prism as an indicator of inlet stability.

However, although many researchers have noted river flow to be a potential component of inlet stability, surprisingly little work has been conducted on the influence of river flow on inlet stability. The majority of research has focused around tidally dominated inlets where river flows have little effect (Walker, 2003). Research that has taken into account the effect of river flow has predominately been in the area of seasonally closed inlet, where there is a significant seasonal decrease in river flow (Shuttleworth *et al.*, 2005). This section will review the mechanisms of inlet closure and the applicable inlet stability relationships for the Te Tumu inlet.

#### 3.3.1 Bruun Ratio

The Bruun Ratio is the ratio of the tidal prism ( $\Omega$  - in  $m^3$ ) to the net annual littoral drift arriving at the inlet ( $M_{tot}$  - in  $m^3/yr$ ). It is based on the concept of whether there is sufficient tidal flushing to remove the sediment transported into the inlet

from the littoral drift system. Based on this ratio overall inlet stability can then be classified on a scale from “relatively good, little bar and good flushing ( $\Omega/M_{tot} > 150$ )”, to cases where “entrances become unstable and overflow channels form rather than permanent inlets ( $\Omega/M_{tot} < 20$ )” (Bruun, *et al.*, 1978 pp. 261 )

Hume & Herdendorf (1992) modified the Bruun stability ratio classification for the northeast coast of the North Island of New Zealand and defined the classifications of inlet stability and navigability shown in Table 3.2.

**Table 3.2:** Classification of inlets based on the tidal prism to littoral drift ratios ( $\Omega/M_{tot}$ ) after Bruun (1978), recreated from Hume & Herdendorf (1992).

$\Omega/M_{tot}$ Ratio	Entrance Condition
$\Omega/M_{tot} > 300$	Little or no ocean bar outside gorge (ocean shoal may occur further out), good entrance conditions and flushing
$150 < \Omega/M_{tot} < 300$	Little ocean bar
$100 < \Omega/M_{tot} < 150$	Low ocean bar, navigation problems usually minor
$50 < \Omega/M_{tot} < 100$	Wider and higher ocean bar, increasing navigation problems
$20 < \Omega/M_{tot} < 50$	Wide and shallow ocean bar, navigation difficult
$\Omega/M_{tot} < 20$	Very shallow ocean bar, navigation very difficult, entrance unstable

In the case of the Te Tumu Cut, which is a river dominated inlet, the tidal prism also includes the freshwater discharge ( $Q$ ) over the ebb tide (from here on referred to as the effective tidal prism). The Bruun ratio can be modified to include river discharge as:  $(\Omega + Q) / M_{tot}$ .

No direct measurements have been made of the effective tidal prism for the Te Tumu Cut. However, based on average flow conditions for the Kaituna River ( $40 \text{ m}^3/\text{s}$ ) and its tributaries ( $1.85 \text{ m}^3/\text{s}$  for Raparapahoe and using the assumptions outlined in Section 5.2.1) an average volume of  $2,240,000 \text{ m}^3$  has been estimated to discharge from the river mouth during an ebb tide, via the 1-dimensional Mike 11 river flow model described in Section 5.3.

Based on an average ebb discharge through the Te Tumu Cut of  $2,240,000 \text{ m}^3$  per tidal cycle and an  $M_{tot}$  of  $40,000 \text{ m}^3$  per year along the Maketū coast (Burton & Healy, 1985) the modified Bruun stability ratio is equal to 56. This corresponds to

the entrance condition of a wide and high ocean bar with increasing navigation problems (Table 3.2). Observations during field work for this project also closely matched this classification description, with access over the delta dangerous at low tide.

It can be seen from the modified Bruun ratio and Hume & Herdendorf's (1992) classification that any significant reduction in the discharge through the Te Tumu Cut, will lead to a decrease in the Bruun stability ratio, and thus likely further decreasing the navigability of the Te Tumu Cut.

### 3.3.2 Cross-sectional Stability of the inlet

Numerous studies have shown that there is a relationship between the cross-sectional area of an inlet's throat and its tidal prism (O'Brien, 1969; Heath, 1975; Jarrett, 1976 and Hume and Herdendorf, 1988, 1992, 1993), with the relationship having the following form:

$$A = C \Omega^n \quad \text{Equation. 3.1}$$

where  $A$  is the inlet throat cross-sectional area ( $\text{m}^2$ ),  $\Omega$  is the tidal prism ( $\text{m}^3$ ) and  $C$  and  $n$  are constants.

Hume & Herdendorf (1992) collated a range of parameters, including cross-sectional area and tidal prism data for 16 inlets along the northeast coast of New Zealand. The relationship between the cross-sectional area and tidal prism for these 16 inlets is shown in Figure 3.3. The position of the Te Tumu inlet, based on the average ebb flow volume and bathymetry data collected in Section 4.4, is also indicated, although it is not accounted for in either of the trend lines.

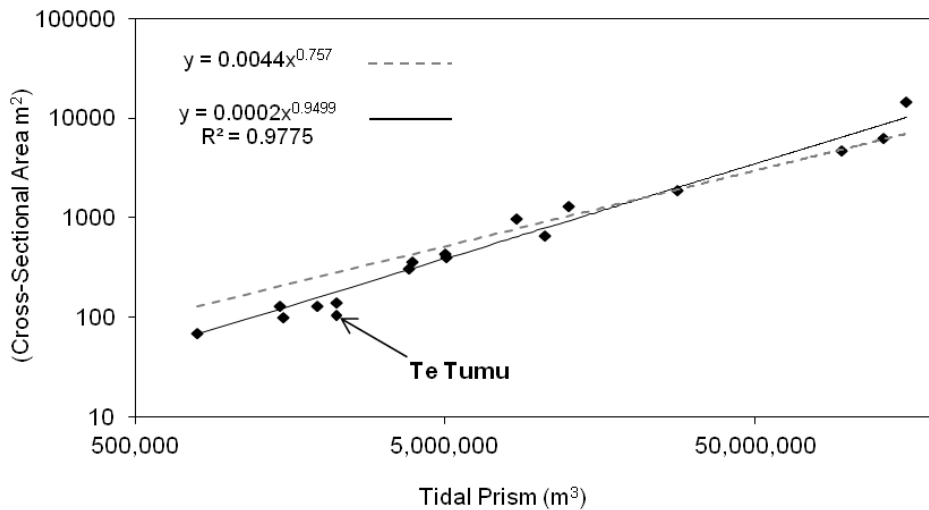


**Figure 3.3:** Inlet cross-sectional area vs. tidal prism relationships. The data points and solid trend line represents data of 16 inlets from Hume & Herdendorf (1992). The grey dashed line represents the relationship for River Mouth type inlets from Hume & Herdendorf (1993).

Following on from this work, Hume & Herdendorf (1993) classified 82 New Zealand inlets into 16 different inlet categories based on the Hume & Herdendorf (1988) scheme. It was found that for the river mouth inlet classification  $C = 4.39 \times 10^{-3}$  and  $n = 0.757$ , giving a relationship with an  $r^2$  value of 0.94 based on a sample size of 4. However, from Figure 3.3 (dashed line) it is evident that this river mouth inlet relationship does not hold true for the Te Tumu Cut, overestimating the cross-sectional area by slightly over 200%. However, the Te Tumu inlet fits closely within the relationship of the 16 inlets on the northeast coast (solid line) from Hume & Herdendorf (1992).

Hume & Herdendorf (1993) note that at river mouth inlets large variations in throat cross-sectional area exist due to large variations in river flow, and therefore river mouth inlets are perhaps not well described by  $A - \Omega$  relationships. Kirk (1991) and Kirk & Lauder (2000) also agree, stating that tidal prism to inlet cross-sectional area relationships are inappropriate for river mouth lagoon systems, due to the inlet being primarily freshwater dominated rather than tidally dominated.

Despite the concerns of Kirk (1991) and Kirk & Lauder (2000) the tidal prism - cross-sectional area relationship has been included and calculated here as it has been applied successfully to similar situations in the Bay of Plenty region in the past. Healy (1985) showed that for the Whakatane River when the mean daily river discharge was multiplied by the ebb tidal duration of 6.5 hours, and added to the tidal prism, a cross-sectional area of 238 m<sup>2</sup> was predicted, matching closely to the measured cross-sectional area of 246 m<sup>2</sup>.

The relationship was also used by Dahm & Kench (2004) for the Opotiki entrance. They measured cross-sectional area and tidal prism on two separate occasions, and compared them against the tidal prism cross-sectional area relationship for New Zealand Inlets. On both occasions the data points were situated above the equilibrium slope, suggesting the cross-sectional area was too large for the measured tidal prism. However, they observed flood scour prior to the measurements being collected and attributed the observed differences to this.

### 3.3.3 Ebb Delta Stability

In New Zealand the tidal prism is the primary control on ebb delta volume, with the angle of outflow in relation to the shoreline being the main secondary factor (Hicks & Hume, 1996). It was also shown that wave energy had some impact, with deltas on the West Coast tending to be smaller than those on the East Coast, for inlets with similar tidal prisms. Based on 17 inlets around New Zealand Hicks & Hume (1996) devised the following relationship between the inlets tidal prism and volume of the delta:

$$V = 1.9 \times 10^{-4} \times \Omega^{1.41} \quad \text{Equation 3.2}$$

Again assuming an effective tidal prism of 2,240,000 m<sup>3</sup> for the Kaituna River mouth (Section 3.3.1), the volume of sediment within the delta is 170,845 m<sup>3</sup>. This relationship further reiterates the point that any significant decrease in the effective tidal prism will lead to an increase in sedimentation around the inlet, as excess sediment from the smaller delta would likely move onshore and into the inlet, due to wave action.

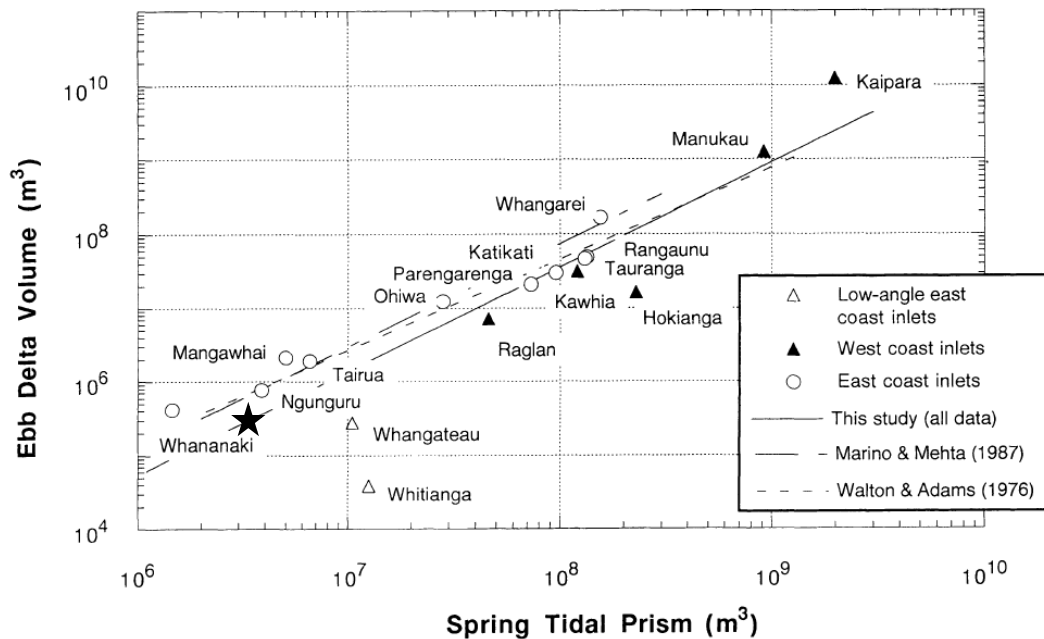


**Figure 3.4:** Relationship between spring tidal prism and ebb delta volume for 17 North Island inlets, from Hicks & Hume (1996). The Te Tumu inlet's position (calculated above) is also added and indicated by the black star.

Based on the methodology of Hicks & Hume (1996) the length / breadth ratio was determined using bathymetry data where available (2008, 2011), and aerial photographs when bathymetry data was unavailable (2003, 2007). Where aerial photographs were used, breaking waves were taken as an indication of the delta edge. The length was measured along the outflow axis and breadth was measured parallel to the shore. The average length / breadth ratio for the delta measurements shown in Figure 3.5 was 0.27 which fits the Type 1, free-form delta category of Hicks & Hume (1996).

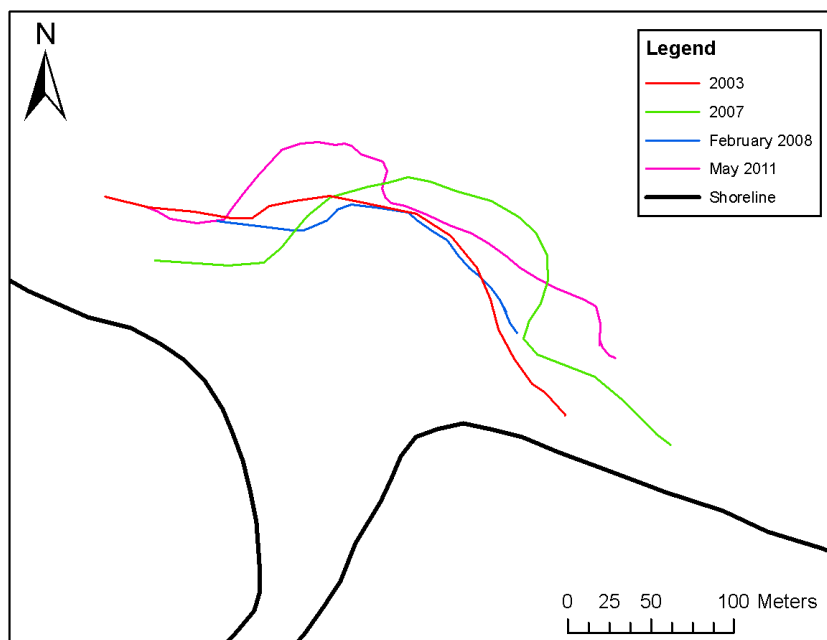


**Figure 3.5:** Schematic showing the ebb delta location, 2003 – 2011. The 2003 & 2007 locations were digitised from aerial photographs while 2008 & 2011 were digitised from hydrographic soundings.

From Figure 3.5 it is evident that in general the ebb delta at the Te Tumu entrance has remained relatively stable in regards to size, location and orientation between 2003 and 2011. The main variation away from the “normal” condition appears to be in 2007, where the delta becomes narrower, longer and orientated more to the north east.

### 3.4 Mechanisms of Inlet Closure

It can be seen from Section 3.3.2 that any significant reduction in flow through an inlet leads to a decrease in the inlet's cross-sectional area, as a result of increased deposition. If the decrease in flow is significant enough the inlet may completely close up. Ranasinghe & Pattiaratchi (2003) reviewed the theories on inlet closure mechanisms and stated they fall into two main categories. Mechanism 1 is the interaction between the inlet currents and longshore currents, whereas Mechanism 2 is the interaction between inlet currents and onshore sediment transport.

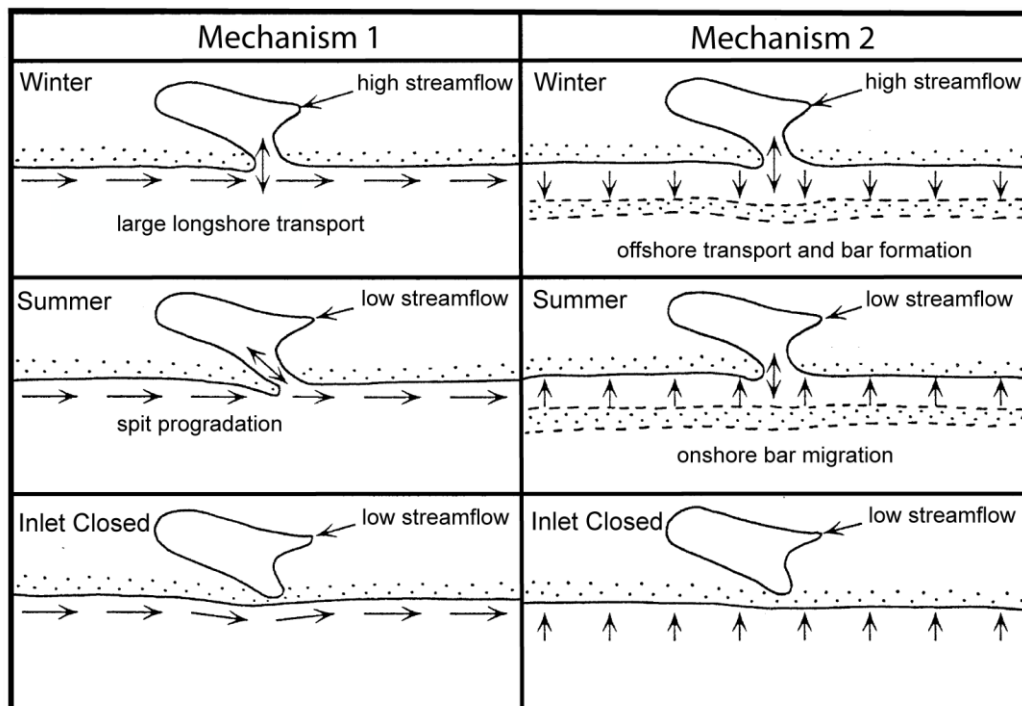


**Figure 3.6:** Schematic depiction of inlet closure by longshore and cross-shore mechanisms, from Ranasinghe & Pattiaratchi (2003).

Mechanism 1 is the result of the inlet interrupting longshore sediment transport and as a result, the formation of an up-drift shoal. Persistent supply of sediment to the shoal will result in the growth of a spit across the inlet mouth. If currents through the inlet mouth are strong enough to scour away deposited sediments then the spit will no longer grow. However, if the current velocities are not strong enough then the spit will continue to prograde until the inlet is completely closed (Figure 3.6, left).

Mechanism 2 only occurs when current velocities through an inlet mouth are small, for example inlets with a low tidal range and thus small tidal prism. This mechanism is the result of the interaction between low current velocities and onshore sediment transport conditions under calm swell wave conditions. When ebb flow currents are low, calm swell wave conditions will result in the onshore movement of sediment from the offshore bar region; providing the ebb flow currents are weak enough this onshore movement of sediment will lead to the closure of the inlet (Figure 3.6, right).

It is speculated that the Te Tumu Cut would conform to Ranasinghe & Pattiaratchi's (2003) Mechanism 1 of inlet. This speculation is based on the repeated cycles of spit breach and subsequent spit growth prior to the Kaituna River mouth becoming fixed at Te Tumu in 1956 as discussed in Section 2.2. Google Earth images in Figure 3.7 also show the partial development across the mouth, however, the river flows are strong enough to maintain the gorge channel and prevent complete closure.



**Figure 3.7:** Historic images from Google Earth showing spit growth across the river mouth.

Hart (2009) developed a theoretical model of the different morphodynamic states of river mouth lagoons, and the drivers between the different states, based on a range of non-estuarine river mouth lagoons on the eastern South Island of New Zealand. Figure 3.8 illustrates Hart's (2009) model and the links between each state. States a: primary and e: secondary breaches of new outlets occur as a result of high energy river and or sea events. Under moderate river and sea conditions outlet migration (b and c) dominates, while outlet closure (d) or stable outlet

configurations (b, c and e) occur during times of low energy river and sea conditions.

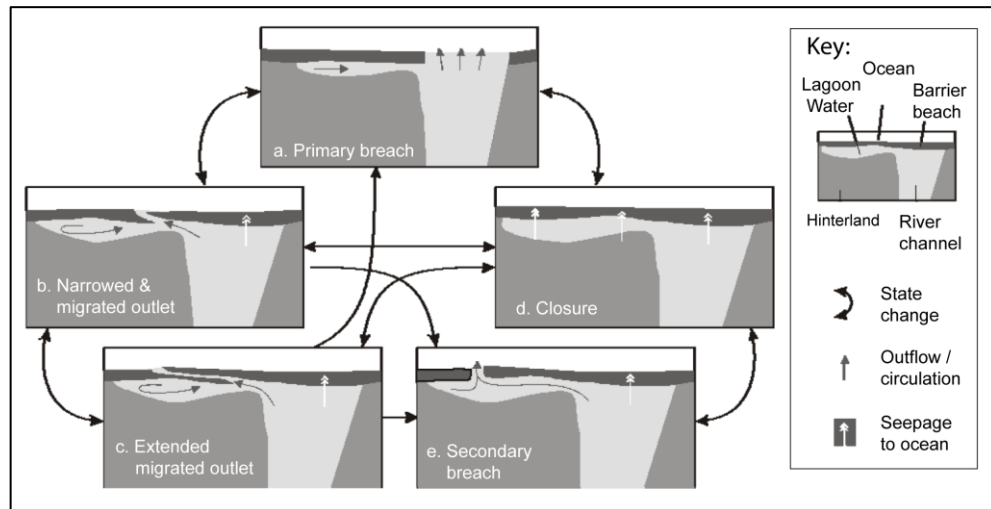


**Figure 3.8:** River mouth lagoon states and state changes (modified from Hart, 2009).

Based on the observed river mouth lagoons assessed in Hart’s (2009) study it was found that the most common lagoon state and stage changes occur during periods of wave dominance. These conditions induced stable or migrating outlets, closed outlets and barrier overtopping by waves. River conditions dominated outlet dynamics only occasionally to rarely, and resulted in primary and secondary breaching. It was also noted that lagoons with moderate river flows (mean  $<50 \text{ m}^3/\text{s}$ , 7-day low  $<16 \text{ m}^3/\text{s}$  and annual floods of  $<500 \text{ m}^3/\text{s}$ ) typically experience longer periods of wave dominance, while lagoons with higher flows (mean  $>50 \text{ m}^3/\text{s}$ , 7-day low  $>16 \text{ m}^3/\text{s}$  and annual floods of  $>500 \text{ m}^3/\text{s}$ ) typically experience less frequent state changes. From this it was concluded that stronger river flows do not lead to more frequent river-induced behaviours, but rather more stable outlets, which experience less frequent lagoon closures and intermediate stages.

The main difference between the river mouth lagoons observed in Hart’s (2009) study and the Kaituna River mouth is that the Te Tumu Cut is fixed by a rock causeway, and therefore, no longer experiences outlet migration as do the outlets Hart’s (2009) model is based upon. The Bay of Plenty coastline also experiences a much lower energy wave climate than that of the South Island’s east coast, with hindcast model results from Gorman *et al.* (2003) showing an  $H_s$  of 0.86 m for the

Bay of Plenty compared to 1.99 m for Banks Peninsula on the east Coast of the South Island.

### 3.5 Engineering Structures to Maintain Inlet Stability

Jetty structures or training walls at the mouth of inlets act to give the inlet positional stability and deepen the main channel by directing current flow and by inhibiting the natural littoral drift system. This is achieved by confining the flow to a limited channel and making the flow paths more hydraulically efficient, thus increasing flow velocities and scour potential (Kieslich, 1981). There are two main types of jetties: single jetties and twin jetties, each of which can vary in shape, size, height and design.

#### 3.5.1 Single Structure Jetties

Single jetties are single structures that can be straight or curved and either perpendicular or at an angle to the shore. Depending on the predominant wave and littoral drift conditions, they are typically located on the updrift side of the inlet. Single updrift jetties act as a barrier to the littoral drift system, minimising the influx of sediment from littoral drift system from entering the inlet (Figure 3.6). With sediment inflow minimised tidal and freshwater inflow current scour becomes more effective (Kieslich, 1981).

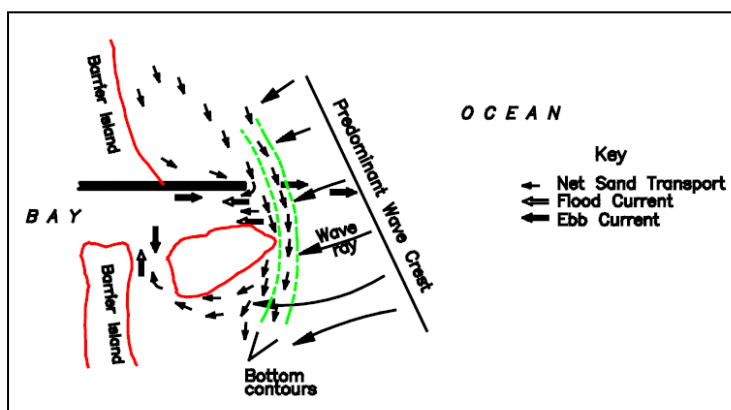


**Figure 3.9:** Schematic showing the current flow paths around a single updrift jetty structure (USCAE, 1995).

The current rock causeway structure at Te Tumu is an example of a single straight jetty, which is located on the downdrift side of the inlet. However, the causeway only extends to the edge of the river mouth, rather than out into the surf zone. This provides positional stability for the river mouth and channel, without interfering with sediment bypassing the inlet within the littoral drift system.

Although single jetties have been widely used in the past, it is now generally accepted that single updrift jetties are not a good protection measure for inlets. Based on data from 12 entrances along the Atlantic, Gulf and Pacific Coasts where single jetties have been used Kieslich (1981) concluded that construction of single jetty systems do not appear to be practical solutions to improving inlet entrances.

Their effects are beneficial updrift as they promote an area of deposition immediately against the jetty. However, single jetties lead to three main problems downdrift:

- Erosion of the downdrift beachface as a result of the littoral system becoming blocked off.
- Deposition within a lee side eddy (Figure 3.9) which may expand into the navigation channel.
- It has been shown that regardless of position and orientation of the jetty in relation to the net longshore sediment transport the seaward portion of the thalweg migrates towards the jetty often resulting in a channel in an unsafe proximity to the jetty (Bruun, 1978).

In attempts to minimise the negative effects often associated with single jetty structures two basic variations were designed, the weir section and the Haupt Jetty. A weir jetty (Figure 3.10) is similar to a single jetty structure; however, it must always be located on the updrift side to function. The weir section is a lower section on the shoreward portion of structure that typically has a crest level close to mean sea level. This allows sediment to be transported by waves and currents over the weir section to be deposited into the sheltered deposition basin. The deposition basin can then be periodically dredged with the sediment being deposited on the downdrift coast (USCAE, 1995).

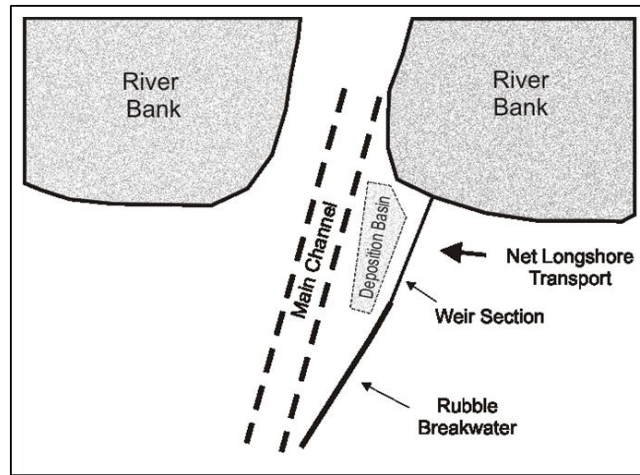


**Figure 3.10:** Schematic of a weir section in a jetty system (Recreated from USCAE, 1995).

The Haupt jetty (Figure 3.11) design is a single jetty that is detached from the shoreline and located on the updrift side of the inlet. The structure is concave to the main ebb currents, forcing them against the structure and thus scouring out a channel along the length of the jetty (USCAE, 1995).

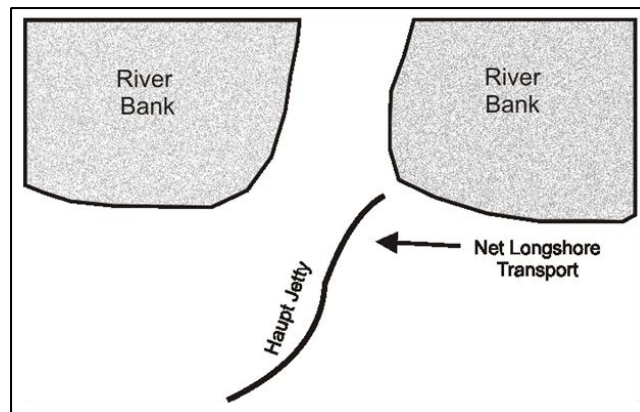


**Figure 3.11:** Schematic of a Haupt jetty system (Recreated from USCAE, 1995).

### 3.5.2 Twin Jetty Structures

Twin jetties are solid structures placed on either side of the inlet (Figure 3.12). They can be perpendicular or at an angle to the shore; diverging, converging or parallel; and of equal or different lengths depending on the predominant wave and littoral drift conditions. Twin jetties force the flood and ebb currents to become more channelized and constrict the entrance, therefore creating a deeper channel, while also blocking longshore sediment transport into the inlet (Komar, 1976; Kieslich, 1981).

The advantage of twin jetty structures over single jetties is that the jetty on the downdrift side prevents the formation of a deposition shoal in the lee side eddy as typically seen in single jetty systems. However, just like single jetty structures, twin jetties typically cause erosion on the downdrift side of the inlet as a result of impeding the littoral drift system (Bruun, 1978).

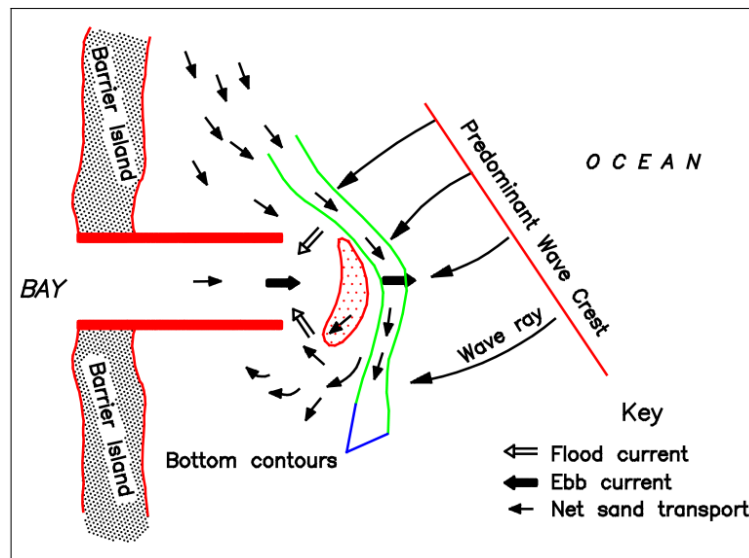


**Figure 3.12:** Schematic of a twin jetty system

The spacing between twin jetties can be crudely estimated using the tidal prism cross-sectional area relationship from Section 3.3.2 if the desired average channel depth is known. However, this relationship uses the tidal prism as a proxy for other factors that directly affect the inlets cross-sectional area, such as peak discharge

and velocity, and therefore, should only be used as an initial estimate (Hughes, 1999).

More recently, work by the United States Army Corps of Engineers (USACE) has developed another empirical relationship that can be used to determine the equilibrium scour depth ( $h_e$ ) between training walls (Hughes, 1999). The relationship is based on sediment grain size ( $d_e$ ), density ( $S_s$  – specific density) and maximum discharge per unit width through the inlet ( $q_e$ ), and is given by:

$$h_e = (0.234q_e^{\frac{8}{9}})/(g(s_s - 1)^{\frac{4}{9}}) d_e^{\frac{1}{3}} \quad \text{Equation 3.3}$$

This relationship has been used on a number of twin jetty inlets in the USA and has shown to provide an exaggerated estimate of equilibrium scour depth (more scour than may actually occur for a given discharge), representing the outer bound of the field data (Hughes, 1999). This relationship can be solved for  $q_e$  to determine the spacing between two jetties based on the required channel depth and inlet discharge conditions.

### 3.5.3 Opotiki Harbour Example

The Opotiki Harbour Inlet, much like the Te Tumu Cut, is a dynamic and continually changing inlet that responds to a complex interaction of wave induced, river flow and tidal currents along with a constantly varying sediment transport regime. During low river flows, the tidal flow through the inlet is insufficient to maintain the channel through the inlet. As a result the inlet becomes difficult, or at times impossible to navigate due to increased sedimentation. For example, in 2007 the inlet was unnavigable for 64 days, due to decreased depths within the channel (Pedersen *et al.*, 2008).

As a result of such problems, the Opotiki District Council commissioned DHI to investigate the significance of the different processes that shape the Opotiki

Harbour Inlet and assess various measures that could be taken to stabilise and deepen the channel through the inlet (Pedersen *et al.*, 2008).

Through extensive field data collection and the use of DHI's numerical modelling software it was concluded that:

- (1) The entrance is dominated by fine sediments transported within the littoral drift system, with an estimated 700,000 – 900,000 m<sup>3</sup> passing the inlet each year, with the direction varying in time depending on the wave conditions. Overall the net transport is estimated at about 7,600 m<sup>3</sup> each year to the west.
- (2) Preliminary assessments concluded that twin jetty structures would provide much better results than a single jetty would. Through sediment transport modelling of various jetty configurations it was found that the construction of twin breakwaters (jetties), spaced 120 metres apart would provide increased navigational conditions.



**Figure 3.13:** Aerial photograph showing the twin jetty structures that DHI (2008) concluded would provide the best navigation improvements, based on the required cost and flooding impacts (Modified from Pedersen *et al.*, 2008).

The proposed design consists of twin jetties spaced 120 metres apart, 400 m to the east of the current inlet. The jetties are aligned approximately 19° west of normal

to the coast, following the direction of the channel and extend out to a depth of 4 m. However, it was noted that their lengths were restricted due to costs, and that an ideal solution would extend further out to sea. Modelling showed that these structures would maintain a minimum channel depth 4.3 m under typical river flow and wave conditions.

### **3.6 Summary**

The Te Tumu Cut is classified as a low mesotidal, medium wave energy inlet according to Hayes (1979), and a straight banked river mouth according to Hume & Herdendorf (1988). However, the use of Hume & Herdendorf's (1988) classification of estuary types for river mouths is disputed by Kirk (1991) who instead suggests a separate classification of coastal lagoons, which would classify the Te Tumu Cut as a river mouth lagoon.

Based on number of widely used empirical relationships between an inlet's tidal prism and cross-sectional area, ebb delta volume and inlet stability when compared to the net annual littoral drift of the region it was shown any significant reduction in freshwater discharge out of the river mouth would lead to increased sedimentation around the Te Tumu inlet. However, Kirk (1991) and Kirk & Lauder (2000) suggest that such relationships are not appropriate for river mouth lagoon systems, as they are primarily controlled by freshwater discharges rather than tidal flows. However, tidal prism cross-section relationships have been used successfully in the past for the Whakatane River mouth and also applied to the Opotiki entrance in the Bay of Plenty and therefore were also calculated for the Te Tumu Cut. It has also been speculated that if there was a significant decrease in freshwater discharge the Te Tumu Cut would begin to close via the Type 1 Ranasinghe & Pattiaratchi (2003) mechanism of inlet closure.

# Chapter 4

## Field Data & Bathymetry Measurements

---

### 4.1 Introduction

In order to model hydrodynamic problems accurately, detailed bathymetric measurements are required (Ramming & Kowalik, 1980; Papanicolaou *et al.*, 2008). Inadequate bathymetry can cause difficulty in the calibration and validation stages of modelling and also lead to incorrect model results. This chapter will outline the different methods used to collect bathymetric data, sediment samples and current velocities in, and around the Te Tumu Cut and Maketū Estuary for this project.

### 4.2 RTK GPS Set Up

RTK (Real Time Kinematic) GPS is a form of GPS technology enabling accuracy in the order of 10 mm + 1 ppm (rms) in the horizontal, and 20 mm + 1 ppm (rms) in the vertical direction. It is based on the principle of a carrier phase-based relative positioning technique, which uses two (or more) receivers to track satellites simultaneously. A base station receiver remains stationary over a known point (benchmark) and the rover receiver can be manually moved around or attached to a vehicle such as a boat. The base station receiver transmits its coordinate and height measurements to the rover receiver, which then using built-in software combines and processes the coordinates and heights of both receivers to obtain an accurate position for the rover receiver (El-Rabbany, 2006).

Benchmark positions were provided by the BoPRC in the New Zealand Map Grid coordinate system and converted to the NZGD2000 Bay of Plenty Circuit using the online LINZ conversion tool, as this was the coordinate system used for this project. All elevation data used and recorded were relative to the Moturiki Datum.

A TrimbleMS 750 base station was set up on the BoPRC KN2R benchmark (Figure 4.1). The RTK GPS system was then verified against the BoPRC KN3R benchmark to check the accuracy of the system. The Northing and Elevation were accurate to within 2 cm, while the Easting was off by approximately 0.4 m. However, it was decided that the accuracy was sufficient for the requirements of this survey.



**Figure 4.1:** Location of the benchmarks used in the RTK GPS system.

### 4.3 Land Based Survey

For approximately one hour either side of low tide, on February 21<sup>st</sup>, a land based RTK GPS survey was conducted over the intertidal area around the river mouth. This was achieved by attaching the RTK GPS rover receiver to a metal staff, and setting it to record coordinates and elevation every 5 m. This was then carried by hand, holding the bottom of the staff so it was just scratching the beach face. Initially a transect was walked along the low tide water line on the western riverbank. A zigzag pattern from the water's edge, to above the high tide line, was then walked to gain bathymetry measurements of the intertidal zone. This process was then repeated on the eastern riverbank. However, the area surveyed on the eastern side was limited as approximately 150 metres inside the river mouth as there was not enough beach face exposed to walk over, as the river bank against the causeway is below the water's surface, even at low tide. The area over which the land based survey was conducted is shown in Figure 4.2.

The main source of error associated with this land based survey technique was human error. Due to the weight of the rover and the staff it was attached to, it was difficult to make sure the bottom of the pole was just scraping the sand at all times, especially over the highly variable topography. It was noted during the survey that these factors would have caused an error of approximately  $\pm 5$  cm in elevation.



**Figure 4.2:** Map showing where the various survey methods were used, excluding the digitised hydrographic chart, which was used for the offshore region.

## 4.4 Single Beam Survey

A Knudsen 320 MP single beam echo sounder (SBES) was used to survey inside, and outside the river mouth over the ebb delta. The surveys were conducted using the University of Waikato's Tai Tumu boat. The SBES and RTK GPS were attached to the boat's stern, and linked into a computer running Trimble's HYDROpro™ software. HYDROpro™ was used to compute and navigate transect lines, record the SBES and RTK GPS data and to calculate the heave and tidal elevations.

The survey was conducted in two parts, due to a small swell making it difficult to survey outside of the river during the initial survey. The first survey was conducted during a spring tide on the 22<sup>nd</sup> of February 2011. The second survey was then conducted 20<sup>th</sup> of May, where data was collected just inside the river mouth to provide an overlap with the first survey, and outside the river mouth over the ebb delta.

There were two main potential sources of error associated with the SBES set up used for this survey. The first potential error was from the GPS system. Prior to starting both surveys, the RTK GPS was checked against the temporary benchmark created on the wharf next to the boat ramp. During the first survey it was found to match perfectly, however, on the second survey the Northing was off by 0.6 m. However, due to time constraints and needing to start the survey before the high tide, this was deemed acceptable.

The second potential source of error arose from the constantly varying water density around the river mouth. Echo sounders are based on the principle of how long an acoustic pulse takes to travel from the transducer to the sea floor and back again, and thus rely on an accurate representation of the speed of sound in water. The Te Tumu Cut is an environment with a constantly changing water density due to the interaction of freshwater from the Kaituna River and saltwater entering through tidal currents. This results in a varying speed of sound, both spatially and temporally, within the river mouth. In order to simplify the process a constant speed of sound in water was assumed. The echo sounder recorded depth values to one decimal place, therefore an estimate of the SBES depth accuracy during the survey was  $\pm 0.2$  m.

#### 4.4.1 Post Processing

Post processing of the SBES data was undertaken using the Trimble NavEdit™ software. There was some random noise present in the raw SBES data, with some points showing depths deeper than 10 metres. However, it was known this was unrealistic, and was likely due to the presence of suspended sediment within the water column. These points were removed using the batch filter function, which removed all depths greater than 10 m, as it is known that there are no depths exceeding this depth in the areas surveyed. The tidal heights recorded from the RTK GPS were then checked against readings from the BoPRC tide gauge located next to the boat ramp. The tidal curves were shown to match within 5 – 10 cm and follow the same general shape (Figure 4.3). The cleaned data was then exported as an ASCII text file with the tide and heave subtracted from the raw depths to generate a file containing Northing, Easting and Depth data points.

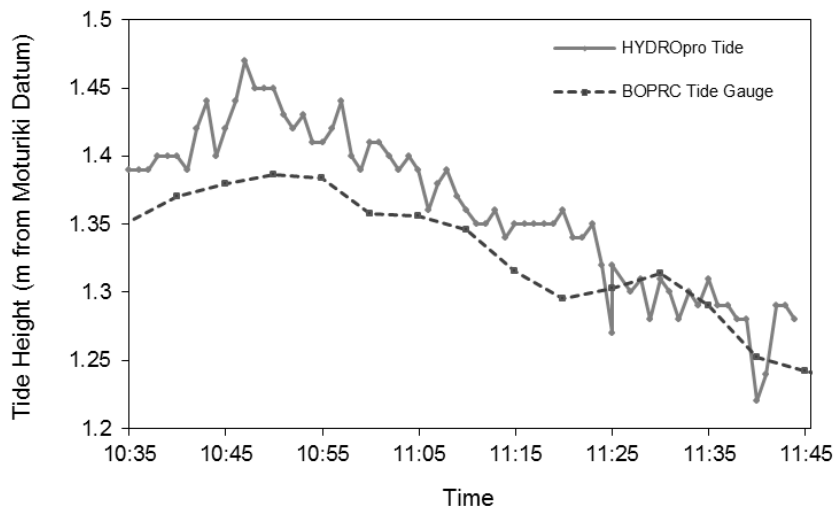


**Figure 4.3:** Comparison between the Ford's Cut tide gauge readings and the tide level obtained using the RTK GPS through the HydroPro software, on the 20/5/2011.

## 4.5 Digitised Hydrographic Chart

Regional bathymetric data were required in order to transform offshore wave data to their nearshore equivalent using the MIKE 21 Spectral Wave (SW) module. Due to the size of the mesh required it was unrealistic to complete a hydrographic survey of the entire Bay of Plenty, and therefore a hydrographic chart from LINZ was digitised.

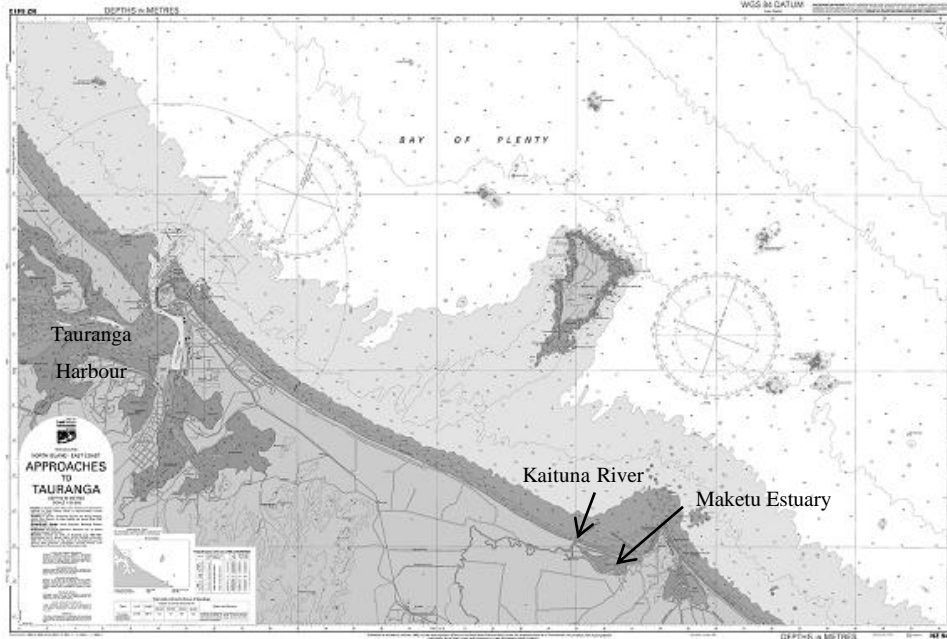


**Figure 4.4:** LINZ Chart NZ5413 - Approaches to Tauranga (LINZ, 2008), which was digitised to obtain the offshore bathymetry.

The NZ5413 – Approaches to Tauranga, 1:50,000 map from LINZ was chosen as it is freely available on the LINZ website, and covers the Western Bay of Plenty region, out to approximately 400 m water depth. ESRI’s ArcMap software was used to digitise the hydrographic chart in the WGS84 coordinate system, as that is what the chart was produced in. The contour lines were traced using the Polyline tool and then converted into point data which consisted of X, Y and Z coordinates. Individual spot heights were then digitised using the point tool, which created xyz points like the contour line points. The digitised data were then transformed in to the BOP2000 circuit coordinate system in order to match the other bathymetric data. The contour and point height files were then combined using the Merge (Data Management) Tool into a single file and exported as an ASCII text file.

## 4.6 Maketū Estuary Bathymetry Data

Bathymetry measurements inside Maketū Estuary were required in order to model the diversion Option N, which includes the reopening of Papahikahawai Channel. Due to the large and shallow nature of Maketū Estuary, conducting a SBES survey was beyond the scope of this study. Therefore, bathymetry data were collated from various sources, to provide full coverage of the estuary. The different data sources are briefly described below.

Discovery Marine Limited was employed by the BoPRC in February 2008 to conduct a SBES survey of the Te Tumu and Maketū entrances. This was achieved using a Garmin Etrex GPS and echo sounder, and was determined to have a vertical error of less than  $\pm 0.15$  m (DHI, 2009). The data used from this survey covered the ebb delta outside the Maketū entrance to approximately 400 m inside the entrance. Discovery Marine Limited was further commissioned by the BoPRC in August 2008 to survey Papahikahawai Channel. A series of zigzag patterns and transects perpendicular to the channel were surveyed along the length of Papahikahawai Channel (DHI, 2009). The main channel, to Ford's Cut was surveyed by Goodhue (2007) using an RTK GPS and echo sounder set up similar to the one described in Section 4.4.

Bathymetry measurements over the intertidal flats, in the middle of the estuary, were determined through image rectification by Goodhue (2007). The image rectification was achieved using a camera set up on an elevated location to the east of Maketū Estuary, and recording a series of still images over a tidal cycle. The water-sand bank interface was then digitised and rectified on each image. Given that the water elevation was known at the time each photograph was taken, a series of proxy depths could be obtained. The error associated with the image rectification technique was estimated at less than  $\pm 0.2$  m.

## 4.7 ADCP Measurements

An Acoustic Doppler Current Profiler (ADCP) was used to collect current measurements around the Kaituna River mouth. A boat mounted ADCP was chosen because the river mouth and delta were too shallow and regularly navigated by recreational fisherman, to safely leave a current meter deployed on the bottom. Measurements were collected to calibrate the Mike 21 Hydrodynamic model, and determine whether the river water disperses out relatively evenly in a fan shape or if it discharges as a jet. Originally it was hoped a transect parallel to the shoreline, just in front of the river mouth could be sampled throughout a tidal cycle. However, it became too shallow to cross over the ebb delta at low tide. Instead semi-circular transects were driven slightly further offshore, for the duration of the survey.

ADCP measurements were collected on the 19<sup>th</sup> of May 2011 using the University of Waikato's RDI 1200 kHz ADCP mounted downward on the Tai Timu vessel. A semi-circular transect ranging from approximately 150 m either side of the river mouth was driven from 9:30 am to 5:30 pm, covering the time from just after high tide until approximately half way through the incoming tide (Figure 4.5).

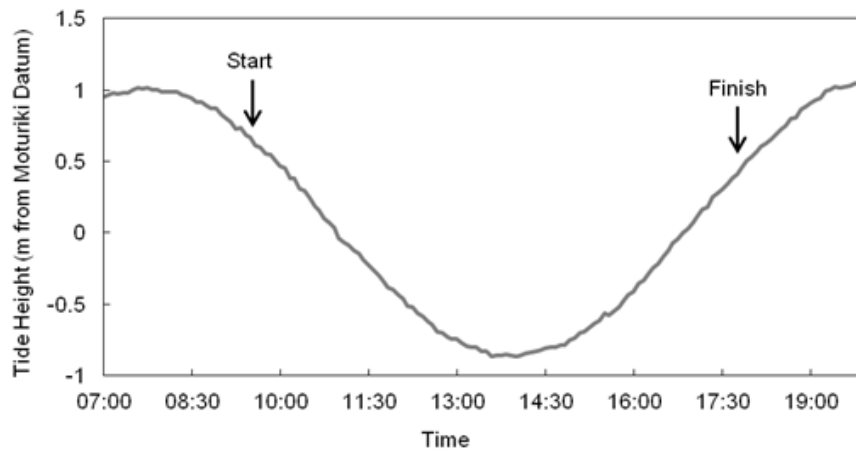


**Figure 4.5:** Tidal elevation plot from the 19<sup>th</sup> of May 2011, indicating the duration of the ADCP survey.

The ADCP was set up to record the  $u$  and  $v$  velocity at 25 cm depth increments directly below the instrument. However, the top 1.03 m of the water column was missed as the instrument was mounted below the water surface and there is a blanking zone before measurements can be obtained.

#### 4.8 Sediment Samples

Surficial sediment samples were collected using a small hand held drop sampler from the locations shown in Figure 4.6. The samples were then processed through the University of Waikato's Malvern Laser Sizer (MS2000). The Laser Sizer calculates the particle size distribution through the diffraction and diffusion of the grains passing through a focused laser beam. Sample 4 contained large amounts of irregular shaped shell fragments which had to be removed prior to it being processed in the Laser Sizer. Therefore, it was first passed through a 1.4 mm sieve, in order to avoid any potential blockage of the Laser Sizer.



**Figure 4.6:** Locations of the sediment samples collected.

## 4.9 Summary

The field data outlined in this chapter was crucial for creating, calibrating and validating the Spectral Wave, Hydrodynamic and Sediment Transport models described in the subsequent chapter. A SBES and RTK GPS survey was conducted around the Te Tumu Cut, and a hydrographic chart of the Bay of Plenty region was digitised specifically for this project. Additional bathymetry measurements in the form of LIDAR and SBES data was provided by the BoPRC in addition to RTK GPS and image rectification data which were collected as part of Goodhue's MSc thesis (2007). The various bathymetry data sets were all converted to the BOP2000 circuit coordinate system and saved as ASCII text files, allowing them to be imported into the Mike 21 Mesh Generation module.

Sediment samples were also collected inside the Kaituna River and around the ebb delta and analysed using a Malvern Laser Sizer. ADCP measurements were collected by driving a semi-circular transect around the river mouth which were to be used to calibrate the Hydrodynamic Model.

# Chapter 5

## *Numerical Modelling*

---

### **5.1 Introduction**

This chapter describes the setup and calibration of the DHI Mike 21 Spectral Wave, Hydrodynamic and Sediment Transport models used to investigate the morphologic response of the Te Tumu Cut to a range of scenarios. By altering the boundary conditions and bathymetry files used, the effects of different river flow and wave conditions on various proposed diversion options for the Kaituna River / Maketū Estuary were able to be investigated.

With the exception of the 1-dimensional Mike 11 model, all models used were 2-dimensional, run over unstructured triangular meshes and solved using a cell-centred finite volume solution technique (DHI, 2011a). A large regional scale wave model was used to transform offshore wave conditions into the nearshore environment. Smaller scale and more detailed local scale Spectral Wave (SW), Hydrodynamic (HD) and Sediment Transport (ST) models were then run and coupled together within the Mike 21 environment. This allowed changes in bed level, water level and current conditions at each time step to be taken into account in each successive time step for the SW, HD, and ST models.

### **5.2 Time Series Data Used to Force the Models**

Discharge data from the Te Matai and Raparapahoe river flow gauges, wave data from the Pukehina wave buoy and tidal heights from the Moturiki tide gauge were supplied by the BOPRC, and wind data was obtained from the Tauranga Airport, through NIWA's CLiFlo database (Station #: 1615). The data sets were provided in the following forms:

- The Te Matai and Raparapahoe discharge data spanned from 01/01/2006 to 01/06/2011 and were provided as 15 minute averaged discharges in litres per second.
- The wave buoy data included hourly averaged significant, mean and peak wave heights, mean and peak periods and mean direction, covering the time period between 01/01/2006 to 17/7/2011.
- Tidal heights were provided as 5 minute averaged water level heights relative to the Moturiki datum and spanned the same time period as the wave data.
- Wind speed and direction data were obtained as hourly averages from the Tauranga Airport, measured 4 m above mean sea level.

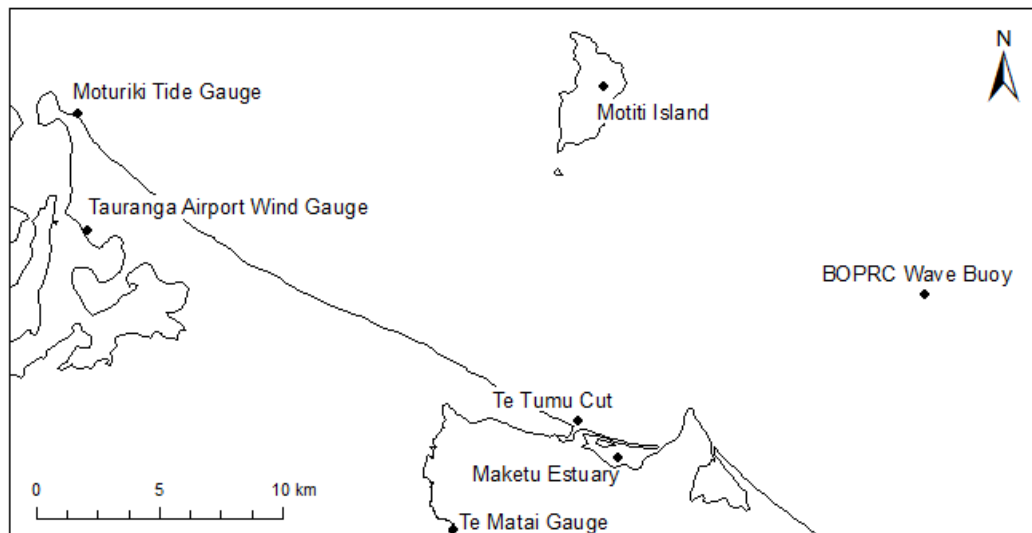


**Figure 5.1:** Locations of the various time series data recording gauges.

All data sets, excluding tidal height (which was interpolated using the Mike Zero piecewise cubic interpolation function), were run through the linear interpolation tool in the Mike Zero toolbox to fill in small periods of missing data. They were then re-saved at the same sampling frequency in which they were provided and exported as .dsf0 files, allowing them to be used as model boundary conditions.

### 5.3 River Flow Model

A pre-existing DHI Mike 11, 1-Dimensional river flow model of the lower Kaituna River was supplied by the Bay of Plenty Regional Council. This model was originally developed in 1991 by the BOPRC to assess inflows into the Maketū Estuary. In 1999–2000 Matthew Surman updated the model and expanded its coverage to upstream of the Maungarangi Bridge, and included the canals and drains of the lower catchment into the existing lower floodplain and the Maketū Estuary model. Individual models of the Waiari and Kopuaroa streams and the Raparapahoe and Ohineangaanga Canals were developed in 2007. These were then connected to the Kaituna Model, creating a 1-dimensional model of the lower Kaituna Catchment as shown in Figure 5.2 (Wallace, 2009).

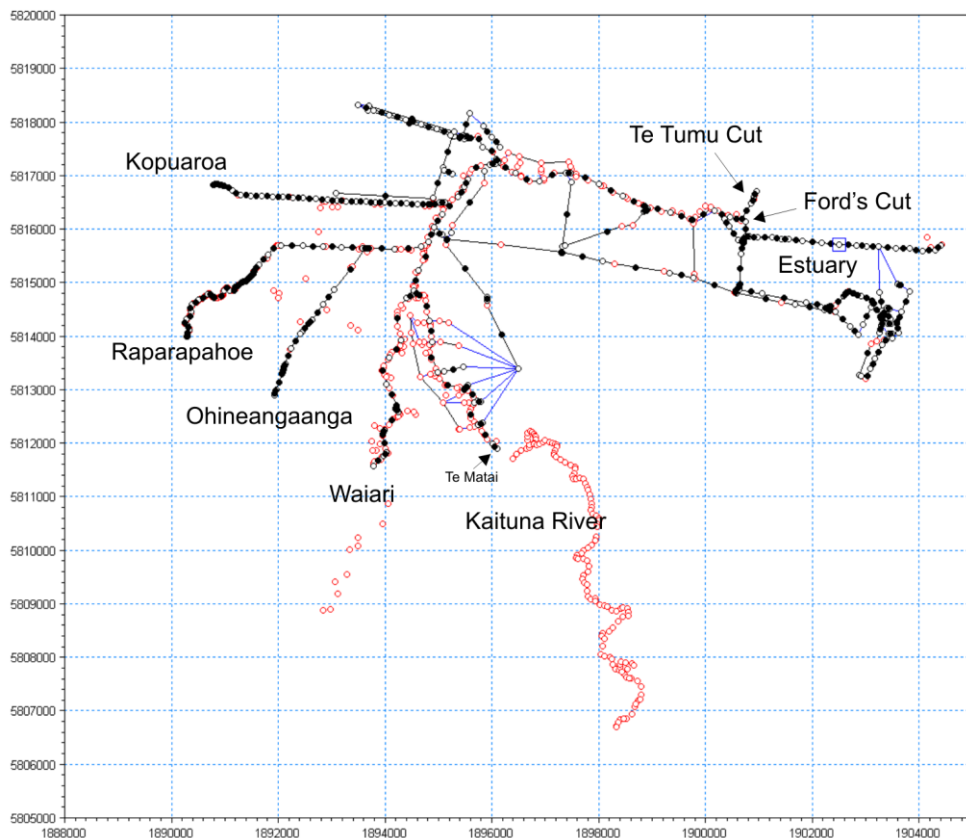


**Figure 5.2:** Annotated screenshot from the Mike 11 network editor showing the extent of the model, and the location of the different boundaries.

The model was edited to include a node at the upstream boundary (BOP2000 Circuit – 395379.62, 801178.64) of the Mike 21 model used. This allowed discharge values to be extracted from the Mike 11 model to be used as input conditions for the upstream boundary of the Mike21 2-Dimensional model.

### 5.3.1 Boundary Conditions

The upstream boundary of the Kaituna river model was at the Te Matai river flow recording site. This was forced by 15 minute averaged discharge data from the Te Matai monitoring station. The downstream boundaries (Te Tumu Cut & Maketū Estuary Inlet), which represent tidal flows from the sea, were forced by 5 minute averaged water level data from the Moturiki tide gauge.

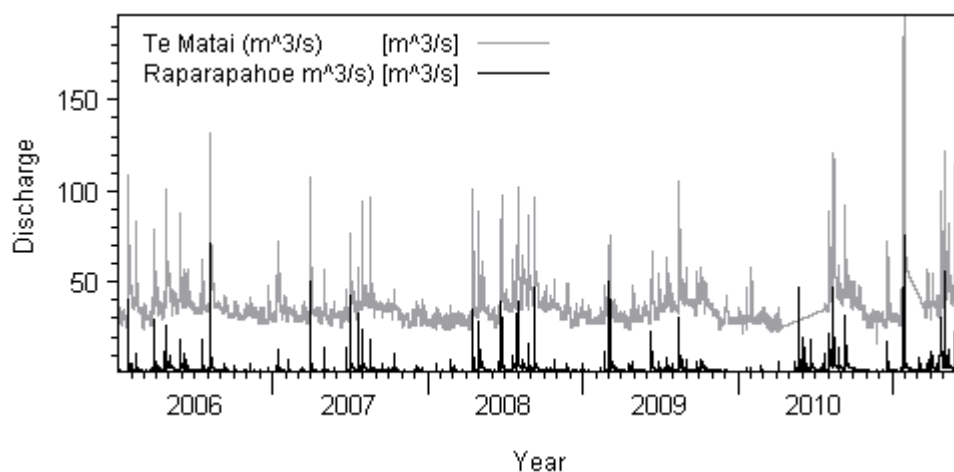


**Figure 5.3:** 15 minute discharge readings from the Bay of Plenty Regional Councils Te Matai and Raparapahoe recording gauges.

The lower Kaituna River also has a range of smaller input sources such as the tributaries of the Raparapahoe, Ohineangaanga, Kopuaroa and Waiari streams and various pumped and non-pumped drains from the surrounding farmland. However, of these input sources the Raparapahoe tributary is the only one that has a permanent long term monitoring site. This allowed the Raparapahoe Stream to be

forced by 15 minute averaged data. However, the other tributaries are too small to justify permanent monitoring sites, and therefore approximations were required.

The approximations used for the smaller tributaries were devised from several studies by the BOPRC and outlined by Wallace (2009) in his Hydraulic modelling of the Kaituna River report. The approximations were based on slope-area calculations and scale discharges from the Raparapahoe stream in relation to the catchment area of the other tributaries. The approximations were (where  $Q_R$  is the discharge from the Raparapahoe stream):

- Ohineangaanga Q = 0.508 x  $Q_R$
- Waiari Q = 1.389 x  $Q_R$
- Kopuaroa Q = 0.51 x  $Q_R$

The use of these assumptions was justified by the fact that any slight error (e.g.  $\pm 1 - 2 \text{ m}^3/\text{s}$ ) in the above relationships would be largely insignificant compared to the on average  $40 \text{ m}^3/\text{s}$  entering from the upper Kaituna River.

## 5.4 Flexible Mesh Generation

The Mesh Generator is module within the Mike Zero package, and is an environment for creating digital flexible meshes (FM). The main advantage, and reason why a flexible mesh was chosen over a rectilinear grid for this project, is that it allows for greater control of the node resolution in specified areas (DHI, 2011a). This method allows smaller elements to be used over areas where the bathymetry is more variable and greater detail is required (e.g. the river mouth) and larger elements where the bathymetry is more uniform, and less detail is required (e.g. the inner shelf zone) and thus optimizes computational time.

Three separate meshes were generated. The first was a large regional scale mesh (Figure 5.4), which covered the area from Papamoa Beach, to the northern (~400 m water depth) and eastern extent of the LINZ 542 chart shown in Figure 4.4. A mesh this size was required to include the effects of wave sheltering from Motiti Island and is shown in Figure 5.4. The second mesh was smaller and only extended out to approximately 25 – 35 m water depth, and 10 km less in the western direction. This smaller local scale mesh (Figure 5.5) was used for the coupled Spectral Wave, Hydrodynamic and Sediment Transport model.

The third mesh created was exactly the same as the local scale mesh, but also included Maketū Estuary, and a reopened Papahikahawai Channel (Figure 5.6). Papahikahawai Channel was reopened by opening up the land boundary between the Kaituna River and Maketū Estuary parallel to the spit. The bathymetry was then manually edited to create a channel 30 m wide and 1 m deep, as outlined in Tuckey (2009).

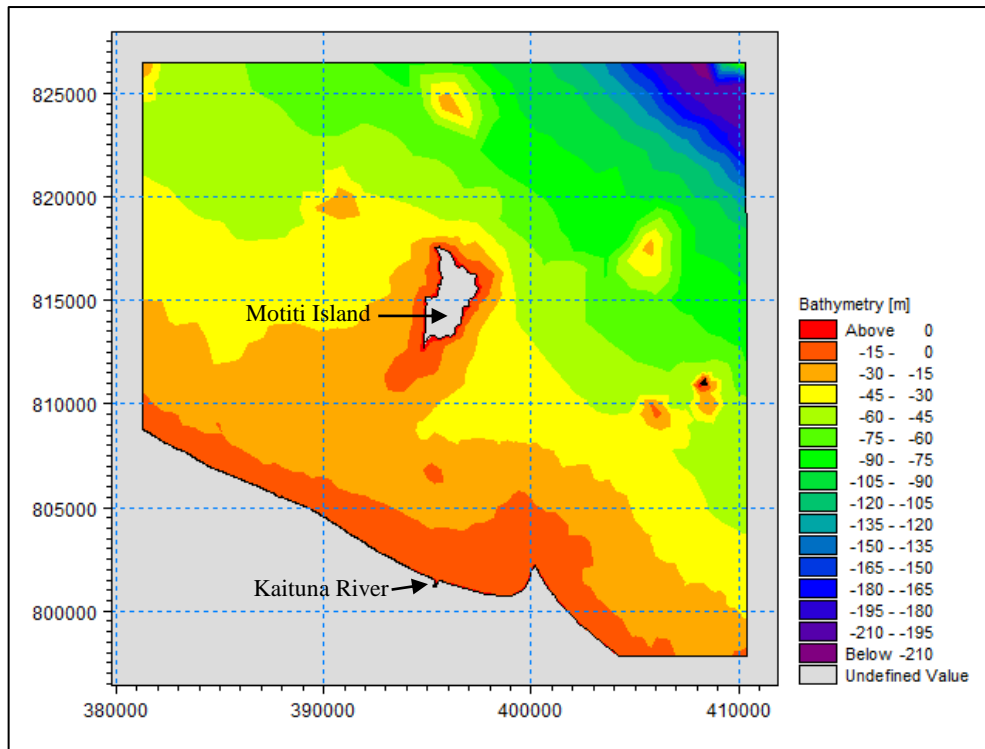


**Figure 5.4:** Interpolated mesh showing the bathymetry used for the regional scale, spectral wave simulations. Depths were obtained from a mixture of a SBES survey, RTK GPS survey and a digitised hydrographic chart.

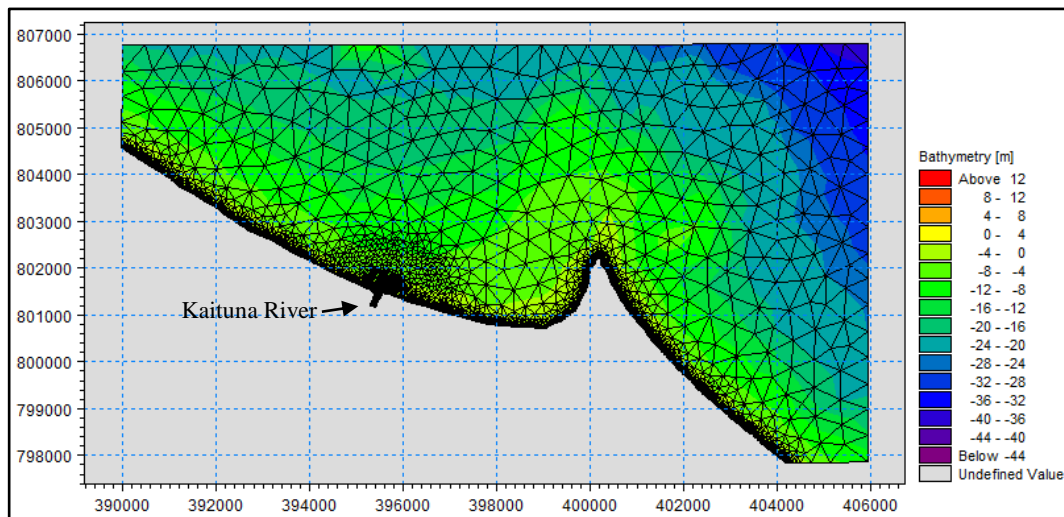


**Figure 5.5:** Interpolated mesh showing the bathymetry and mesh elements used for the coupled local Hydrodynamic, Spectral Wave and Sediment Transport modelling of the Status Quo and Option J scenarios. Depths were obtained from a mixture of a SBES survey, RTK GPS survey and a digitised hydrographic chart.

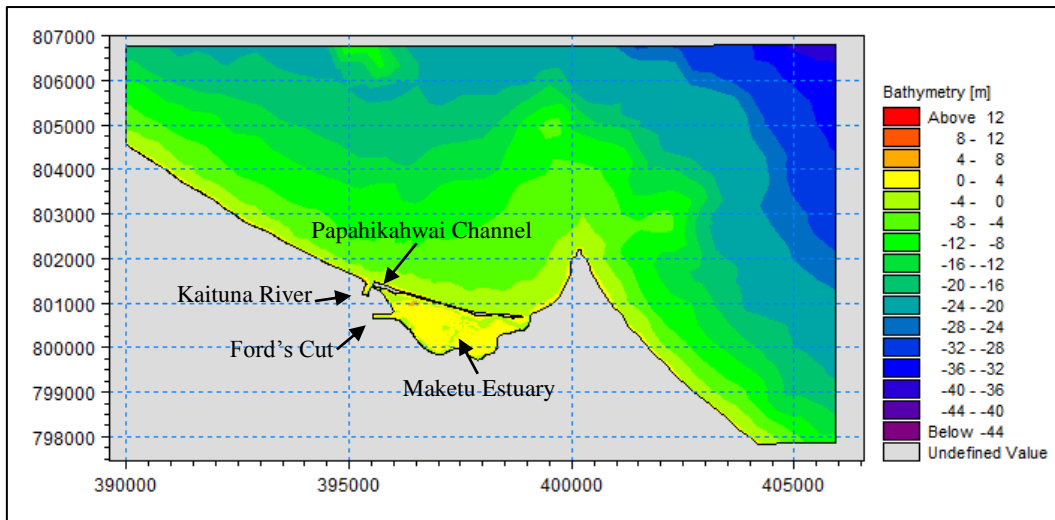


**Figure 5.6:** Interpolated mesh showing the bathymetry used for the coupled local Hydrodynamic, Spectral Wave and Sediment Transport modelling of Option N. Depths were obtained from a mixture of SBES surveys, an RTK GPS survey, a digitised hydrographic chart and tidal levels from orthorectified photographic images.

Six separate zones of the mesh were defined, and given varying mesh resolutions. The finest mesh resolution zone contained the area inside the Te Tumu Cut and along the sand dunes, as this was the area of primary interest, and with the most variable bathymetry. The remaining zones formed progressively larger semicircles with coarser mesh resolutions radiating out from the river mouth.

The constraints for each zone were that the smallest allowable angle for any of the triangular mesh elements was  $26^\circ$ , and that the maximum area of any one triangle within the respective zone was 150, 250, 500, 10,000 and 200,000  $m^2$  for zones 1 – 5 respectively. An example of the local scale triangular flexible mesh used is shown in Figure 5.5. For the second local scale mesh that included Maketū Estuary, the same constraints as above were used along with a zone containing Maketū Estuary which had a maximum allowable area of 150  $m^2$ . Although the above resolutions may sound large, they are the maximum areas allowed, and the mesh generation algorithm creates smaller elements around the more complex boundaries.

The very coarse mesh resolutions used for the offshore regions are justified by the fact that the bathymetry data covering this area was also of coarse resolution, with large distances between contour lines due to the low slope of offshore region, and

sparse point depth coverage from the digitised bathymetric chart. Therefore a finer mesh resolution would not add any detail.

Once the mesh had been generated ASCII text files from the SBES surveys (4.4), RTK GPS land survey (Section 4.3), LiDAR data (Section 4.6) and the digitised hydrographic chart (Section 4.5), were imported into the Mesh Generator. These points were then interpolated onto the mesh using the built in Triangular Natural Neighbour Interpolation function. The three meshes were then used to run the models described in Sections 5.5, 5.6 and 5.7.

## 5.5 Simulation Time Scales

Initial model runs showed that long period (30+ days) simulations produced unrealistic results, with significant erosion occurring at the western boundary shoreline and around the Kaituna River mouth. Through simulations of varying time scales it was found that simulations over a 2 week period produced the most accurate results. Therefore two week simulations were used for the simulations described in Section 5.9

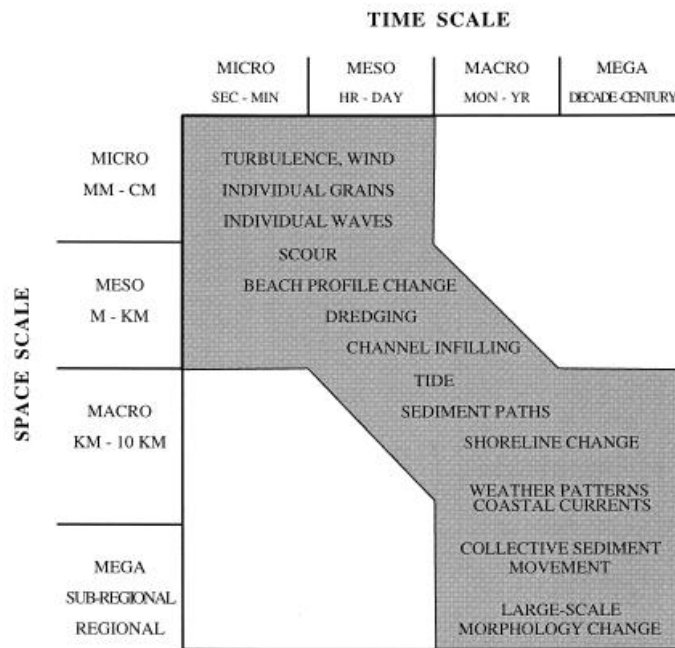


**Figure 5.7:** Time and spatial scale compatibility for nearshore morphodynamic modelling. The shaded area indicates the time and spatial scales that processes that can realistically be evaluated while the white areas indicate temporal and spatial scales unfeasible for modelling, from Ranasinghe *et al.* (1999).

Figure 5.7 shows the spatial, and corresponding temporal scales required to model a range of nearshore morphodynamic processes. Nearshore scour is located near the start of both the meso spatial and temporal classes, indicating that scour can occur over a few meters and within hour time scales. Conversely channel infilling is shown to occur towards the outer extent of the of the meso spatial and temporal time scales, indicating this processes acts on scales up to one kilometre and over a day to multiple days. Both scour and channel infilling fall within the meso time

scale and therefore should be able to be successfully represented in the two week model simulations used for this project.

## **5.6 Spectral Wave Modelling**

The BOPRC wave buoy is located at a depth of 64 m, approximately 16 km to the east of the Te Tumu Cut, 13 km offshore from Pukehina Beach (Figure 5.1). A regional wave model was developed to transform offshore wave data from BOPRC's wave buoy, into the nearshore region. This was achieved using DHI's 2-dimensional Spectral Wave (SW) Model. The SW model simulates the growth, transformation and decay of wind and swell waves in the open coast and nearshore environment (DHI, 2011b). The SW simulations for this project used the directionally decoupled parametric formulation, which is based on a parameterization of the wave action conservation equation of Holthuijsen (1989).

### **5.6.1 Wave Model Resolution**

In selecting the resolution of directional discretisation for the wave model a tradeoff between resolution and computational time was required. For swell waves with a small directional distribution of wave energy, a resolution of  $< 10^\circ$  is recommended. For wind waves with a larger directional distribution of energy, resolution values of  $< 30^\circ$  are recommended (DHI, 2011b). A value of  $22.5^\circ$  was used for the SW simulation in this project as this falls between recommended values for swell and wind waves and allowed for realistic computational times and is also the same value used in the nearby Opotiki Entrance study by Pedersen *et al.* (2008), previously mentioned in Section 3.5.4. The spatial resolution for the regional scale, and local scale meshes are described in Chapter 5.4.

### **5.6.2 Wave Model Parameters**

The wave data used to force the open ocean boundary of the regional Spectral Wave model was hourly averaged significant wave height ( $H_s$ ), mean direction

and peak wave period ( $T_p$ ) from the BOPRC's wave buoy. As shown by Figure 5.8 this data closely matched wave conditions from the literature cited in Section 1.3.4. The wave buoy is located at a depth of approximately 62 m and thus the waves have not likely undergone any significant transformations, such as shoaling and therefore could be applied as an open boundary condition for the Spectral Wave Model. This was confirmed through the SW model validation in Section 5.6.3.

As there was no information on the standard deviation on the directional spreading of waves from the wave buoy, a constant value of  $23.28^\circ$  was assumed, as this is typical of wind-waves (DHI, 2011b). This value was chosen as the mean wave period of the wave buoy data was 7 seconds, which typically represents wind generated waves. All other parameters used in setting up the spectral wave model are outlined in Table 5.1

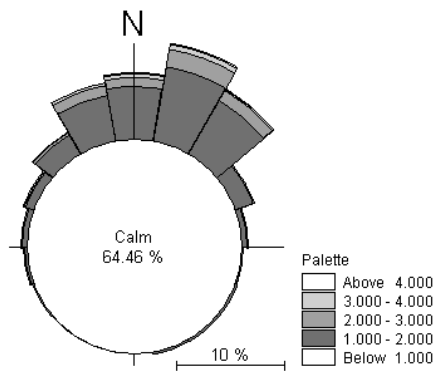


**Figure 5.8:** Rose Plot of Significant Wave Height from the BOPRC's wave buoy, 2006 – 2011.

**Table 5.1:** Parameters used for the regional scale, Spectral Wave Model.

<b>Parameters</b>	<b>Value</b>
<b>Basic Equations</b>	
Spectral Formulation	Directionally decoupled parametric formulation
Time Formulation	Quasi stationary formulation
<b>Spectral Discretization</b>	
Discretization Type	360 degree rose
Number of Directions	16
<b>Water Level Conditions</b>	
Type	None
<b>Current Conditions</b>	
Type	None
<b>Diffraction</b>	
Type	Diffraction
Smoothing Factor	1
Number of Smoothing Steps	1
<b>Wave Breaking</b>	
Model	Wave breaking
Type of Gamma	Specified gamma
Gamma Data	
Format	Constant
Constant Value	0.8
Alpha	1
Gamma (wave steepness)	0.9
<b>Bottom Friction</b>	
Model	Sand grain size, d50
Format	Constant
Constant Value	0.000493 m

### 5.6.3 Wave Model Validation

A 20 day significant wave height and peak wave period time series, from the location of the BOPRC wave buoy, was extracted from the regional wave model results and plotted against the raw data from the wave buoy. The Mean Absolute Error (MAE) and Root Mean Square Error (RMSE) were also evaluated for both, using the following formulas from Winter (2007), where  $y_i$  and  $x_i$  are the predicted and observed values respectively.

$$MAE = \frac{1}{N} \sum_{i=1}^N |y_i - x_i| \quad \text{Equation 5.1}$$

$$RMSE = \sqrt{\frac{1}{N} \sum_{i=1}^N (y_i - x_i)^2} \quad \text{Equation 5.2}$$

The MAE is a measure of the average magnitude of the error for a set of predictions without considering their direction. The RMSE is also a measure of the average magnitude of the error. However, as the errors are squared before they are averaged it gives a higher weighting to larger errors. Used together the MAE and RMSE provide an indication of the variance within the errors. When the MAE is equal to the RMSE, the variance is zero, and the larger the variance within the individual errors, the larger the difference between the MAE and RMSE (Willmott & Matsuura, 2005).

The significant wave height was shown to match with a MAE and RMSE of 0.09 and 0.11 metres respectively and is shown in top panel of Figure 5.9. A MAE and RMSE of 0.04 and 0.05 seconds respectively were calculated between the modelled and wave buoy peak period. The largest differences between observed and predicted  $H_s$  occur between the 4<sup>th</sup> and 11<sup>th</sup> of February during which time there was no measured wave buoy data, and values were estimated through linear interpolation. All predicted peak period values matched almost exactly to the measured values.

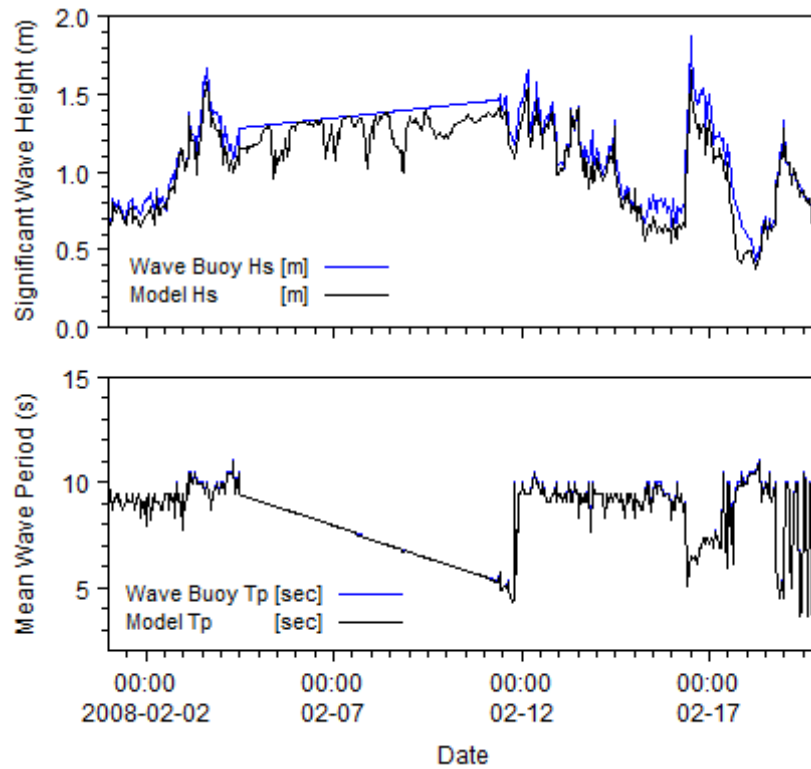


**Figure 5.9:** Modelled and observed significant wave height and average wave period at the location of the BOPRC wave buoy over 21 days in February 2008.

As the observed and predicted  $H_s$  and  $T_p$  values match closely this provides justification for using the wave buoy data as an open boundary condition, further offshore than the wave buoy is located. Although the predicted and observed data match closely this does not provide complete validation of the model. As the wave buoy is located in deep water (compared to the average wave height and wave length), waves propagating from the ocean boundary to the wave buoy have undergone very little transformation. Therefore Figure 5.9 and the error statistics calculated provide justification for using the wave buoy data as open boundary conditions, but do not validate wave transformation processes.

#### **5.6.4 Local Scale Spectral Wave Model**

A time series of significant wave height, peak period, mean wave direction and directional spreading index were extracted from the regional scale spectral wave model results and applied as a boundary condition to the local scale coupled model. The local scale spectral wave model was run with same parameters as described in Table 5.1, with the exception of the Water Level and Current Conditions which were included from the Hydrodynamic Model. This local scale model was coupled with the hydrodynamic and sediment transport models described in subsequent sections. It was this coupled, local scale model that was used to run the various simulations described in Section 5.8.

#### **5.6.5 Spectral Wave Model Limitations**

The main limitation of spectral wave modelling was the use of a constant, large standard deviation for the directional spreading angle. A constant value was used as the wave buoy did not contain the information required to calculate the directional spreading standard deviation. A large directional spreading standard deviation is usually associated with wind waves, and smaller directional spreading standard deviations with swell waves. The use of a constant standard deviation of  $23.28^\circ$  in all simulations assumes that all of the wave conditions represented wind generated waves, rather than swell waves. This causes a decrease in the driving forces of any swell waves, and as a consequence results in weaker longshore currents and less sediment transport (DHI volume 4, 2008). However, analysis by Macky *et al.* (1995) of wave steepness data from the Katikati wave buoy between 1991 and 1993 suggested many of the measured waves originated close to the wave buoy and thus indicates a predominance wind generated waves along the Bay of Plenty Coastline.

## 5.7 Hydrodynamic Modelling

The Mike 21 Hydrodynamic Model (HD) simulates changes in water level and flow conditions as a result of various forcing conditions such as tides, waves, wind and river or point source inflows. This is achieved through solving the depth integrated, incompressible, Reynolds averaged Navier-Stokes equations, also known as the 2-dimensional shallow water equations (DHI, 2011c).

The single largest limitation of the 2-dimensional models used is that stratification is neglected. 2-Dimensional hydrodynamic models simplify 3-dimensional environments by solving the depth-integrated incompressible Reynolds averaged Navier-Stokes equations (Papanicolaou, *et al.*, 2008; DHI, 2011c). However, river mouth environments, such as the Kaituna River mouth, represent areas of complex interaction between fresh riverine and saline marine waters. The different densities between the fresh and saline water can lead to hypopycnal outflows, where the freshwater discharges as a layer above the salty sea water (Wright, 1977). However, despite the assumption of negligible stratification and the application of a 2-dimensional hydrodynamic model the sediment transport model was shown to recreate measured bed levels accurately, especially inside the river, as described in Section 5.8.3.

### 5.7.1 HD Boundary Conditions and Model Parameters

The HD model was run using the local scale meshes described in Section 5.4. The upstream river boundary was forced by a time series of discharge values extracted from a node in the Mike 11 river flow model at the same location as the river boundary of the HD model. Wave driven currents from the Spectral Wave Model, in the form of  $S_{xx}$ ,  $S_{xy}$  and  $S_{yy}$  radiation stresses, were applied over the entire domain. Similarly wind data was forced over the entire domain. However, the wind was assumed to be spatially constant, changing only in time. The northern open boundary was forced by the Moturiki water level data, and varied in time, but was constant along the length of the boundary.

**Table 5.2:** Parameters used for the Mike 21 Hydrodynamic model.

<b>Parameter</b>	<b>Value</b>
<b>Flood and Dry</b>	
Drying depth	0.005 m
Flooding depth	0.05 m
Wetting depth	0.1 m
<b>Density</b>	Barotropic
<b>Eddy Viscosity</b>	
Type	Smagorinsky Formulation
Format	Constant
Value	0.28
<b>Bed Resistance</b>	
Type	Manning Number
Format	Constant
Value	26 m <sup>(1/3)</sup> /s
<b>Coriolis Forcing</b>	Varying in domain
<b>Wind Forcing</b>	
Type	Constant
Wind Friction Factor	0.001255
<b>Wave Radiation</b>	
Type	From SW simulation

### 5.7.2 Hydrodynamic Model Calibration

In order to calibrate the current velocities produced by the model, an ADCP survey was conducted over the majority of a tidal cycle (Section 4.7). Vector plots of each ADCP transect were then created using Matlab's built in Quiver command. The top 0.5 m of vectors (-1.03 – -1.53 m below MSL) were plotted separately from the readings below -1.53 m in order to determine whether there were different current vectors for the fresh surface water and the saline bottom waters. Quiver plots of every reading along each transect were highly variable, possibly due to turbulence over the ebb tidal delta associated with the combination of wave action and tidal currents, so it was decided to use the mean of every six points along each transect. A subset of these averaged transects is shown in Figure 5.10 and compared against the current vectors produced by the Hydrodynamic model over the same time period.

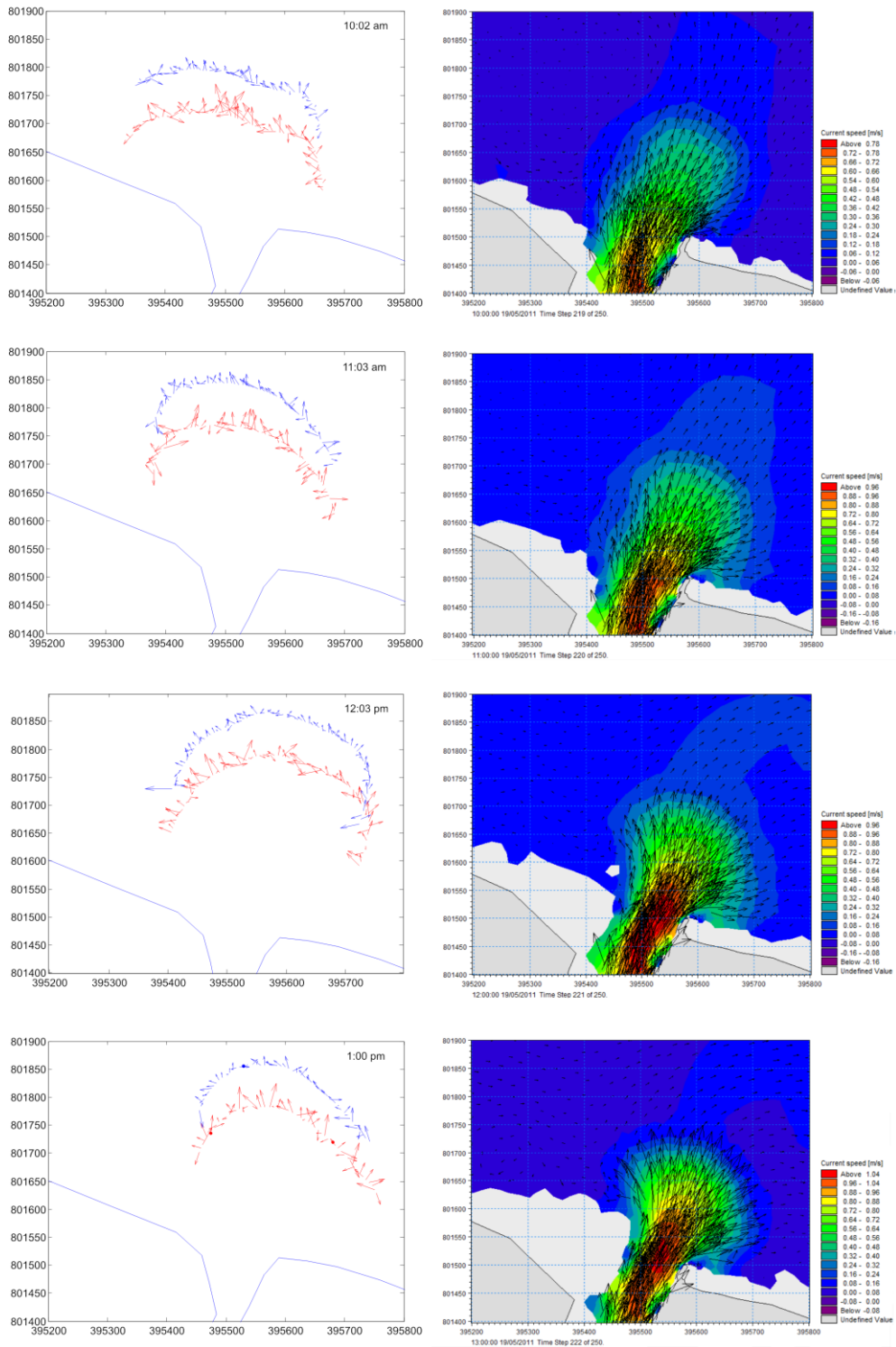


**Figure 5.10:** A subset of the vector diagrams from the ADCP transects, compared to the current vectors predicted by the Hydrodynamic model. The red vector arrows represent the - 1.53 m and deeper currents, while the blue vectors represent the currents between - 1.03 – -1.53 m depth. The blue vectors are offset in the North direction from the red vector arrows for easier viewing. A full comparison of all the ADCP transects measured is shown in Appendix 2 (Note: vector arrow lengths are not to the same scale between the ADCP and modelled vectors).

Originally it was planned to extract the  $u$  and  $v$  velocities from a model simulation over the same time period as the ADCP data collection. Statistics such as the MAE and RMS could then be calculated to provide a quantitative indication of how well the model predicted current vectors compared to the measured current vectors. However, this was unsuccessful due to the highly variable nature of the  $u$  and  $v$  velocities in the ADCP data. Instead the quiver plots were used to provide a visual qualitative justification for the modelled current directions.

It appears from the modelled current vectors shown in Figure 5.10 and Appendix 2, that the river discharge currents decelerate fairly rapidly outside of the river mouth, just prior to the location where the ADCP transects were collected. Therefore a possible explanation for the highly variable ADCP data, especially in the transects taken during the incoming tide, is due to the fact that the transects were taken outside the area of river discharge dominance. Thus the variable ADCP data represents the complex interaction of tides, waves and any remaining river discharge currents which had not yet completely decelerated into the ambient water. However, the water depth was insufficient to run transects at any significant distance closer to the river mouth as it would become too hazardous, particularly around low tide.

### 5.7.3 Bed Resistance Values

Due to the highly variable nature of the ADCP data collected the hydrodynamic model could not be calibrated or validated to a quantifiable number. This caused difficulty and uncertainty in choosing the appropriate bed resistance value for the hydrodynamic model.

Mehta & Joshi (1988) note that a major complication with determining bed resistance values for tidally influenced inlets is that the flow depth and bedforms present such as ripples, dunes, or a flat bed can change within a tidal cycle. However, it was concluded for many engineering purposes a tide-averaged bed resistance is usually acceptable.

The DHI (2011c) Mike 21 Flow Model FM – Hydrodynamic User Guide states that Manning numbers of 20 - 40 m<sup>1/3</sup>/s are common, and a value of 32 m<sup>1/3</sup>/s is recommended if no other information is available. This corresponds well with the work of Mehta & Joshi (1988) who stated Manning's  $n$ , which is the reciprocal of the Manning Number, can be estimated by the empirical relationship of:

$$n = \frac{h_c^{1/6}}{\alpha_2 + \alpha_3 \log A_c} \quad \text{Equation: 5.3}$$

where  $h_c$  is the throat depth,  $\alpha_2$ ,  $\alpha_3$  are coefficients of 30 and 5 respectively and  $A_c$  is equal to the throat cross-sectional area. Based on a cross-sectional area of 97 m<sup>2</sup> and a throat depth of 3.5 m from the bathymetric survey conducted for this project, a Manning's  $n$  of 0.031 is predicted using Equation 5.3. This is the equivalent of a Manning's Number of 32.5 m<sup>1/3</sup>/s.

The model was entirely calibrated on the results of the Sediment Transport model as further explained Sections 5.8.2 and 5.8.3. Several simulations were run using various bed resistance values, wave breaking parameters, slightly different grain sizes and it was found that a Manning's Number of 27 m<sup>1/3</sup>/s and the sediment properties calculated in Section 6.2 produced the most accurate results, and thus was used for all of the various simulations. Although a Manning's Number of 27 m<sup>1/3</sup>/s is smaller (increased bed resistance) than the 32 m<sup>1/3</sup>/s recommended in the DHI user manual, and predicted by the equation of Mehta & Joshi (1988) it

matches the values used for the offshore region of the Mike 11 model developed by the BOPRC (Figure 7.11).



**Figure 5.11:** Map showing the Manning Numbers from BOPRC's Mike 11 Kaituna River flow model.

## 5.8 Sediment Transport Modelling

The DHI Mike 21 Non-cohesive Sediment Transport (ST) model was used to predict the sediment transport associated with the currents predicted by the Spectral Wave and Hydrodynamic models. The ST model simulates the erosion, transport and deposition of non-cohesive sediments under the effect of currents and waves (DHI, 2011d). It was dynamically linked to the HD and SW model, and any bed level changes were reflected in the successive time step of the HD and SW model.

### 5.8.1 Model Parameters & Forcing

Simulating sedimentation around the Te Tumu Cut was the main objective for the sediment transport modelling. Therefore, the model was set up with sediment properties representative of the river mouth. The ST model has the ability to use spatially varying sediment characteristics; however, this would have required extensive sediment sampling in order to accurately map the entire model domain. Instead uniform sediment characteristics have been used throughout the model.

A mean grain size ( $d_{50}$ ) and geometrical spreading ( $((d_{84}/d_{16})^{1/2})$ ) of 0.493 mm and 1.64 respectively (Section 6.2) were used as the representative sediment characteristics. As no information was available on the relative sediment density and porosity, typical values for quartz and feldspar rich sediments of 2650 kg/m<sup>3</sup> and 40% were assumed.

Sediment transport rates under the combined effect of waves and currents in the ST model are found through linear interpolation of Quasi 3D (Q3D) Sediment Transport Tables. These Q3D Sediment Transport Tables were created using the DHI STP Q3D application. The STP Q3D application is a detailed infra-wave sediment transport programme, which uses a Q3D description of the hydrodynamic and sediment transport conditions to determine sediment transport rates under a range of predefined conditions (DHI, 2011e). The settings used for the generation of the Q3D Sediment Transport Tables, used for all sediment transport modelling in this thesis are outlined in Appendix 3. The parameters used in the ST model itself are given in Table 5.3.

**Table 5.3:** Parameters used in the Mike 21 Sediment Transport model.

<b>Parameters</b>	<b>Value</b>
<b>Model Definition</b>	
Model Type	Wave and Current
<b>Time Parameters</b>	
Start Time	5
Time Step Factor	1
<b>Sediment Properties</b>	
Format	Constant
Porosity	0.4
Grain Diameter	0.493 mm
Grading Coefficient	1.65
<b>Forcings</b>	
Waves	Wave field from SW simulation
<b>Morphology</b>	
<b>Model definition</b>	
Max Bed Level Change	2 m/day
Speed Up Factor	1
<b>Time Parameter</b>	
Start Time Step	0
<b>Bank Erosion</b>	
Type	Slope Failure
Format	Constant
Value	30°

### 5.8.2 Sediment Transport Model Calibration

A critical requirement of the Sediment Transport Model was for it to be able to successfully recreate the bathymetry in and around the Te Tumu Cut. In order to ensure that the Sediment Transport Model was able to produce realistic and reliable results the model needed to be calibrated. This was achieved by comparing model results from a two week simulation over the same time period during which a previous bathymetry survey was conducted. Bathymetry data inside the river mouth and over the delta was collected by Discovery Marine Limited for the Bay of Plenty Regional Council on the 18<sup>th</sup> and 19<sup>th</sup> of February 2008.

To assign a numerical value to the accuracy of the model, a simulation was run from the 5<sup>th</sup> of February to the 20<sup>th</sup>. Five transects were extracted from the model results on the 19<sup>th</sup> of February and compared to transects of the same positions from the Discovery Marine Limited survey. The location of the five transects are shown in Figure 5.12.

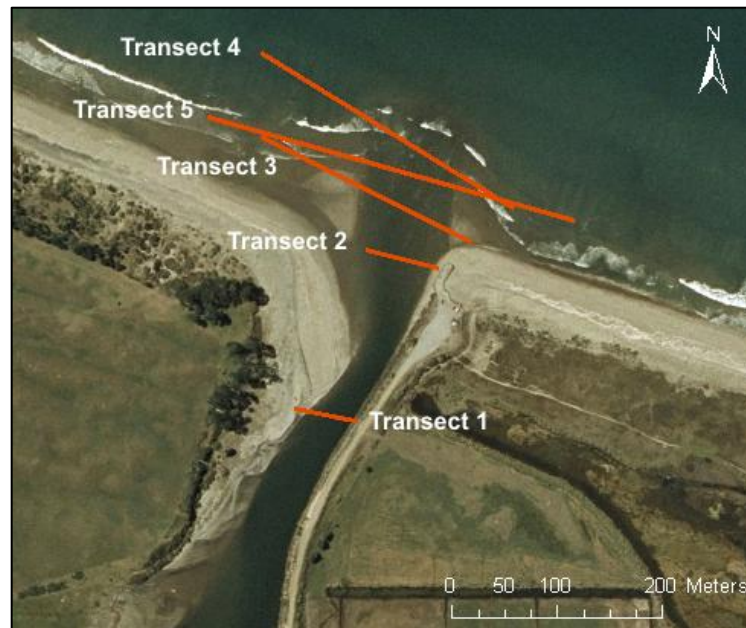


**Figure 5.12:** Location of the 5 transects used to compare the Sediment Transport Model results against the 2008 DML survey. The transects are of varying lengths and angles to the shoreline in order to obtain the largest transects possible from the 2008 Discovery Marine Limited survey.

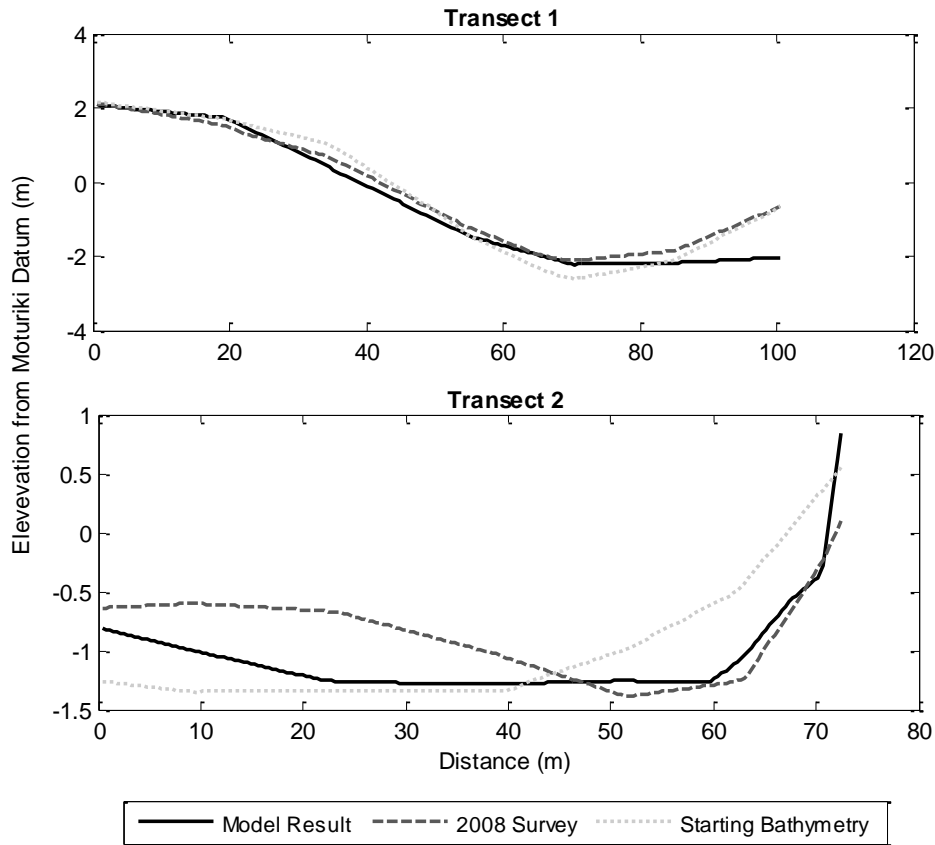


**Figure 5.13:** Transects within the Kaituna River comparing the Sediment Transport Model results against the 2008 DML survey.

Transects 1 and 2 were taken across the main river channel. Both transects showed an accurate recreation of the bed levels within the channel, which in both transects occurred on the eastern side of the river, along the edge of the rock causeway.

Transects 3, 4 and 5 were taken from outside the river mouth, over the ebb delta. Transect 3 shows the movement off the channel through the delta is successfully recreated, with the model showing the channel has moved to the east compared to the starting bathymetry. However, the model predicted a slightly narrower and shallower channel within this transect. Transect 4 was not recreated very accurately, with a difference of slightly over 1 m between the modelled bed level, and the 2008 DML survey on the western part of the transect. The model recreated the shape of transect 5 over the western half almost completely accurately, however, it predicted a higher bed level than the survey over the eastern half, indicating excess deposition in this area.

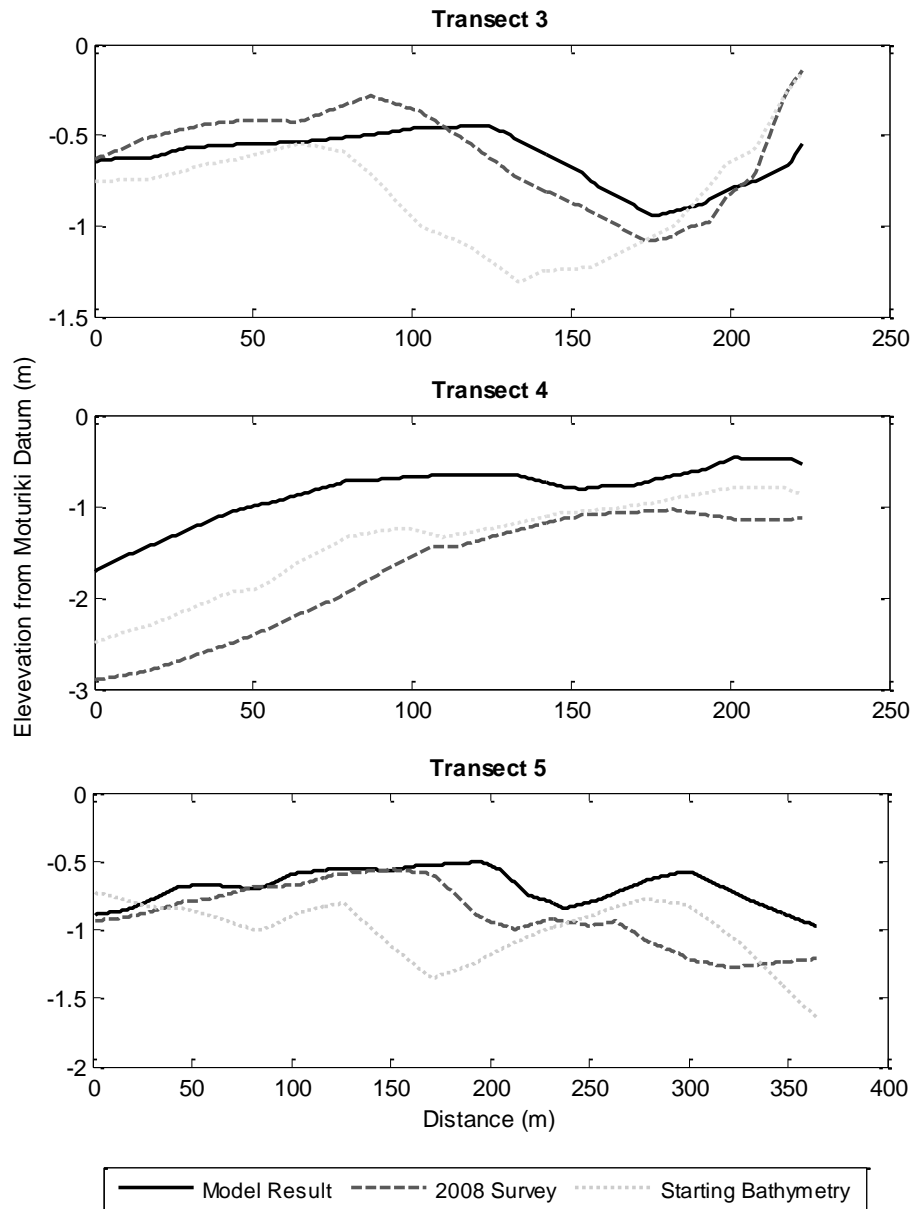


**Figure 5.14:** Transects outside the Kaituna River over the ebb delta comparing the Sediment Transport Model results against the 2008 DML survey.

Table 5.4 shows the MAE and RMSE calculated for each transect and the average MAE and RMSE of all five transects. In general the model tends to over predict the bed level outside the river mouth over the delta, but matches fairly accurately within the river mouth.

**Table 5.4:** Error statistics comparing the bed level from the model results against the 2008 survey along the five transects shown in Figure 5.10.

<b>Transect</b>	<b>Mean Absolute Error (MAE) (m)</b>	<b>Root Mean Square Error (RMSE) (m)</b>
<b>1</b>	0.27	0.40
<b>2</b>	0.28	0.34
<b>3</b>	0.14	0.16
<b>4</b>	0.87	0.96
<b>5</b>	0.21	0.28
<b>Average</b>	<b>0.35</b>	<b>0.43</b>

### 5.8.3 Sediment Transport Model Limitations

As the hydrodynamic model could not be calibrated against the ADCP measurements, and there was no shallow water wave buoy to compare wave conditions against, the coupled spectral wave, hydrodynamic and sediment transport model was entirely calibrated through the sediment transport model. This meant that any errors within the spectral wave and hydrodynamic model were accounted for and included in the calibration error of the sediment transport model in Section 5.8.2.

The Mike 21 FM Sediment Transport Model does not include sediment inflow boundaries under the combined effects of waves and currents. However, sediment inflows can be included when the effect of waves are not taken into account. Therefore one possible cause of error within the sediment transport modelling stems from the fact that sediment inflows from Kaituna River were excluded. It was assumed that the effects of wave driven sediment transport were more important than sediment inflows from the Kaituna River itself. It was thought the majority of suspended sediment from the Kaituna River would be lost as washload out to sea. This was based on the personal communication with Ben Tuckey (2011) and results from Kirk (1991) on various South Island rivers.

Suspended sediment yields also generally follow a power function in the form of  $L = aS^b$ , where (L) is equal to the suspended sediment load, (S) is equal to the streamflow and (a) and (b) being rating curve parameters (Crawford, 1991). This means that a significant proportion of the suspended sediment discharging out of the Kaituna River would likely occur during high flows, which were not looked at during this thesis.

It must also be noted, that there is uncertainty involved with the use of any numerical model. Studies have shown large differences can occur between modelled results for identical forcing conditions between various 2D modelling packages (de Vriend *et al.*, 1993). This was largely attributed to the different sediment transport formulas used (Nicholson, *et al.*, 1997). However, despite this, the coupled morphological model developed for this project was shown to sufficiently recreate the bed levels in response to the natural forcing conditions of the calibration period, especially inside the river mouth.

## 5.9 Modelled Scenarios

Five different re-diversion scenarios were assessed. They were all forced by the same tidal curve (Figure 5.15), which was the tidal curve observed during the sediment transport modelling calibration period. This tidal curve was used for all simulations as it represents a natural spring – neap cycle. Simulations of various river flow and wave conditions were run for each scenario.

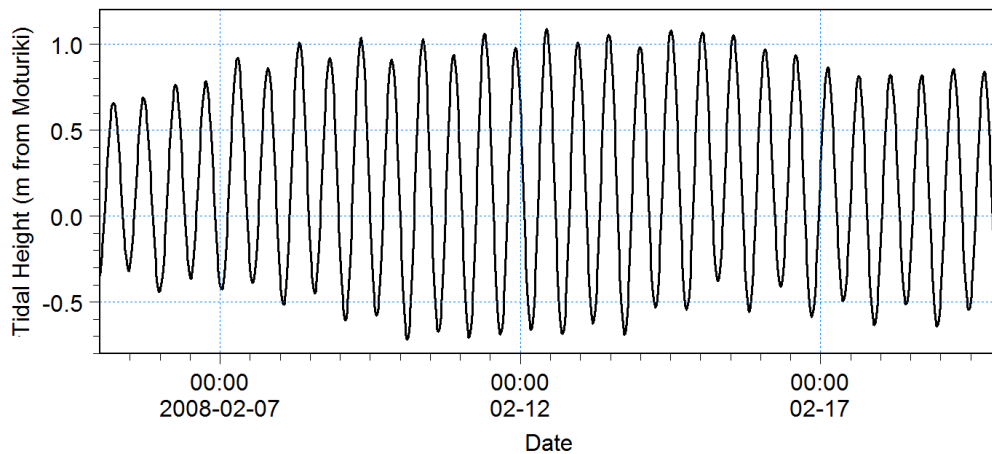


**Figure 5.15:** Tidal elevations recorded at the Moturiki tide gauge during the calibration period. This tide curve was also used for all of the other simulations.

The five scenarios and how they were set up are explained in the bullet points below. Following this, the subsections outline the simulations run representing the various combinations of river and wave conditions each scenario was run with.

- **Status Quo**

For the Status quo – or normal scenario, the bathymetry obtained from the February 2011 survey conducted for this project, and resulting mesh file created were used. The upstream river boundary was forced by the results of the Mike 11 Kaituna River model which was set up to simulate the river’s present configuration.

- **Option J**

Simulations representing the Kaituna River / Maketū Estuary re-diversion Option J (lowering Ford's Cut culverts to -1.6 RL) were also run using the mesh file created from the 2011 bathymetry data. As Ford's Cut is upstream of the river boundary of the Mike 21 model, the Ford's Cut culverts were lowered in the Mike 11 model. The Mike 11 model was then rerun and a time series of discharge values were extracted from a node at the location of the Mike 21 boundary.

- **Option J with twin jetty structures**

The same setup as described above for Option J was used with the addition of twin jetty structures extending out through the surfzone. Two trials were run, the first with the jetties spaced 45 m apart and a second run with jetties spaced 35 m apart. In both cases the jetties extended out to sea a distance of 200 m from the shoreline at a direction of 15° from North, along the rivers natural outflow axis. The eastern sub-tidal riverbank that has accumulated along the side of wharf / training wall structure at the river mouth was also removed, editing the bed levels to match the surrounding riverbed levels.

- **Option N with and without flap gated culverts**

For the Kaituna River / Maketū Estuary re-diversion Option N, unlike the re-diversion Option J, the river configuration is changed downstream of the Mike 21 Model Boundary. Therefore, the mesh that included Maketū Estuary and the re-opened Papahikahawai Channel (Figure 5.6) was used. The upstream river boundary was forced by the same Mike 11 discharge results as the status quo option.

Simulations were run with and without the addition of one way flap gates, which allowed water to flow from the Kaituna River into Maketū Estuary, but not in the opposite direction. For simulations where the flap gate culverts were enabled they were added in as one-way culverts in the Mike 21 HD module. The dimensions used for the culverts were based on a report by Wallace *et al.* (2008), which stated

that Papahikahawai Channel would be reopened to 30 m wide in the upstream portion, with twin 10 m wide culverts with an invert level of -1 m RL.

### **5.9.1 Calibration Time**

The first simulation run was over the same time period during which the Sediment Transport model was calibrated (05/02/2008 – 20/02/2008). This time period was chosen as it was a time of typical summer time conditions with an average  $H_s$  and  $T_p$  of 1.15 m and 7.9 s respectively over the two week period and an average flow of 27 m<sup>3</sup>/s at Te Matai. Individual simulations were run using these conditions for each of the scenarios outlined above.

### **5.9.2 Average Wave & River Flow Conditions**

These simulations were run using constant, long term average conditions over a two week period. The average wave conditions simulated were a  $H_s$  and  $T_p$  of 0.8 m and 10 s respectively propagating 20° from North (Section 1.3.4) with a directional spreading standard deviation of 23.28°.

The river boundary was forced from the results of a Mike 11 river flow simulation of average conditions. These were a constant discharge of 39.5 m<sup>3</sup>/s at Te Matai and 1.8 m<sup>3</sup>/s for the Raparapahoe stream. The smaller tributaries were also included and scaled based on the assumptions outlined in Section 5.3.1.

### **5.9.3 7-Day Annual Low Flow & Average Wave Conditions**

These simulations were run using constant, long term average wave conditions over a two week period. The average wave conditions simulated were a  $H_s$  and  $T_p$  of 0.8 m and 10 s respectively propagating 20° from North (Section 1.3.4) with a directional spreading standard deviation of 23.28°.

The river boundary conditions were forced from the results of a Mike 11 river flow simulation that was run using 7 day Annual low flow conditions. These were 28.95 m<sup>3</sup>/s at Te Matai and 0.67 m<sup>3</sup>/s for the Raparapahoe stream, based on values taken from the EBoP (2007) Meteorological Summary Report.

#### **5.9.4 2 x Average Height & Average River Flow Conditions**

These simulations were run using a constant significant wave height twice that of the long term average significant wave height, over a 2 week period. The average wave conditions simulated were a H<sub>s</sub> and T<sub>p</sub> of 1.6 m and 10 s respectively propagating 20° from North (Section 1.3.4) with a directional spreading standard deviation of 23.28°.

The river boundary was forced from the results of a Mike 11 river flow simulation of average conditions. These were a constant discharge of 39.5 m<sup>3</sup>/s at Te Matai and 1.8 m<sup>3</sup>/s for the Raparapahoe stream. The smaller tributaries were also included and scaled based on the assumptions outlined in Section 5.3.1

## **5.10 Summary**

This chapter described the creation and setup of three flexible meshes and the creation and calibration of a coupled spectral wave, hydrodynamic and sediment transport model. Comparing simulated bed levels from a two week model run in 2008, to a bathymetry survey which was conducted during the same time period showed the sediment transport model successfully recreated the bed level with a mean absolute error of 0.35 m. Bed levels within the river channel were recreated almost exactly, however, bed levels over the delta were in general, over predicted. Following this, the various model scenarios (the different re-diversion options) and simulations (the different forcing conditions) to be investigated were described, the results of which are presented in the subsequent chapter.

# Chapter 6

## *Results*

---

### **6.1 Introduction**

This chapter presents the results obtained throughout this project. Firstly the results of the sediment sample analysis are described and then the results of the morphology modelling are presented. The results of the different modelled scenarios are described as comparisons to the bed levels predicted by the model for the Kaituna River mouth's present configuration, which is referred to as the Status Quo scenario.

### **6.2 Sediment Sample Analysis**

The sediment samples collected, ranged in mean grain size from 0.32 mm to 0.76 mm; with all samples exhibiting similar geometrical spreading values of approximately 1.65 (Figure 6.1; Table 6.1). Sample 4 contained significant amounts of irregular shaped particles. Therefore, it had to be passed through a 1.4 mm sieve before it was run through the Laser Sizer, in order to avoid potential blockage. Despite this, Sample 4 was still shown to be significantly coarser than the other samples. According to the Wentworth scale, Samples 2, 3 and 5 are classified as medium sands while Samples 1 and 4 are coarse sands. The full Laser Sizer results sheets for each sample are presented in Appendix 1.

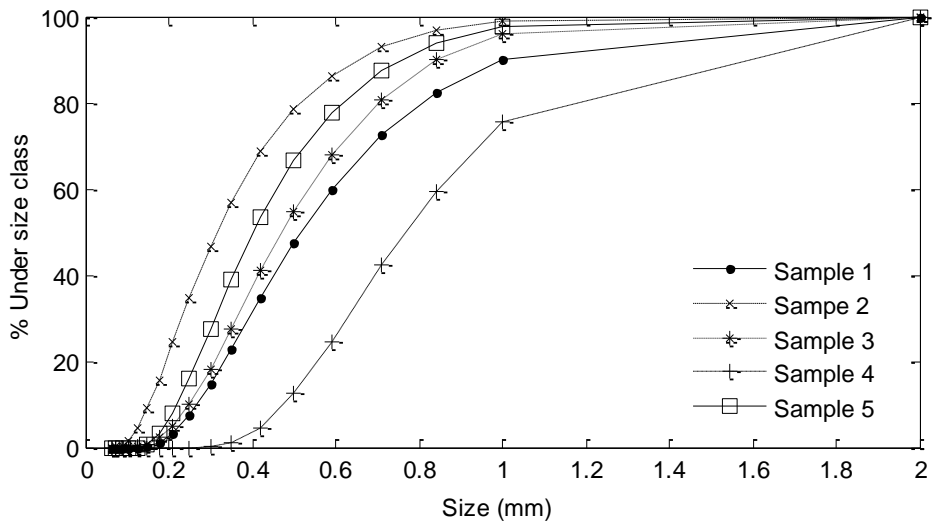


**Figure 6.1:** Particle size distributions for the five sediment samples collected.

**Table 6.1:** Sediment sample statistics, where  $d_{50}$  = mean grain size and  $((d_{16}/d_{84})^{1/2})$  = geometrical spreading.

Sample #	$d_{50}$ (mm)	Geometrical Spreading
1	0.53	1.70
2	0.32	1.76
3	0.46	1.62
4	0.76	1.60
5	0.40	1.56
<b>Average</b>	0.49	1.65

The Mike 21 Sediment Transport model can solve simulations with spatially varying sediment properties. However, creating a sufficiently detailed sediment map of the Te Tumu area would require a vast amount of samples to be collected on, and offshore, which was beyond the scope of this thesis. Therefore, the mean grain size and geometrical spreading of the five samples was used as a constant value across the entire domain. It has also been noted in previous studies using the Mike 21 Sediment Transport model, that the use of varying sediment properties generally tends to confuse the interpretation of results (DHI, 2008 vol. 4).

## **6.3 Morphological Modelling Results**

The following subsections present the results of the various model simulations outlined in Section 5.8, with bed levels shown for each of the diversion scenarios after a two week simulation. Comparisons for each of the diversion options are then made in contrast to the Status Quo option, subjected to the same forcing conditions as the corresponding diversion options.

### **6.3.1 Calibration Time – Varying Conditions**

Comparing the Option J bed level map to the Status Quo bed levels (Figure 6.2), it can be seen that there is a change in bed level in a number of regions around the river mouth. The most prominent area of change is indicated by the (A) marker. Here the main channel is approximately 35 metres shorter than predicted in the Status Quo simulation. The channel is also slightly narrower at the location of marker (C) under Option J. The swash bar on the western side of the delta split into three smaller swash bars under Option J (B). Despite these changes over the delta, there was no significant change in bed level inside the river mouth.

Comparing the results of Option N – with flapgates included to the Status Quo scenario, there are two main areas of difference. The first is indicated by the Marker (A), and highlights the channel through the delta becoming longer, with the -1 and -1.25 metre contours surrounding the channels becoming 40 and 20 metres longer respectively. Marker (B) indicates the area inside the river mouth which became deeper by 0.25 metres.

When the flapgates were removed from Papahikahawai Channel, the predicted bed levels through the main channel of the Te Tumu Cut were very similar to the simulation with flapgates included. However, the -1 metre contour around the ebb channel (A) became 50 metres longer and the -1.5 metre contour extended 40 metres further seaward than in the Status Quo simulation. Similarly to the Option N – with flapgates simulation the bed level upstream of Papahikahawai Channel (B) became 0.25 metres deeper compared to the Status Quo simulation.

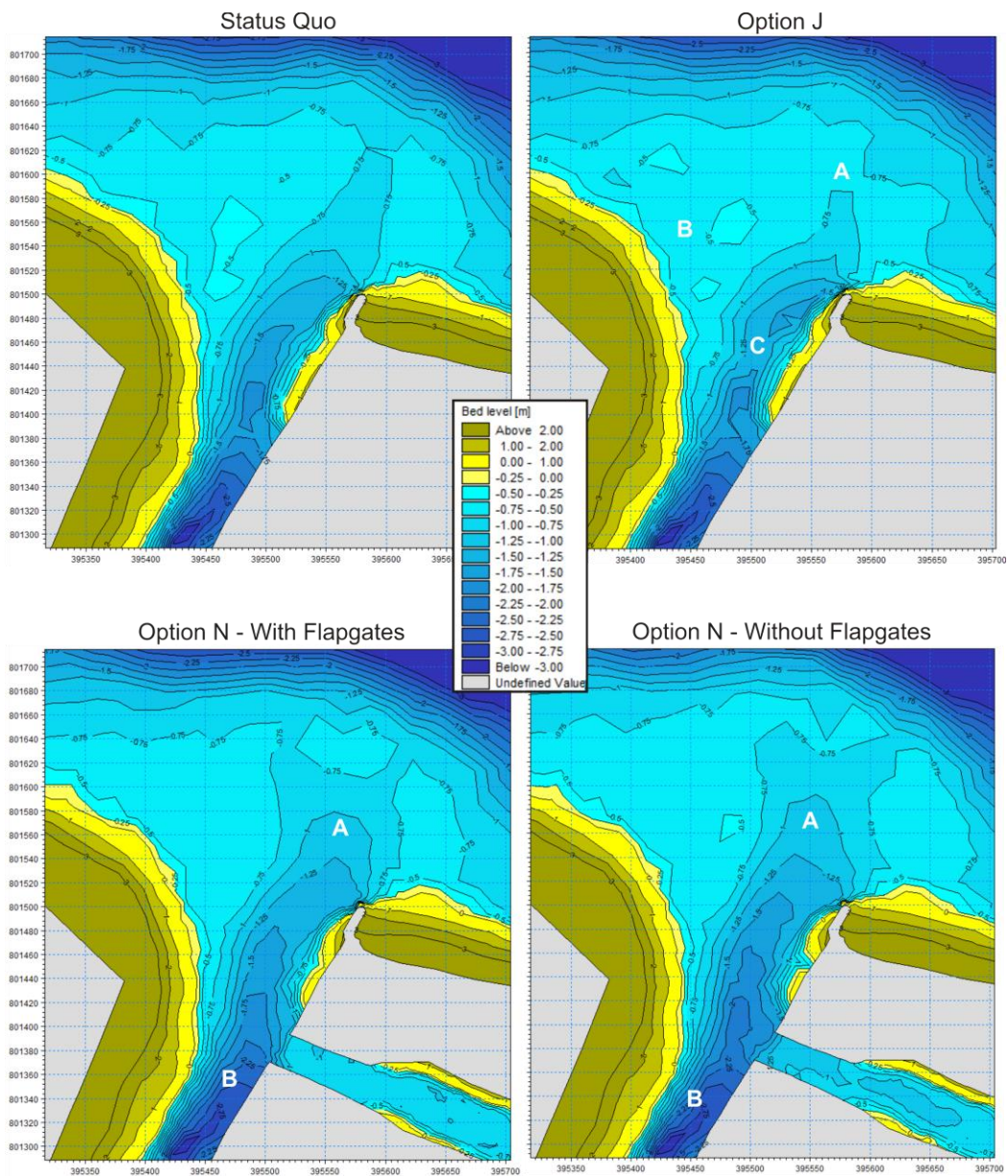


**Figure 6.2:** Predicted bed levels after a 14 day simulation run over the same time in which the sediment transport model was calibrated.

### 6.3.2 Constant Average Wave and River Flow Conditions

Figure 6.3 shows the predicted changes in bed level around the Kaituna River mouth for Option J, and Option N with and without one way flapgates installed, after a two week simulation forced by average waves and river flow conditions, as described in Section 5.8.2

Comparing the Option J bed level map to the Status Quo bed levels it can be seen that there is a change in bed level in a number of regions around the river mouth. The most prominent area of change is indicated by the (A) marker. Here the -0.75 m contour, indicating the main channel through the delta, extends approximately 45 metres further seaward. However, the -1 m and -1.25 m contours do not extend as far as the Status Quo option. A small scour depression is also present in the main channel, just below the (A) marker, which was not seen in the Status Quo simulation. Markers (B) and (C) highlight changes in the bed level within the swash platforms. Compared to the status Quo simulation the western swash platform containing marker (B) is slightly larger and shows the development of a small marginal flood channel which has cut through the -0.25 m contour, resulting in a small detached swash bar. Conversely the swash platform on the eastern side (C) became deeper. Marker (D) indicates a small area of increased deposition along the inner eastern river bank.

The main difference observed between the Status Quo simulation and Option N, with the addition of one way flapgates, is that the main channel extends further seaward through the ebb delta. This is indicated by marker (A), where the -1 metre contour extends 60 m further seaward compared to the status Quo Option. Bed levels upstream of Papahikahawai Channel have also become slightly deeper, with a maximum bed level change of -0.25 m. A marginal flood channel has also developed, with the -0.5 metre contour on the western side of the delta becoming detached from the shoreline and moving seaward.

When Papahikahawai Channel is opened without floodgates the main channel grew significantly. The -1 metre contour extended a further 40 metres seaward and became twice as wide. Similarly the -0.75 metre contour grew 20 metres in length and approximately doubled in width. The channel also became deeper

inside the river mouth as indicated at location (B), where the bed level became deeper by 0.25 metres.

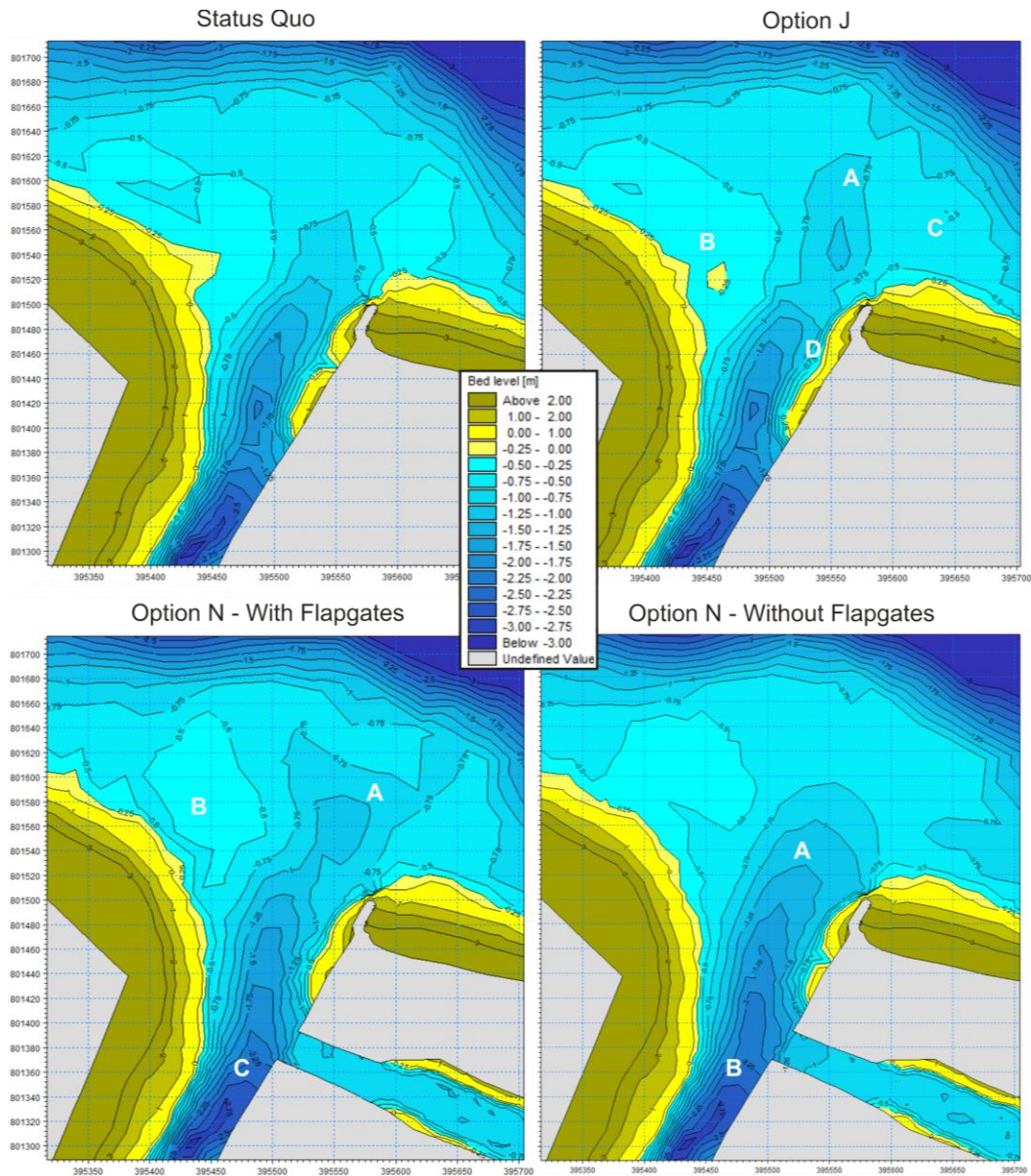


**Figure 6.3:** Predicted bed levels after a 14 day simulation of constant average river flow and wave conditions.

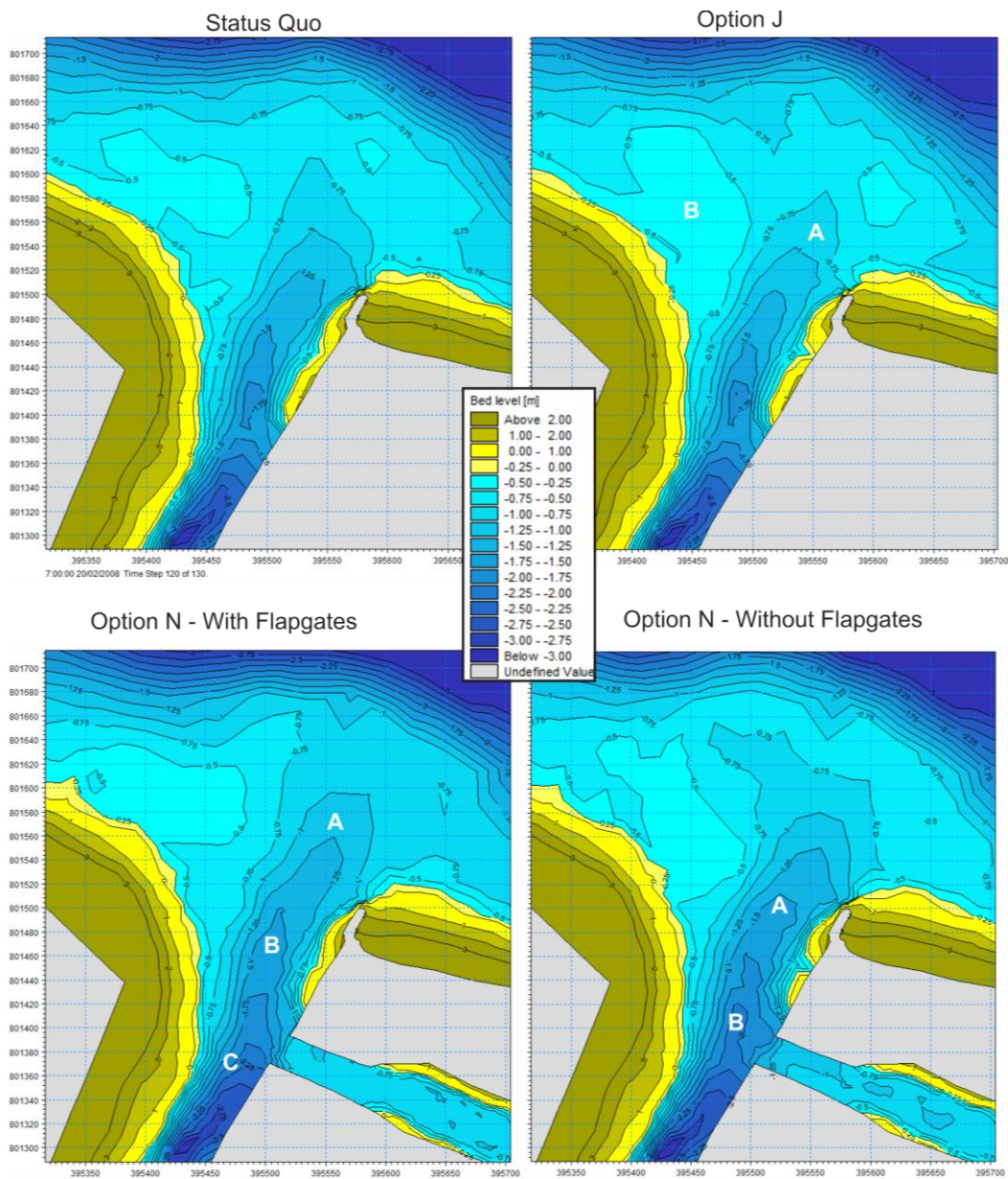
### **6.3.3 Constant Average Wave and Average Annual 7 Day Low River Flow Conditions**

Figure 6.4 shows the predicted changes in bed level around the Kaituna River mouth for Option J and Option N with, and without one way flapgates installed after a two week simulation forced by average waves and average annual 7 day low river flow conditions, as described in Section 5.8.2. Although these simulations were forced by seven day low flow river conditions, they were still run for a two week period. Therefore they can be thought of as an extreme case of prolonged low flow conditions.

Compared to the Status Quo option the bed levels predicted for the Option J scenario are fairly similar. The main difference is that the -0.75, -1 and -1.25 metre contours around the ebb channel (A) are 20 metres shorter and slightly narrower than the Status Quo simulation. The -0.5 m contour on the western swash platform is larger (B), and represents sediment deposition, creating a shallower swash platform.

The main difference observed between the Status Quo simulation and the Option N – with the addition of one way flapgates, is that the channel through the delta became longer and deeper. The -1.5, -1.25 and -1 metre contours surrounding the channel, extended approximately 40 metres further seaward (A & B). Bed levels upstream also became deeper, with a maximum decrease in bed level of 0.5 m indicated by marker (C).

Comparing Option N – without flapgates to the Status Quo simulation it can be seen that the -1.25 and -1 metre contours both extend 20 metres further seaward (A), and the -0.75 metre contour 40 metres further offshore, in addition to becoming a lot broader. The channel also became deeper inside the river mouth as indicated at location (B), where the bed level became deeper by approximately 0.5 m.



**Figure 6.4:** Predicted bed levels after a 14 day simulation of constant average annual 7 day low river flow and average wave conditions.

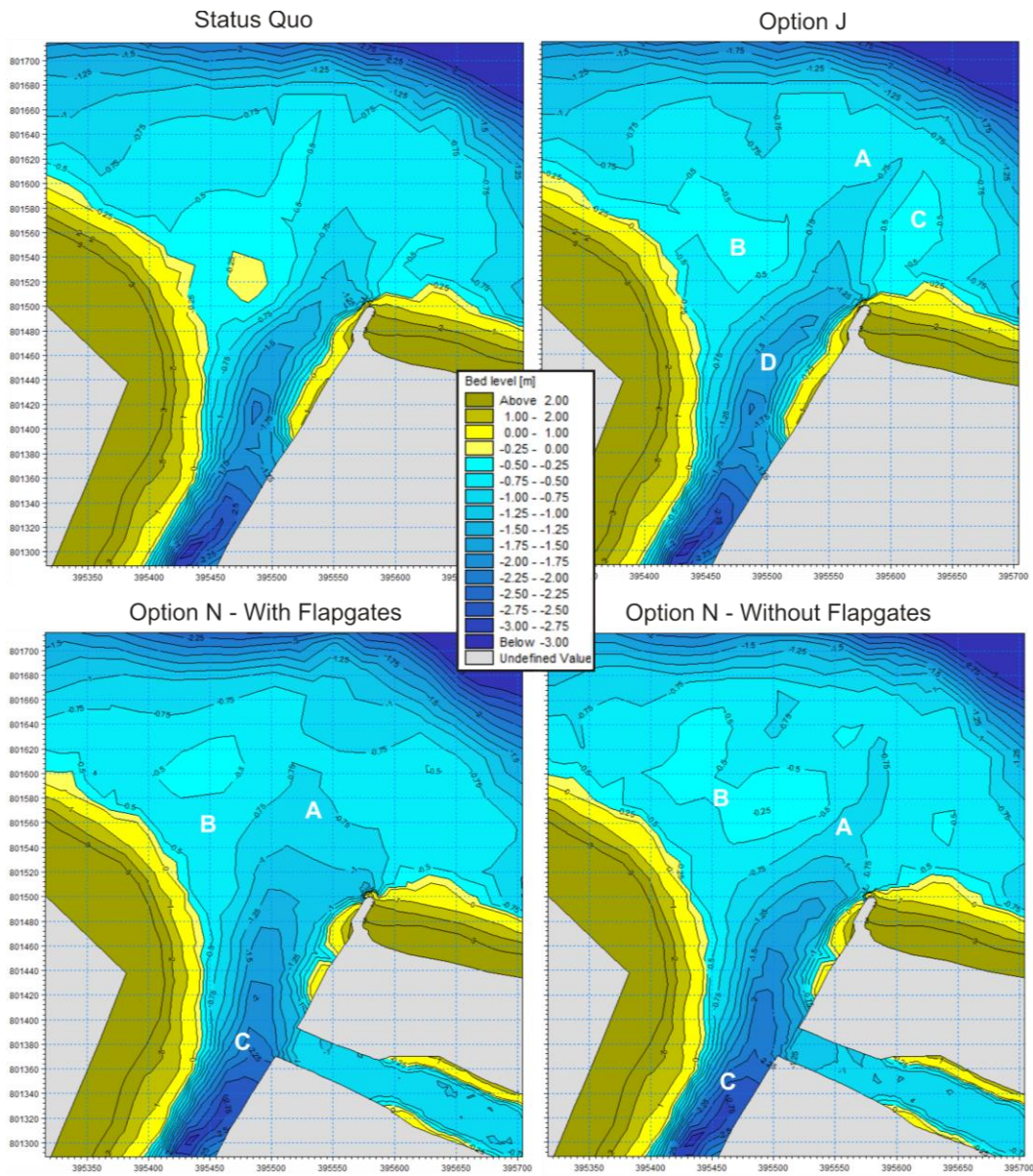
### **6.3.4 Constant 2x Times the Average Wave and Annual Average River Flow Conditions**

Figure 6.5 shows the predicted changes in bed level around the Kaituna River mouth for Option J and Option N with, and without one way flapgates installed after a two week simulation forced by average river flow, and twice the average significant wave height conditions.

Comparing the Option J bed level map to the Status Quo bed levels it can be seen that there is a change in bed level in a number of regions around the river mouth (Figure 6.4). The main area of change is indicated by the (A) marker. Here the -0.75 m contour, indicating the main channel through the delta, extends approximately 40 metres further seaward. The -1, -1.25 and -1.5 metre contours all extend slightly further out (< 20 m) as well. Markers (B) and (C) highlight changes in the bed level over the swash platforms. Compared to the status Quo simulation the western swash platform containing marker (B) decreased in size, indicating erosion in this area. Conversely the swash platform on the eastern side (C) has become larger, indicating deposition.

The main difference observed between the Status Quo simulation and the Option N, with the addition of one way flapgates, is that the main channel through the delta (A) became a lot larger. The -0.75 and -1 metre contours became significantly wider, more than doubling in width, and the -0.75 metre contour extended 30 metres further seaward. The sand mound on the western side of the delta (B) became detached from the shoreline and decreased in size, and indicates a deepening of the western marginal flood channel.

When the flapgates were removed from Papahikahawai Channel the main channel became slightly wider, with the -1 and -1.25 metre contours increasing in size. However, not to the extent seen in Option N – with the addition of flapgates. The accumulation of sand seen on the western swash platform of the Status Quo simulation was seen to move offshore (B) and likely indicates the formation, and increasing size of the marginal flood channel.



**Figure 6.5:** Predicted bed levels after a 14 day simulation of constant average river flow and 2x wave conditions.

### **6.3.5 Decreased River Flows Compared to Average Conditions**

In all four scenarios, the main channel through the river mouth and delta extended further seaward, and became slightly wider in the constant average 7 day low river flow simulations, compared to the average river flow conditions simulations. The largest increase in channel size occurred in the Option N – with flapgates scenario where the -1.25 and -1 metre contour lines surrounding the channel, extended 60 and 20 metres further seaward respectively, than seen in their respective average river flow simulations. Similar changes were also seen in the other three scenarios, however, at a lesser extent.

### **6.3.6 Increased Wave Heights Compared to Average Conditions**

Comparing the four modelled simulations of average river flow and wave conditions scenarios to their respective modelled simulations for the average river flow and 2x average wave height scenario, the effects of wave conditions can be analysed. In three of the four scenarios (Status Quo, Option N with, and Option N without flapgates) the channel through the river mouth became shorter and narrower, each to varying extents. The Option N – without flapgated culverts scenario showed the largest decrease in channel size with the -1 and -1.25 metre contours around the channel becoming much shorter and narrower, whereas the other two scenarios exhibited much smaller changes. Conversely, the Option J scenario showed an increase in channel length through the river mouth and into the delta under the 2x average wave conditions simulation.

### **6.3.7 Addition of Twin Training Walls**

Figure 6.6 shows the predicted bed levels when twin training wall structures spaced 35 and 45 metres apart are added to the Te Tumu Cut. The simulations were run for 14 days and subjected to average river flow and wave conditions. When the training walls were spaced 45 metres apart, the channel was seen to form along western wall until ~100 m from the seaward end, where the bed level then became relatively even. A 40 m long by 45 m wide ebb delta sediment deposit was also observed at the seaward end of the structures

Conversely, when the training walls were spaced 35 metres apart the bed level became uniform perpendicular to the training walls, indicating a uniform channel between the two walls. The 35 metre spaced training walls also resulted in a deeper bed level towards the seaward end, compared to the 45 metre spaced training walls. A narrower (35 m), but longer (50 m) ebb delta sediment deposit was seen to form at the seaward end of the twin training wall structures.

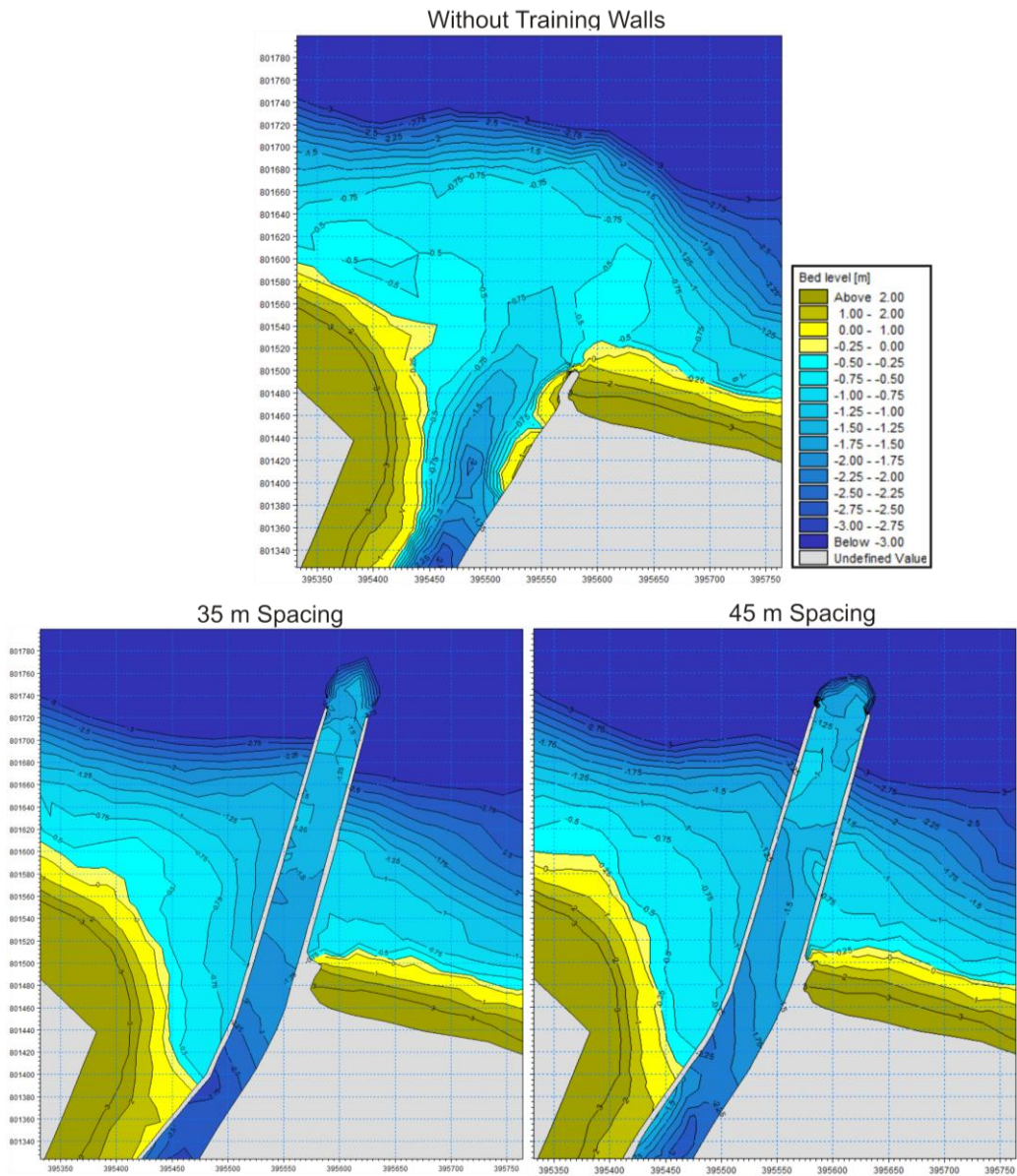


**Figure 6.6:** Predicted bed levels with the addition of twin training wall structures places 35 and 45 m apart. The simulations were run for 14 days and forced by average river flow and wave conditions as described in Section 5.8.



# Chapter 7

## *Discussion & Conclusion*

---

### **7.1 Introduction**

A morphological model of the Te Tumu Cut was developed to assess the effects of various potential re-diversion options for the Kaituna River in to Maketū Estuary. The change in bed levels were predicted as a result of the different diversion options under a range of conditions, the results of which are described in Chapter 6.

This chapter expands on the results chapter and explains why such results were observed, the validity of the results, and considerations for further developing the morphological model used. This is then concluded by a summary of the findings of this project and how they relate to the aims stated in Section 1.4.

## **7.2 Analysis of Model Results**

The following subsections provide further analysis on the results obtained in Chapter 6 and offers explanations as to why such results were observed.

### **7.2.1 Option J**

Comparing each of the simulations run for Option J to the corresponding simulations for the Status Quo – existing river / estuary configuration it is evident that in general the lowering of the culverts at Ford's Cut tends to cause increased sedimentation around, and within the Kaituna River mouth. This was shown in all four of the simulations looked at, when the channel is classified as everything deeper than the -1 metre contour surrounding the channel.

The increased sedimentation can be attributed to the increase in the flood tide volume of water entering the river. Figure 7.1 illustrates the differences in discharges at the Mike 21 model boundary (Figure 7.2) between the Status Quo and Option J scenarios, produced by the Mike 11 river flow model. There is no difference in peak ebb discharges. However, under all three river flow conditions (calibration time, mean annual flow and mean annual 7 day low flow conditions) the peak flood discharges increased (became more negative) by on average 10 m<sup>3</sup>/s under diversion Option J.

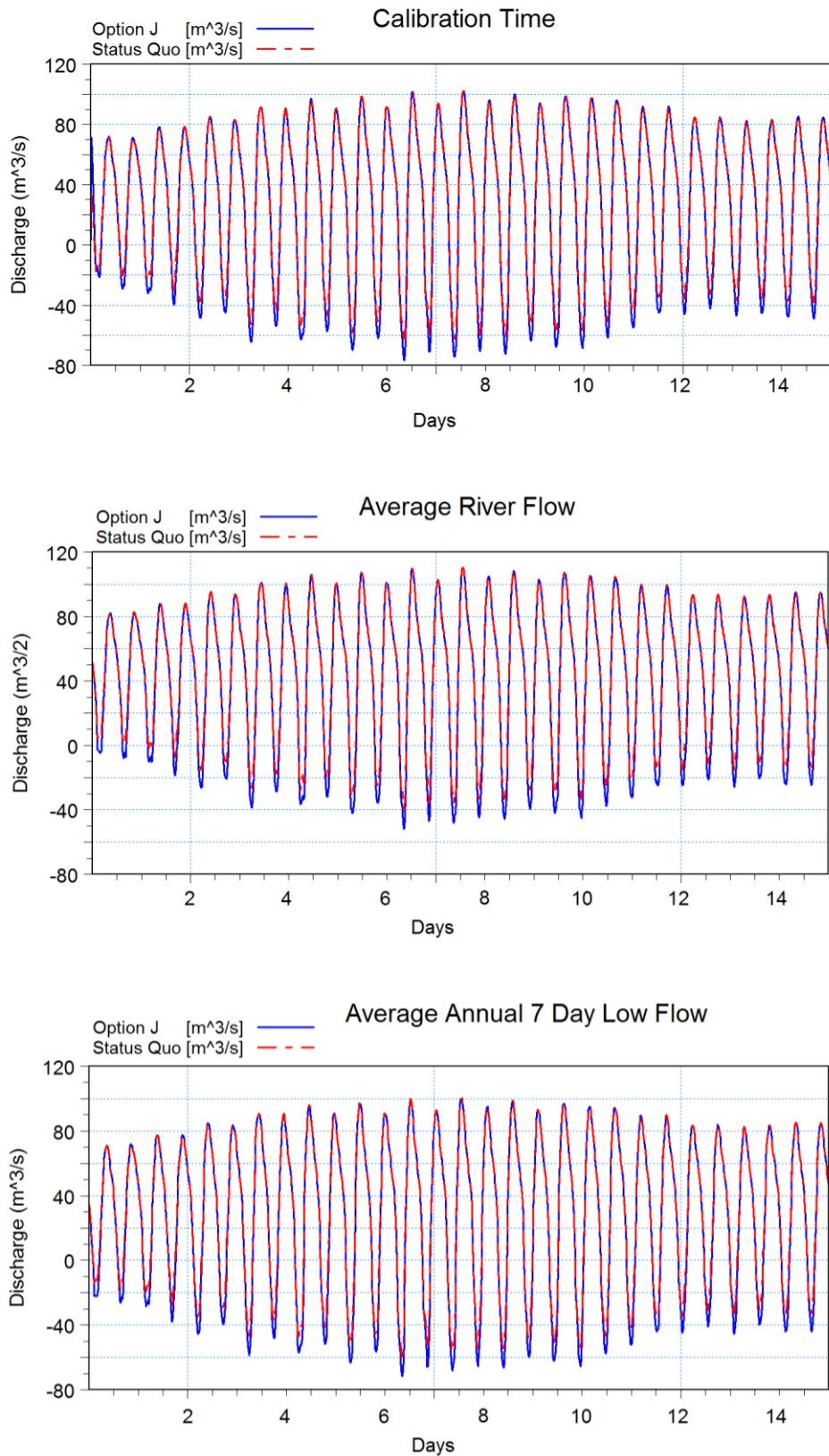


**Figure 7.1:** Discharge time series from the Mike 11 model used to force the upstream model boundaries of the coupled Mike 21 model for the Status Quo and Option J scenarios.



**Figure 7.2:** Map showing the two transects where discharge values were extracted from the model results for Option J and Option N.

The increase in flood discharge into the river under Option J is a result of the majority of increased flow into the estuary through Ford's Cut, occurring during the incoming tide (Figure 7.3). The tidal prism of a tidal basin is a function of the basins intertidal area (Heath, 1975). Therefore, lowering the invert level of the Ford's Cut culverts for Option J, effectively increases the intertidal area and thus the tidal prism on the incoming tide. However, as the culverts only allow water to flow from the river into the estuary and not back into the river, the ebb discharges through the river mouth remain the same as the present configuration.

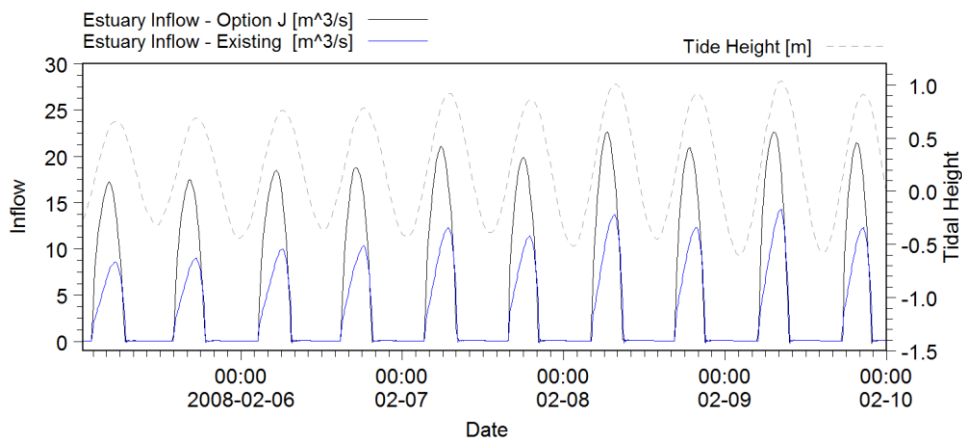


**Figure 7.3:** Plot showing the predicted increased discharge through Ford's Cut under the diversion Option J, compared to the existing inflows. Taken from the Mike 11 model with a constant annual average discharge of 39.5 m<sup>3</sup>/s.

Wright (1977) stated that tides have three basic effects on tidally influenced river mouths: (1) tidal mixing removes vertical density gradients, reducing the effects of buoyancy; (2) creates bidirectional sediment transport paths, with tides accounting for a greater fraction of sediment transport than the river for at least part of the year; and (3) creates a constantly varying land-sea boundary in both the vertical, and horizontal directions during the rise and fall of the tide.

Lowering the culverts at Ford's Cut increases the flood tidal volume and thus also the flood sediment transport carrying capacity within the river. This acts to alter equilibrium bidirectional sediment transport, causing increased flood sedimentation until a new equilibrium bed level is formed.

However, it is during the ebb tide, when river flow and tidal currents are acting in the same direction, when peak discharges and current velocities occur. Therefore it is the ebb flows which have the predominant influence on erosion and deposition within the throat of the river mouth. As the ebb flows remained unaltered by Option J there was no significant, large scale changes in bed level.

## 7.2.2 Option N – With Flapgated Culverts

On average, during the 14 day simulation, 220,000 m<sup>3</sup> of water per tidal cycle entered Maketū Estuary through the floodgates in Papahikahawai Channel. In addition to this, 139,000 m<sup>3</sup> entered the estuary through the Ford's Cut culverts (same as the Status Quo scenario). The change in discharges through the river mouth, downstream of Papahikahawai Channel, compared to the Status Quo scenario is shown in Figure 7.4. Similarly to Option J, although to a greater extent, there is an increase in the flood tidal prism through the river mouth, of approximately 10 – 30 m<sup>3</sup>/s. As expected there is no corresponding change in ebb flow volume.

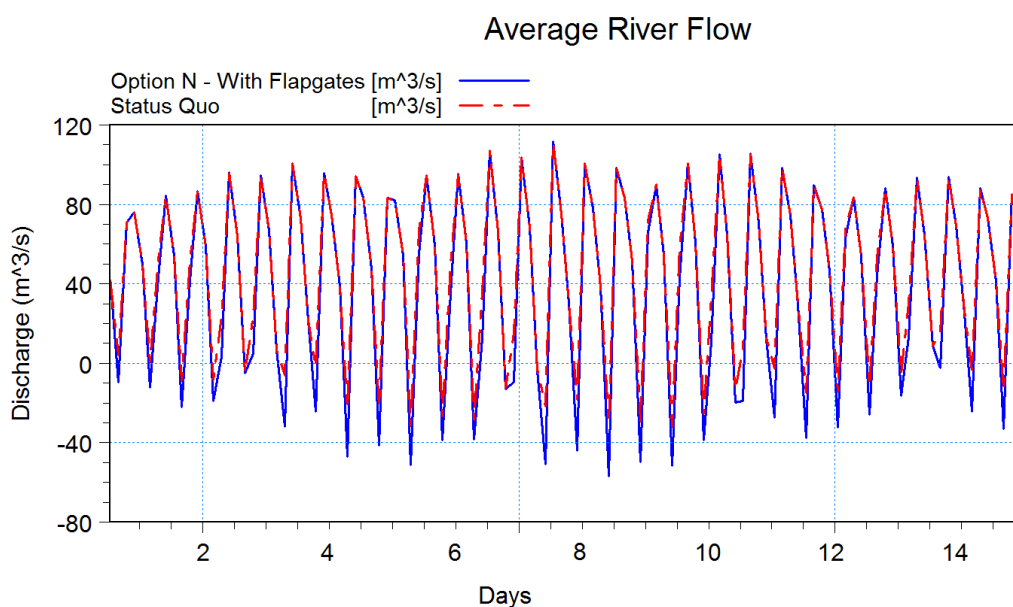


**Figure 7.4:** Comparison of discharge values taken from the average river flow and wave condition simulations for the Status Quo and the Option N - with flapgates scenarios. The discharge values were extracted from a transect downstream of Papahikahawai Channel (Figure 7.2).

Contrary to the results of Option J, where the increased peak flood tidal discharge, volume, and corresponding increase in sediment transport carrying capacity caused sedimentation within the channel, this was not seen for Option N – with flapgates. A possible explanation for this is that when mesh was edited to reopen Papahikahawai Channel, the bathymetry on the river side, immediately surrounding the opening, had to be edited to match the invert level of the culverts.

This simulated a dredging event, which would be required for the culverts to be installed. Therefore, this caused a loss of sediment from the river mouth system.

It was expected sediment from the surrounding coastline would enter the inlet and replace the “dredged sediment” fairly rapidly, returning the inlet back in to an equilibrium state, as rapid morphological readjustment of river entrances and tidal inlets is well documented (Kench & Parnell, 1991; Dahm & Kench, 2004). However, it is possible an equilibrium state had not been reached at the end of the 14 day simulation due to: the assumption of no river derived sediment inputs, as it was deemed insignificant, and low longshore sediment transport rates associated with a constant large directional spreading standard deviation for the waves (Section 7.3.3). A combination of these factors may have resulted in the unexpected increase ebb channel size.

### 7.2.3 Option N – Without Flapgated Culverts

When Option N was run without the flapgated culverts, both the peak flood tidal discharges and peak ebb flow discharges increased compared to the Status Quo scenario (Figure 7.5). However, in general the flood tidal discharges increased more than the ebb flows. This indicates that not all of the water entering Maketū Estuary through Papahikahawai Channel, exits the estuary back through Papahikahawai Channel. This extra volume of water must therefore discharge out through the Maketū Estuary inlet instead.

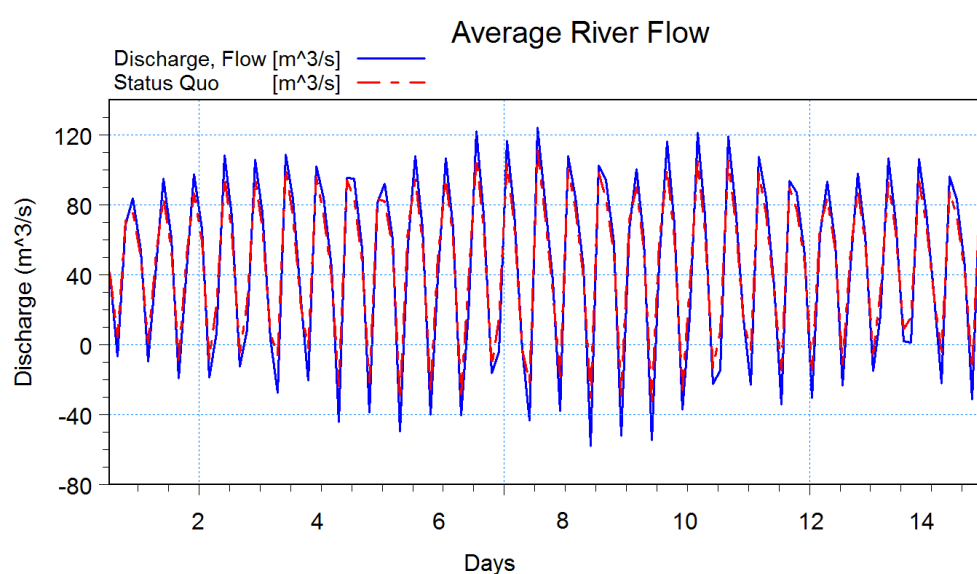


**Figure 7.5:** Comparison of discharge values taken from the average river flow and wave condition simulations for the Status Quo and the Option N - without flapgates scenarios. The discharge values are taken from a transect downstream of Papahikahawai Channel (Figure 7.2).

Similarly to the Option N – with flapgated culverts scenario, the increase in channel size could partially be attributed to a loss of sediment from the river mouth system when the bathymetry was edited to reopen Papahikahawai Channel. However, for this scenario, the channel became even longer than the scenario with flapgates. This extra increase in depth, and size, of the channel can be explained by the increase in peak ebb discharges and corresponding increase in current speeds that occur.

This corresponds with the inlet cross-sectional area – tidal prism relationship discussed in section Chapter 3.3.2, which describes the positive relationship between effective tidal prism, and inlet throat cross-sectional area. The change in cross-section area is shown in Figure 7.6. Although the deepest point in the cross-section became shallower by 0.2 metres under Option N – Without flapgates, the channel became much wider on the eastern side, leading to an increase in the cross-sectional area.

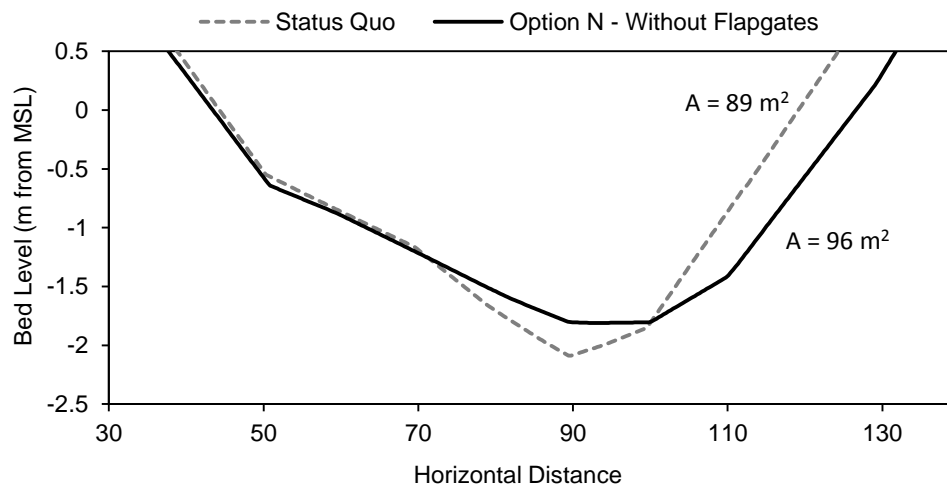


**Figure 7.6:** Inlet throat cross-section comparison between the Status Quo and Option N - Without Flapgates options for average river flow and wave conditions. The cross-section areas are calculated from the bed level to MSL (0 m) and were extracted from the last time-step in each of 14 day simulations.

#### 7.2.4 Decreased River Flow Conditions

In contrast to expectation, and similar situations reported in the literature, the ebb channel was seen to extend further through the delta and become slightly deeper under the constant average annual 7 day low flow river conditions, compared to the constant average discharge conditions. Figure 7.7 compares the discharge time series extracted from the Mike 11 river model, used to force the upstream boundary for the Status Quo and both Option N scenarios, between average conditions and average annual 7 day low flow conditions. Based on Figure 7.7 it was expected that the increased peak flood discharge values would cause an increase in the shoreward sediment transport carrying capacity, and the associated decrease in peak ebb flow values would lead to a decrease in the scour and offshore sediment transport capacity.

This hypothesis was also in line with the literature, with a similar model created by Siegle *et al.*, (2004), who also used the DHI, Mike 21 Sediment Transport module. They showed that for the Teign Inlet (Teignmouth, UK) increases in river discharge resulted in larger quantities of offshore directed sediment displacement. Thus the converse of their results indicates that decreases in river discharge should lead to a decrease in the offshore transport of sediment. However, this was not seen in any of the simulations run for this project, with each scenario resulting in an increase in ebb channel size through the delta, and no areas of decreased erosion within the inlet, which would indicate a decrease in offshore sediment transport.

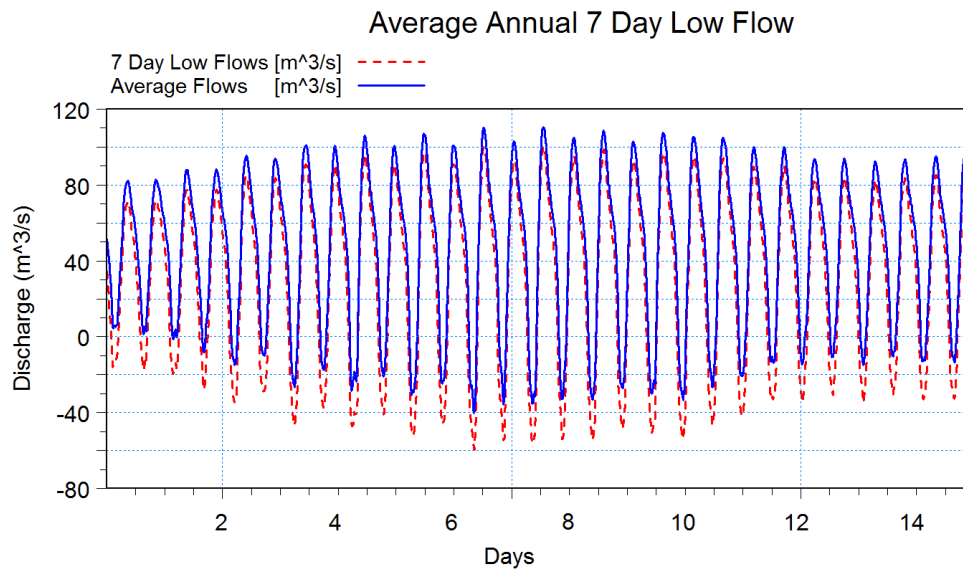


**Figure 7.7:** Discharge time series from the Mike 11 model used to force the upstream model boundaries for the coupled Mike 21 model for the Status Quo and Option N scenarios. Similar differences between average and 7 day low flow discharges were also seen in the time series used to force the Option J scenario. However, they are not shown here for the sake of clarity in this figure.

### 7.2.5 Increased Wave Height Conditions

In three out of the four scenarios (all except Option J), forced by average river flows and twice the average wave height conditions, the channel through the ebb delta became shorter compared to their respective simulations of average river flow and wave height conditions (although, the channel in the Option N – with flatgates scenario, became wider). These three scenarios are in accordance with the general literature, which state that inlets that are subjected to high wave energy climates, tend to have smaller ebb deltas than inlets of similar tidal prisms, but lower energy wave climates (Komar, 1976, 2006; Hicks & Hume, 1996). This is due to the waves “pushing” sand shoreward over the delta, and at times in through the inlet, causing an increase in the size of the flood delta, or in the case of the scenarios for the Te Tumu Cut, a decrease in size of the channel.

Alternatively to the idea of Komar (1976, 2006) and Hicks and Hume (1996), Ranasinghe *et al.*, (1999) showed for an idealised seasonally closed inlet, the effect of wave action depended on wave steepness. Through various model simulations of an idealised seasonally closed inlet Ranasinghe *et al.* (1999) concluded that their results reflected Dean's (1973) condition for on-offshore sediment transport (Equation. 7.1).

Dean's (1973) condition states that onshore sediment transport occurs when wave steepness ( $H_o$  (offshore wave height) /  $L_o$  (offshore wave length)) is less than  $(H_o/L_o)_{crit}$ , while offshore transport occurs otherwise. Dean's condition is given as:

$$\left(\frac{H_o}{L_o}\right)_{crit} = \frac{A\pi W}{gT} \quad \text{Equation: 7.1}$$

where A is a constant (taken as 4.5 after Larson, 1988) and W is the sediment fall velocity.

Their model results showed when wave steepness was greater than  $(H_o/L_o)_{crit}$ , cross-shore processes helped to keep the inlet open, as expected due to offshore sediment transport. Conversely wave steepness values less than Deans criterion promoted onshore sediment movement and helped inlet closure.

Figure 7.8 shows Dean's (1973) critical conditions for onshore and offshore sediment transport based on the mean grain size of 0.943 mm found in Chapter 6.2 and the corresponding settling velocity of 0.0599 mm/s (based on the equation of van de Graaff, 1994). According to this criterion the average wave conditions for the Te Tumu Cut should promote onshore sediment transport, whereas when the wave height is doubled but the wave period remains the same (i.e. the 2x average wave height simulations) offshore sediment transport should occur. Therefore, under the 2x average wave height conditions offshore sediment transport should increase due to the combined effect of ebb tidal flows and undertow associated with waves steeper than Dean's criterion. However, as the ebb channel was only seen to increase in one of the four simulations (Option J), the effect of increased wave height cannot be explained by the same processes as the results of (Ranasinghe *et al.*, 1999).

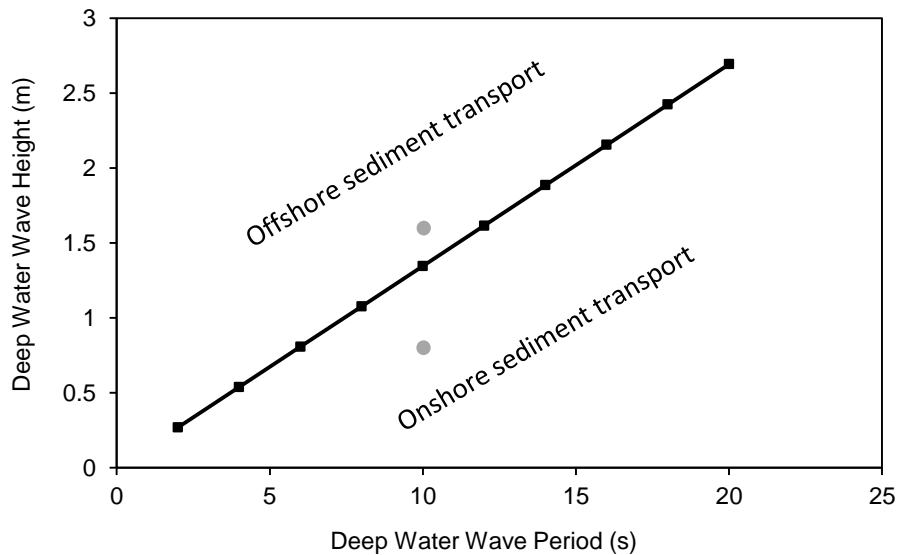


**Figure 7.8:** Dean's criterion for onshore - offshore sediment transport. The average wave (below the line) and 2x average wave heights (above the line) used in the model simulations are indicated by the grey dots.

A possible explanation for no general consensus on the effect of increased wave heights within the four scenarios is that the inlet is in different stages of inlet sediment bypassing.

Bruun & Gerritsen (1959) described three methods through which sand can move past tidal inlets: (1) by wave induced sand transport along the terminal lobe, (2) transport of sand in channels by tidal currents and (3) the migration of channels and sandbars (Figure 7.9). They also showed that the type of bypassing that occurs could be determined from the Bruun Ratio, with ratios of  $> 200 - 300$  associated with the inlet bypassing type 1, and low ratios ( $< 10 - 20$ ) associated with type 2 and 3 bypassing (FitzGerald, 1982).

According to the Bruun Ratio calculated for the Te Tumu Cut ( $\Omega/M_{tot} = 56$ ) in Section 3.3.1 sediment should bypass the inlet by the processes of transport through channels by tidal currents and by the migration of channels and sandbars. This is further reinforced when the results of the sediment transport modelling are viewed as a movie, or frame by frame. This clearly shows the movement of mounds of sediment becoming detached from the western side of the shoreline and swash platform, moving into, and, or around the ebb channel and then onto the eastern swash platform. Therefore it is possible that the inlet is in different

stages of inlet sediment bypassing in each of the scenarios between the average wave and twice the average wave height simulations, thus confusing interpretations of the results.

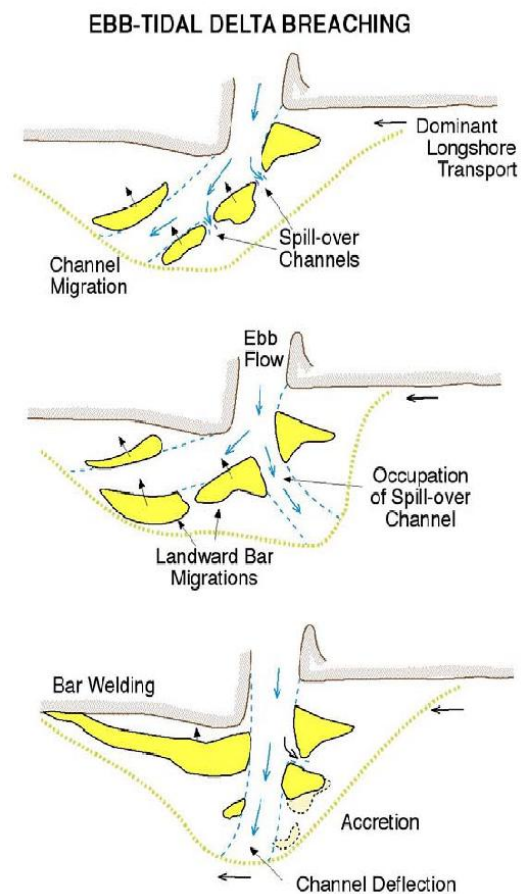


**Figure 7.9:** Schematic of the ebb tidal delta breaching process of inlet sediment bypassing from FitzGerald *et al.* (2000).

## 7.2.6 Twin Jetty Structures

Training walls inhibit a large proportion of the sediments transported to inlets and therefore lead to a dominance of ebb-directed sediment transport. In addition to this training confine the flow to a limited channel and make the flow paths more hydraulically efficient, thus increasing flow velocities and scour potential (Kieslich, 1981).

Figure 7.10 shows the equilibrium scour depth predicted for a range of jetty spacing's based on the USACE equation (Equation 3.3), when a sediment grain size of 0.000496 m (6.2) and an equilibrium maximum discharge of 82m<sup>3</sup>/s (Figure 7.1) are used to represent the end of the 14 day simulation.

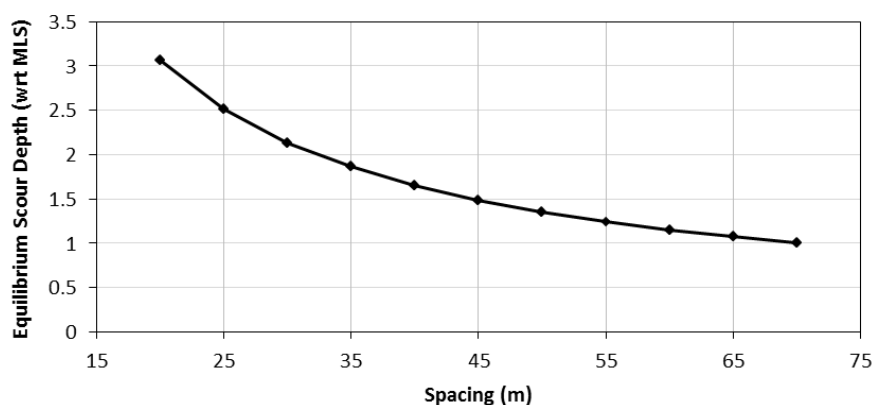


**Figure 7.10:** Estimated scour depth of the Kaituna River mouth using the USACE formula for annual average flow conditions with varying training wall spacing.

In both the 45 metre and 35 metre spaced simulations the effect of the twin training wall structures were seen with the prediction of lower bed levels after a two week simulation, with and without the training walls. As expected the 35 metre spacing simulation produced lower bed levels of the two.

When comparing the bed levels predicted by the sediment transport model and the USACE equation for equilibrium scour depths no matches were seen. This was due to the channel depths becoming progressively shallower seaward from the river mouth and therefore there was not one bed level for the length of the channel as suggest by the USACE equation. However, it must be noted that the USACE

equation tends to predict maximum equilibrium scour depths as it is based on peak discharges, which in reality may not exist long enough to allow the predicted equilibrium scour depth to occur (Hughes, 1999; Dahm & Kench, 2004).

Another possible explanation for this is that both the 35 m and 45 m spaced training wall simulations were orientated at 15° from north which was deemed to be the typical orientation of the channel through the delta based on a series of aerial photographs. However, both simulations were also forced by wave conditions that were deemed to represent the average conditions, which for the propagation direction was 20° from north. This meant that the waves were of almost ideal conditions to enter into between the two training walls, thus also allowing sediment to be transported into inside the twin structures by wave action, whereas the USACE equation does not take into account the effect of wave induced currents (Hughes, 1999).

Despite the disparity between the USACE equation and the morphological model developed for this project, both the 35 metre and 45 metre spaced training wall simulations indicate the potential of such structures to create a deeper channel than the Status Quo simulation. However, to fully assess the suitability and ideal configuration of such structures a much more specialised and specific study is required to assess factors such the ideal width, orientation and length of the structures, their effects of flood releases, scour potential from flood events, the magnitude of currents produced within and around the structures and their effects of vessels entering the entrance and the long term effects on the neighbouring shorelines (Komar, 1976; Dahm & Kench, 2002, 2004).

### 7.3 Summary & Conclusions

Following the diversion of the Kaituna River from Maketū Estuary out to sea in 1956, there have been concerns over the estuary's deteriorating health. The primary concerns have surrounded the increased sedimentation which has been estimated at 13,640 m<sup>3</sup> per year by Domijan (2007). Although, this is not entirely attributed to the diversion, with reports of sedimentation occurring prior to the diversion as well, it is accepted that the diversion has played a role in increasing the sedimentation rate.

In response to these concerns the Bay of Plenty Regional Council has outlined a number of potential re-diversion options to partially or fully restore the Kaituna River back in to Maketū Estuary. However, the options which aim to completely restore flow into the estuary require the Te Tumu Cut to be blocked off. Ultimately, the loss of the Te Tumu Cut is undesirable as at present it is a frequently used access point for recreational boat users and fisherman. The advantage of the options to partially restore the river flow into Maketū Estuary is that the Te Tumu Cut can remain unblocked. However, a consequence of partially re-diverting the river is the alteration of the discharge and flood currents through the Te Tumu Cut, and thus also the sedimentation patterns, which could potentially leave the Cut unnavigable.

In order to investigate the morphological response to three of the outlined potential re-diversion options, a 2-dimensional morphological model was created using the DHI modelling suite. This consisted of a regional spectral wave model to transform offshore wave data into the nearshore region, which in turn was used to force a local scale, coupled, spectral wave, hydrodynamic and sediment transport model of the Te Tumu Cut Region. This was then used to predict the response of the Te Tumu Cut to the Diversion Option J (lowering of the Ford's Cut Culverts) and Option N (reopening Papahikahawai Channel with and without oneway flapgated culverts).

Simulations were run for: (1) average river flow and wave conditions, (2) 7-day low river flows with average wave conditions, (3) average river flow conditions with twice the average significant wave height conditions and (4) over the time in which the model was calibrated, which was classified as typical summer

conditions. Simulations of these conditions were run for each of the three different potential re-diversion diversion options and the Status Quo simulation.

Based on the results of the simulations described above the following conclusions were drawn:

- (1) Option J was shown to increase the flood tidal volume of water through the Te Tumu Cut, however, the ebb flows remained unchanged. This resulted in an increase in the shoreward sediment transport carrying capacity, leading to the main channel through the ebb delta becoming shorter by approximately 20 metres in the four simulations run.
- (2) Option N – with flapgated culverts also caused an increase in the volume of water entering the Te Tumu Cut during the flood tide, while peak ebb discharges remained unaltered. However, unlike Option J, this caused an increase in the size of the channel. A possible explanation for this was that a loss of sediment occurred from the river mouth system when the bed level was decreased in order to reopen Papahikahawai Channel and an equilibrium state had not yet been reached again.
- (3) Option N – without flapgated culverts caused an increase in the flood and ebb tidal discharges. However, a larger increase in flood discharges compared to ebb flows was seen. This indicated that not all of the water entering Maketū Estuary through Papahikahawai Channel exits back through Papahikahawai Channel, but instead discharges through the Maketū Estuary mouth. However, the water that did exit through Papahikahawai Channel and subsequently discharged through the Te Tumu Cut during the ebb tide caused an increase in peak ebb flow and volume, and resulted in a small increase in the size of the channel through the river mouth.
- (4) The modelled results showed that none of the re-diversion options investigated, under average conditions, and conditions thought to promote increased sedimentation, i.e. increased wave height and low river flows (Despite the lack of consensus on the effect of increased wave height

between scenarios, and the lack of explanation for the increase in channel size seen in the low flow simulations) resulted in dramatic changes in the bathymetry or morphology of the Te Tumu Cut. Therefore, all of the scenarios looked at in this project are viable options for the re-diversion of the Kaituna River into Maketū Estuary, based solely on the resulting effects to the Te Tumu Cut.

- (5) Preliminary simulations with the addition of twin jetty structures extending through the ebb delta showed that they can be successfully used at the Te Tumu Cut to create a deeper channel through the delta. However, a more thorough investigation is required to determine the ideal configuration and effects on neighbouring coastlines, which was beyond the ability of the coupled morphological model created for this project.

Based on the results of this project I personally recommend that Option N – without flapgated culverts is the best option in terms of increasing the inflow of water into Maketū Estuary while at the same time having minimal effect on the morphology of the Te Tumu Cut. However, this is solely based on the morphodynamic effects on the Te Tumu Cut and increasing the inflow of water in to Maketū Estuary, and does not consider effects such as the salinity or water quality of the additional water entering the estuary.

## 7.4 Recommendations for Further Research

Suggestions for future work involving the application of the coupled morphological model developed for this project include the following:

- (1) Collection of another current velocity dataset from within the vicinity of the river mouth. This could be achieved by deploying an array of current meters inside the river channel or by completing another ADCP survey, but this time inside the river to gain an estimate of discharges. Such datasets could then be used to specifically calibrate the hydrodynamic model and aid in the choice of bed resistance values.
- (2) Collection of another bathymetry survey, preferably following a period of low flow condition, which could be used to further validate the sediment transport model.
- (3) Investigate why simulations longer than two weeks produced excessive erosion around the Te Tumu Cut. This would allow the various simulations to assess the long term effects of the different re-diversion option.
- (4) Using the long term simulation model recommended for development above, to assess the effects of various river training structures on the neighbouring coastlines, and determine the ideal structure type and configuration in regards to minimal downdrift erosion for maximum channel depths within the Te Tumu Cut.

## References

---

- Bates, D. (2010). *Kaituna Maketū Rediversion Path Forward*. Memorandum to C. Meadowcroft, dated 15/7/2010. Environment Bay of Plenty. Whakatane.
- Bell, R. G., & Goring, D. G. (1998). Seasonal Variability of Sea Level and Sea-surface Temperature on the Northeast Coast of New Zealand. *Estuarine, Coastal and Shelf Science*, 46, 307-318.
- BOPRC. (2011). *Kaituna Catchment Control Scheme*. Retrieved from <http://www.boprc.govt.nz/environment/rivers-and-drainage/kaituna-catchment-control-scheme/>
- Bruun, P., & Gerritsen, F. (1959). Natural bypassing of sand at coastal inlets. *Journal of Waterways and Harbour Div., American Association of Civil Engineering*, 85, 75-107.
- Bruun, P., & Gerritsen, F. (1960). *Stability of coastal inlets*. Amsterdam: North-Holland Pub. Co.
- Bruun, P., Mehta, A. J., & Johnsson, I. G. (1978). *Stability of Tidal Inlets :Theory and Engineering* (Vol. 23). Amsterdam; New York: Elsevier Scientific Pub. Co.
- Burton, J., & Healy, T. (1985). Tidal Hydraulics and Stability of the Maketū Inlet, Bay of Plenty. *Australasian Conference on Coastal and Ocean Engineering* (pp. 697-702). A.C.T. Institution of Engineers, Australia.
- Crawford, C. G. (1991). Estimation of suspended-sediment rating curves and mean suspended-sediment loads. *Journal of Hydrology*, 129 (1-4), 331-348.
- Dahm, J., & Kench, P. (2002). Feasibility Study: Opotiki Entrance Navigation Improvements. *Report Prepared for Opotiki District Council*.
- Dahm, J., & Kench, P. (2004). Opotiki Entrance: Navigation Improvements: Feasibility Study Phase 2. *Report Prepared for Opotiki District Council*.
- Dean, R. G. (1973). Heuristic Models of Sand Transport in the Surf Zone *Conference on Engineering Dynamics in the Surf Zone*, 208-214. Sydney, Australia.
- de Vriend, H. J., Zyserman, J., Nicholson, J., Roelvink, J.A., Péchon, P., Southgate, H.N. (1993). Medium-term 2DH coastal area modelling. *Coastal Engineering*, 21, 193-224.
- DHI. (2011a). Mike Zero Preprocessing & Postprocessing - User Guide Generic Editors and Viewers.

- DHI. (2011b). Mike 21 SW - Spectral Waves FM Module User Guide.
- DHI. (2011c). Mike 21 Flow Model FM - Hydrodynamic Module User Guide.
- DHI. (2011d). Mike 21 Flow Model FM - Sand Transport Module User Guide.
- DHI. (2011e). Mike Zero Module, Built-in Help Menu - Generation of Q3D Sediment Transport Tables.
- Domijan, N. (2000). *The Hydrodynamic and Estuarine Physics of Maketū Estuary*. Unpublished PhD thesis, The University of Waikato, Hamilton.
- Easton, H. R. (2002). *Coastal erosion and sedimentation oh Pukehina Beach and Waihi Estuary*. Unpublished MSc thesis, The University of Waikato, Hamilton.
- EBoP. (2007). *Meteorological Summaries, Environmental Publications 2007/06*. Whakatane: Environment Bay of Plenty.
- EBoP. (2008). *Kaituna River and Maketū Estuary Discussion Document on Potential Re-diversion Options*. Whakatane: Environment Bay of Plenty.
- EBoP. (2009). *Kaituna River and Ongatoro/Maketū Estuary Strategy*. Whakatane: Environment Bay of Plenty.
- El-Rabbany, A. (2006). *Introduction to GPS: the Global Positioning System*. Boston, MA: Artech House.
- FitzGerald, D. M. (1982). Sediment Bypassing at Mixed Energy Tidal Inlets. *Coastal Engineering*, 1094-1118.
- FitzGerald, D. M., Kraus, N. C., & Hands, E. B. (2000). Natural mechanisms of sediment bypassing at tidal inlets (Vol. CHETN-IV-30): US Army Corps of Engineers.
- Foster, G. A., Healy, T. R., & de Lange, W. P. (1994). Sediment Budget and Equilibrium Beach Profiles Applied to Renourishment of an Ebb Tidal Delta Adjacent Beach, Mt. Maunganui, New Zealand. *Journal of Coastal Research*, 10(3), 564-575.
- Goodhue, N. (2007). *Hydrodynamic and Water Quality Modelling of the Lower Kaituna River and Maketū Estuary*. Unpublished MSc thesis, The University of Waikato, Waikato.
- Gordon, A. D. (1990). Coastal Lagoon Entrance Dynamics *22nd International Conference of Coastal Engineering* (pp. 2880-2893): Delft, ASCE.
- Gorman, R. M., Bryan, K. R., & Laing, A. K. (2003). Wave Hindcast for the New Zealand Region: Nearshore Validation and Coastal Wave Climate. *New Zealand Journal of Marine & Freshwater Research*, 37, 567-588.

- Griffiths, G. A., & Glasby, G. P. (1985). Input of River-derived Sediment to the New Zealand Continental Shelf: 1. Mass. *Estuarine, Coastal and Shelf Science*, 21, 773-787.
- Hart, D. E. (2009). Morphodynamics of Non-Estuarine River Mouth Lagoons on High-Energy Coasts. *Journal of Coastal Research* (Special Issue 56), 1355-1359.
- Hayes, M. O. (1979). Barrier island morphology as a function of tidal and wave regime. In Leatherman, S. P. (Ed.). *Barrier Islands from the Gulf of St Lawrence to the Gulf of Mexico*. Academic Press, New York, 1-27.
- Hayes, M. O. (1980). General morphology and sediment patterns in tidal inlets. *Sedimentary Geology*, 26, 139-156.
- Healy, T. (1985). *Assessment of Stability and Natural Hazard Risk of the Whakatane Spit and Inlet in Relation to Proposed Marina Development*. Paper presented at the Australasian Conference on Coastal and Ocean Engineering, A.C.T. Institution of Engineers, Australia.
- Healy, T. R., Harray, K. G., & Richmond, B. (1977). *The Bay of Plenty coastal erosion survey: Preliminary survey*. Hamilton: Bay of Plenty Catchment Commission; University of Waikato.
- Heath, R. A. (1975). Stability of some New Zealand Coastal Inlets. *N.Z. Journal of Marine and Freshwater Research*, 9(4), 449-457.
- Hicks, M., & Hume, T. (1996). Morphology and Size of Ebb Tidal Deltas at Natural Inlets on Open-sea and Pocket-bay Coasts, North Island, New Zealand. *Journal of Coastal Research*, 12(1), 47-63.
- Hubbard, D. K., Oertel, G., & Nummedal, D. (1979). The role of waves and tidal currents in the development of tidal-inlet sedimentary structures and sand body geometry: Examples from North Carolina, South Carolina and Georgia. *Journal of Sedimentary Petrology*, 49(4), 1073-1092.
- Hughes, S. A. (1999). *Equilibrium Scour Depth at Tidal Inlets: Coastal Engineering Technical Note IV-18*: U.S. Army Corps of Engineers.
- Hume, T. M., Snelder, T., Weatherhead, M., & Liefing, R. (2007). A Controlling Factor Approach to Estuary Classification. *Ocean & Coastal Management*, 50, 905-929.
- Hume, T. M., & Herdendorf, C. E. (1988). A geomorphic classification of estuaries and its application to coastal resource management - A New Zealand Example. *Ocean & Shoreline Management* 11, 249-274.
- Hume, T. M., & Herdendorf, C. E. (1992). Factors Controlling Tidal Inlet Characteristics on Low Drift Coasts. *Journal of Coastal Research*, 8(2), 355-375.

- Hume, T. M., & Herdendorf, C. E. (1993). On the use of empirical stability relationships for characterising estuaries. *Journal of Coastal Research*, 9(2), 413-422.
- Jarrett, J. T. (1976). *Tidal Prism - Inlet Area Relationships: GITI Report 3*: Department of the Army Corps of Engineers.
- Kench, P. S. & Parnell, K.E. (1991). The Morphological Behaviour and Stability of a Small Tidal Inlet: Waipu, New Zealand. In: Bell, R.G., Hume, T.M. and Healy T.R. (Ed.). *Coastal Engineering – ‘Climate for Change’, Proceedings 10<sup>th</sup> Australasian Conference and Ocean Engineering*, Water Quality Centre Publication 21:221-226.
- Kieslich, J. M. (1981). Tidal inlet response to jetty construction (Vol. GITI Report 19): Department of the US Army Corps of Engineers.
- Kingston Reynolds Thom & Allardice (KRTA) (1986). *Maketū Estuary Study: Stage 1 Report. Report to the Bay of Plenty Catchment Commission*: KRTA Limited.
- Kirk, R. M. (1991). River-beach Interaction on Mixed Sand and Gravel Coasts: A Geomorphic Model for Water Resource Planning. *Applied Geography*, 11, 267-287.
- Kirk, R. M., & Lauder, G. A. (2000). *Significant Coastal Lagoon Systems in the South Island, New Zealand*. Wellington, New Zealand: Department of Conservation.
- Kjerfve, B. (1994). Coastal Lagoons. In B. Kjerfve (Ed.), *Coastal Lagoon Processes*: Elsevier Science Publishers.
- Komar, P. D. (1976). *Beach Processes and Sedimentation*. New Jersey: Prentice-Hall.
- Komar, P. D. (1996). Tidal-Inlet Processes and Morphology Related to the Transport of Sediments. *Journal of Coastal Research* (Special Issue No. 23), 23-45.
- Lam, N. T., Stive, M. J. F., Verhagen, H. J., & Wang, Z. B. (2007). *Morphodynamics of Hue Tidal Inlets*. Ho Chi Minh City, Vietnam.
- Larson, M. (1988). *Quantification of Beach Profile Change - Report No. 1008*. University of Lund.
- LINZ. (2006). *New Zealand Map Systems (NZMS): Series 260*. Auckland: Land Information of New Zealand (LINZ).
- Macky, G., Latimer, G. J., & Smith, R. K. (1995). Wave Climate of the Western Bay of Plenty, New Zealand, 1991-93. *New Zealand Journal of Marine & Freshwater Research*, 29, 311-327.

- Mehta, A. J., & Joshi, P. B. (1988) Tidal inlet hydraulics. *Journal of Hydraulic Engineering*, 114(11), 1321-1338.
- Murray, K. N. (1978). *Ecology and Geomorphology of the Maketū Estuary, Bay of Plenty*. Unpublished PhD thesis, The University of Waikato, Waikato.
- NIWA. (2011). *WRENZ - Water Resources Explorer NZ*. Retrieved from <http://wrenz.niwa.co.nz/webmodel/>
- Nicholson, J., Broker, I., Roelvink, J. A., Price, D., Tanguy, J. M., Moreno, L. (1997) Intercomparison of coastal area morphodynamic models. *Coastal Engineering*, 31, 97-123.
- O'Brien, M. P. (1931). Estuary Tidal Prisms Related to Entrance Areas. *Civil Engineer*, 1, 738-739.
- Papanicolaou, A. N., Elhakeem, M., Krallis, G., Parakash, S., & Edinger, J. (2008). Sediment Transport Modelling Review - Current and Future Developments. *Journal of Hydraulic Engineering* (January).
- Park, S. G. (2003). *Kaituna River Diversion to Maketū Estuary*. Whakatane, N.Z.: Environment Bay of Plenty.
- Park, S. G. (2007). *Lower Kaituna catchment and water quality*. Whakatane, N.Z.: Environment Bay of Plenty.
- Pedersen, C., Tuckey, B., Saviolo, J., Olesen, K., & van Kalken, T. (2008). *Opotiki Harbour Access Modelling and Preliminary Design - Volume 1: Summary Report*: DHI NZ.
- Pickrill, R. A., & Mitchell, J. S. (1979). Ocean Wave Characteristics Around New Zealand. *New Zealand Journal of Marine & Freshwater Research*, 13(4).
- Quayle. (1984). The Climate and Weather of the Bay of Plenty Region, New Zealand. *Meteorological Service Miscellaneous Publication.*, 115(1)
- Ramming, H., & Kowalik, Z. (1980). *Numerical modelling of marine hydrodynamics: Applications to dynamic physical processes*. New York: Elsevier Scientific Publishing Company.
- Ranasinghe, R., & Pattiaratchi, C. (2003). The seasonal closure of tidal inlets: Cause and effects. *Coastal Engineering Journal*, 45(4), 601-627.
- Ranasinghe, R., Pattiaratchi, C., & Masselink, G. (1999). A Morphodynamic Model to Simulate the Seasonal Closure of Tidal Inlets. *Coastal Engineering*, 37, 1-36.

- Richmond, C., & Forbes, S. (1990). *Maketū Estuary Restoration Strategy: A Proposal to Central and Local Government*. Auckland, New Zealand: Department of Conservation.
- Shuttleworth, B., Woidt, A., Paparella, T., Herbig, S., & Walker, D. (2005). The dynamic behaviour of a river dominated tidal inlet, River Murray, Australia. *Estuarine, Coastal and Shelf Science*, 64, 645-657.
- Siegle, E., Huntley, D. A., & Davidson, M. A. (2004) Physical Controls on the dynamics of inlet sandbar systems. *Ocean Dynamics*, 54, 360-373.
- SmartGrowth. (2008). Eastern Corridor Strategy - October 2008: SmartGrowth.
- Stafford, D. M. (1967). *Te Arawa - A History of the Arawa People*: AH & AW Reed.
- Titchmarsh, R., (1998). *Bank Erosion: Ford's Cut, Maketu*. Draft report prepared for Department of Conservation.
- Tuckey, B. (2009). *Kaituna River to Maketū Estuary Re-diversion: Model Calibration and Initial Hydrodynamic Impact Assessment*. Auckland, New Zealand: DHI NZ.
- USACE. (1995). *Coastal Inlet Hydraulics and Sedimentation*. Washington, DC: U.S. Army Corps of Engineers (USACE).
- van de Graaff (1994). Coastal and dune erosion under extreme conditions. *Journal of Coastal Research Special Issue*, 12, 253-262.
- Walker, D. J. (2003). Assessing environmental flow requirements for a river-dominated tidal inlet. *Journal of Coastal Research*, 19(1), 171-179.
- Wallace, P. (2009). *Hydraulic Modelling of the Kaituna River - Report Prepared for Environment Bay of Plenty*: River Edge Consulting Limited.
- Wallace, P., Tarboton, K., & Pak, I. (2008). Kaituna River to Maketū Estuary rediversion - recommended options (pp. 29). Whakatane: EBoP.
- Wigley, G. N. (1990). *Holocene Tephrochronology and Evolution of the Te Puke Lowlands, Bay of Plenty, New Zealand*. Unpublished MSc thesis, University of Waikato, Waikato.
- Wildland Consultants. (2007). Vegetation and Habitat Types of the Lower Kaituna River, Western Bay of Plenty. *Contract Report 1281, prepared for Environment Bay of Plenty*.
- Willmott, C. J., & Matsuura, K. (2005). Advantages of the Mean Absolute Error (MAE) Over the Root Mean Square Error (RMSE) in Assessing Average Model Performance. *Climate Research*, 30, 79-82.

Winter, C. (2007). On the evaluation of sediment transport models in tidal environments. *Sedimentary Geology*, 202, 562-571.

Wright, L. D. (1977). Sediment transport and deposition at river mouths: A synthesis. *Geological Society of America Bulletin*, 857-868.



# Appendix 1: Sediment Sample Laser Sizer Results



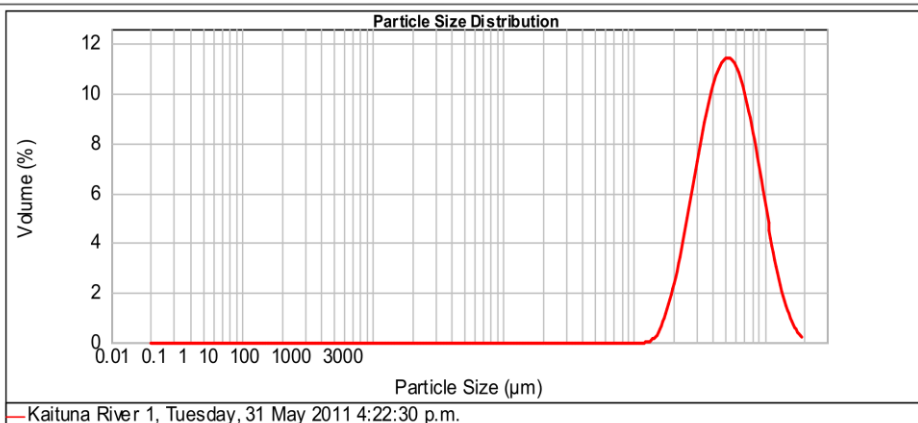
Department of Earth & Ocean Sciences  
School of Science and Engineering  
The University of Waikato  
Private Bag 3105  
Hamilton, New Zealand

## Result Analysis Report

<b>Sample Name:</b> Kaituna River 1	<b>SOP Name:</b> Marine Sediment	<b>Measured:</b> Tuesday, 31 May 2011 4:22:30 p.m.
<b>Sample Source &amp; type:</b>	<b>Measured by:</b> mckinnon	<b>Analysed:</b> Tuesday, 31 May 2011 4:22:31 p.m.
<b>Sample bulk lot ref:</b>	<b>Result Source:</b> Measurement	

<b>Particle Name:</b> Marine Sediment	<b>Accessory Name:</b> Hydro 2000G (A)	<b>Analysis model:</b> General purpose	<b>Sensitivity:</b> Enhanced
<b>Particle RI:</b> 1.500	<b>Absorption:</b> 0.2	<b>Size range:</b> 0.020 to 2000.000 um	<b>Obscuration:</b> 19.77 %
<b>Dispersant Name:</b> Water	<b>Dispersant RI:</b> 1.330	<b>Weighted Residual:</b> 2.468 %	<b>Result Emulation:</b> Off
<b>Concentration:</b> 1.4326 %Vol	<b>Span :</b> 1.406	<b>Uniformity:</b> 0.44	<b>Result units:</b> Volume
<b>Specific Surface Area:</b> 0.0131 m <sup>2</sup> /g	<b>Surface Weighted Mean D[3,2]:</b> 458.191 um	<b>Vol. Weighted Mean D[4,3]:</b> 584.998 um	

**d(0.1): 268.825 um      d(0.5): 517.070 um      d(0.9): 995.980 um**



Size (µm)	d/Under %										
0.050	.00 0	0.980	.00 0	37.000	.00 0	105.000	.00 0	300.000	4.65 1	840.000	2.41 8
0.060	.00 0	2.000	.00 0	44.000	.00 0	125.000	.00 0	350.000	2.87 2	1000.000	0.15 9
0.120	.00 0	3.900	.00 0	53.000	.00 0	149.000	.13 0	420.000	4.75 3	2000.000	00.00 1
0.240	.00 0	7.800	.00 0	63.000	.00 0	177.000	.96 0	500.000	7.49 4		
0.490	.00 0	15.600	.00 0	74.000	.00 0	210.000	.18 3	590.000	9.80 5		
0.700	.00 0	31.000	.00 0	88.000	.00 0	250.000	.49 7	710.000	2.61 7		

Operator notes:

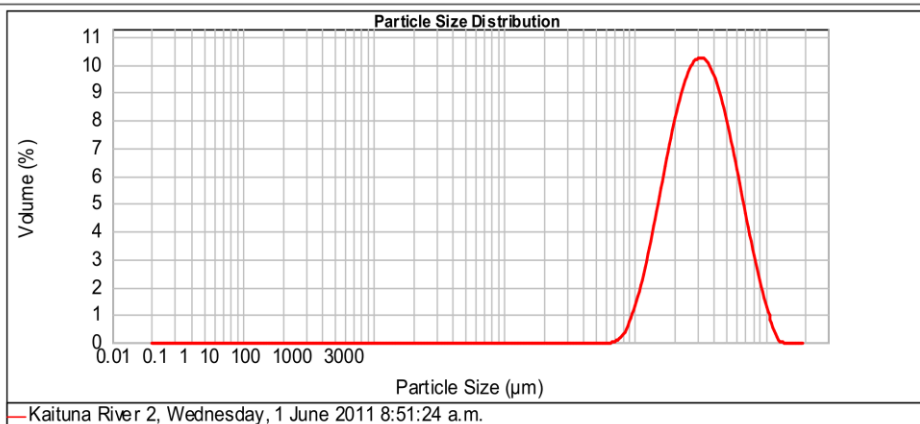
## Result Analysis Report

<b>Sample Name:</b> Kaituna River 2	<b>SOP Name:</b> Marine Sediment	<b>Measured:</b> Wednesday, 1 June 2011 8:51:24 a.m.
<b>Sample Source &amp; type:</b>	<b>Measured by:</b> mckinnon	<b>Analysed:</b> Wednesday, 1 June 2011 8:51:25 a.m.
<b>Sample bulk lot ref:</b>	<b>Result Source:</b> Measurement	

<b>Particle Name:</b> Marine Sediment	<b>Accessory Name:</b> Hydro 2000G (A)	<b>Analysis model:</b> General purpose	<b>Sensitivity:</b> Enhanced
<b>Particle RI:</b> 1.500	<b>Absorption:</b> 0.2	<b>Size range:</b> 0.020 to 2000.000 um	<b>Obscuration:</b> 21.78 %
<b>Dispersant Name:</b> Water	<b>Dispersant RI:</b> 1.330	<b>Weighted Residual:</b> 1.068 %	<b>Result Emulation:</b> Off

<b>Concentration:</b> 0.9492 %Vol	<b>Span :</b> 1.577	<b>Uniformity:</b> 0.489	<b>Result units:</b> Volume
<b>Specific Surface Area:</b> 0.022 m <sup>2</sup> /g	<b>Surface Weighted Mean D[3,2]:</b> 272.304 um	<b>Vol. Weighted Mean D[4,3]:</b> 364.909 um	

**d(0.1): 153.200 um                      d(0.5): 315.303 um                      d(0.9): 650.305 um**



Size (µm)	Under %										
0.050	.00 0	0.980	.00 0	37.000	.00 0	105.000	.67 1	300.000	6.66 4	840.000	6.69 9
0.060	.00 0	2.000	.00 0	44.000	.00 0	125.000	.39 4	350.000	6.98 5	1000.000	8.98 9
0.120	.00 0	3.900	.00 0	53.000	.00 0	149.000	.06 9	420.000	8.64 6	2000.000	00.00 1
0.240	.00 0	7.800	.00 0	63.000	.00 0	177.000	5.74 1	500.000	8.53 7		
0.490	.00 0	15.600	.00 0	74.000	.02 0	210.000	4.33 2	590.000	6.29 8		
0.700	.00 0	31.000	.00 0	88.000	.35 0	250.000	4.72 3	710.000	2.79 9		

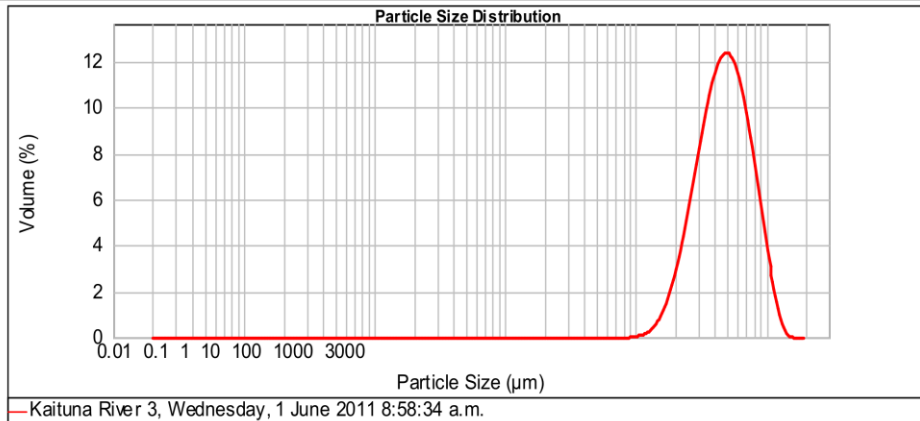
**Operator notes:**

## Result Analysis Report

<b>Sample Name:</b> Kaituna River 3	<b>SOP Name:</b> Marine Sediment	<b>Measured:</b> Wednesday, 1 June 2011 8:58:34 a.m.
<b>Sample Source &amp; type:</b>	<b>Measured by:</b> mckinnon	<b>Analysed:</b> Wednesday, 1 June 2011 8:58:35 a.m.
<b>Sample bulk lot ref:</b>	<b>Result Source:</b> Measurement	

<b>Particle Name:</b> Marine Sediment	<b>Accessory Name:</b> Hydro 2000G (A)	<b>Analysis model:</b> General purpose	<b>Sensitivity:</b> Enhanced
<b>Particle RI:</b> 1.500	<b>Absorption:</b> 0.2	<b>Size range:</b> 0.020 to 2000.000 um	<b>Obscuration:</b> 17.56 %
<b>Dispersant Name:</b> Water	<b>Dispersant RI:</b> 1.330	<b>Weighted Residual:</b> 1.940 %	<b>Result Emulation:</b> Off
<b>Concentration:</b> 1.1375 %Vol	<b>Span :</b> 1.263	<b>Uniformity:</b> 0.389	<b>Result units:</b> Volume
<b>Specific Surface Area:</b> 0.0145 m <sup>2</sup> /g	<b>Surface Weighted Mean D[3,2]:</b> 414.828 um	<b>Vol. Weighted Mean D[4,3]:</b> 514.356 um	

**d(0.1): 249.325 um      d(0.5): 470.928 um      d(0.9): 843.992 um**



Size (µm)	Under %										
0.050	.00 0	0.980	.00 0	37.000	.00 0	105.000	.03 0	300.000	8.27 1	840.000	9.79 8
0.060	.00 0	2.000	.00 0	44.000	.00 0	125.000	.20 0	350.000	7.55 2	1000.000	5.89 9
0.120	.00 0	3.900	.00 0	53.000	.00 0	149.000	.76 0	420.000	0.86 4	2000.000	00.00 1
0.240	.00 0	7.800	.00 0	63.000	.00 0	177.000	.17 2	500.000	4.86 5		
0.490	.00 0	15.600	.00 0	74.000	.00 0	210.000	.02 5	590.000	7.97 6		
0.700	.00 0	31.000	.00 0	88.000	.00 0	250.000	0.10 1	710.000	0.84 8		

Operator notes:

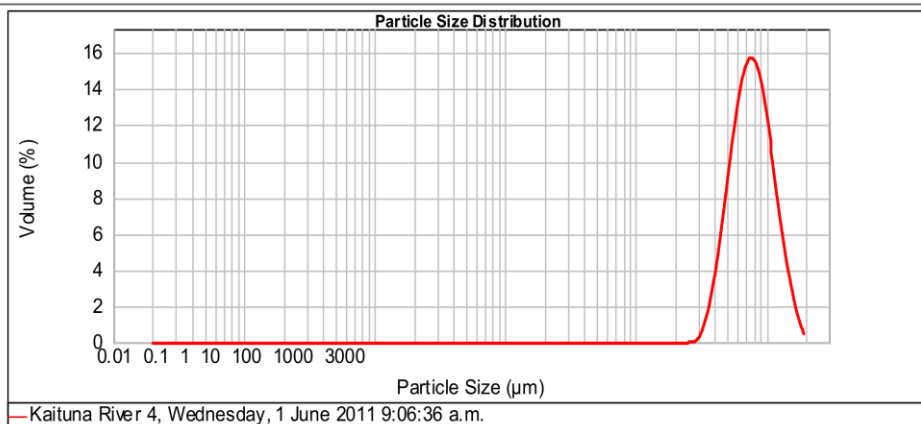
## Result Analysis Report

<b>Sample Name:</b> Kaituna River 4	<b>SOP Name:</b> Marine Sediment	<b>Measured:</b> Wednesday, 1 June 2011 9:06:36 a.m.
<b>Sample Source &amp; type:</b>	<b>Measured by:</b> mckinnon	<b>Analysed:</b> Wednesday, 1 June 2011 9:06:37 a.m.
<b>Sample bulk lot ref:</b>	<b>Result Source:</b> Measurement	

<b>Particle Name:</b> Marine Sediment	<b>Accessory Name:</b> Hydro 2000G (A)	<b>Analysis model:</b> General purpose	<b>Sensitivity:</b> Enhanced
<b>Particle RI:</b> 1.500	<b>Absorption:</b> 0.2	<b>Size range:</b> 0.020 to 2000.000 um	<b>Obscuration:</b> 12.48 %
<b>Dispersant Name:</b> Water	<b>Dispersant RI:</b> 1.330	<b>Weighted Residual:</b> 3.757 %	<b>Result Emulation:</b> Off

<b>Concentration:</b> 1.3609 %Vol	<b>Span :</b> 1.004	<b>Uniformity:</b> 0.311	<b>Result units:</b> Volume
<b>Specific Surface Area:</b> 0.00834 m <sup>2</sup> /g	<b>Surface Weighted Mean D[3,2]:</b> 719.196 um	<b>Vol. Weighted Mean D[4,3]:</b> 820.708 um	

**d(0.1): 477.613 um                      d(0.5): 764.784 um                      d(0.9): 1245.569 um**



Size (µm)	Under %										
0.050	.00 0	0.980	.00 0	37.000	.00 0	105.000	.00 0	300.000	.06 0	840.000	9.57 5
0.060	.00 0	2.000	.00 0	44.000	.00 0	125.000	.00 0	350.000	.92 0	1000.000	5.60 7
0.120	.00 0	3.900	.00 0	53.000	.00 0	149.000	.00 0	420.000	.63 4	2000.000	00.00 1
0.240	.00 0	7.800	.00 0	63.000	.00 0	177.000	.00 0	500.000	2.55 1		
0.490	.00 0	15.600	.00 0	74.000	.00 0	210.000	.00 0	590.000	4.67 2		
0.700	.00 0	31.000	.00 0	88.000	.00 0	250.000	.00 0	710.000	2.33 4		

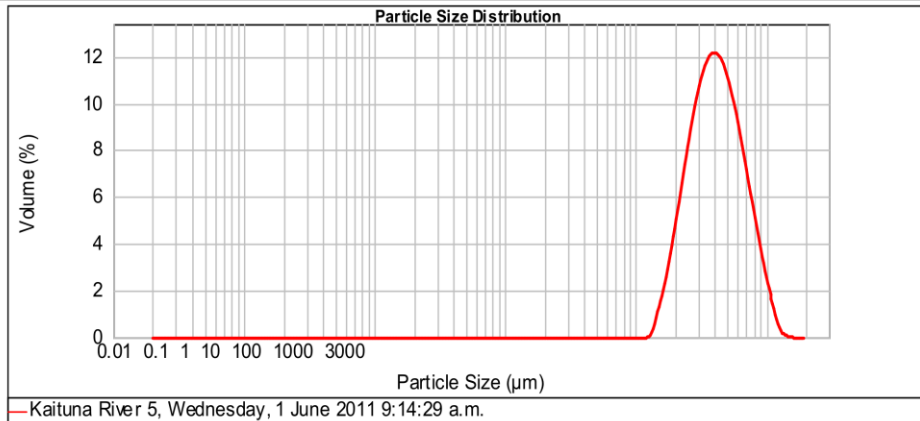
**Operator notes:**

## Result Analysis Report

<b>Sample Name:</b> Kaituna River 5	<b>SOP Name:</b> Marine Sediment	<b>Measured:</b> Wednesday, 1 June 2011 9:14:29 a.m.
<b>Sample Source &amp; type:</b>	<b>Measured by:</b> mckinnon	<b>Analysed:</b> Wednesday, 1 June 2011 9:14:30 a.m.
<b>Sample bulk lot ref:</b>	<b>Result Source:</b> Measurement	

<b>Particle Name:</b> Marine Sediment	<b>Accessory Name:</b> Hydro 2000G (A)	<b>Analysis model:</b> General purpose	<b>Sensitivity:</b> Enhanced
<b>Particle RI:</b> 1.500	<b>Absorption:</b> 0.2	<b>Size range:</b> 0.020 to 2000.000 um	<b>Obscuration:</b> 21.41 %
<b>Dispersant Name:</b> Water	<b>Dispersant RI:</b> 1.330	<b>Weighted Residual:</b> 1.707 %	<b>Result Emulation:</b> Off
<b>Concentration:</b> 1.2498 %Vol	<b>Span :</b> 1.319	<b>Uniformity:</b> 0.406	<b>Result units:</b> Volume
<b>Specific Surface Area:</b> 0.0164 m <sup>2</sup> /g	<b>Surface Weighted Mean D[3,2]:</b> 365.402 um	<b>Vol. Weighted Mean D[4,3]:</b> 451.054 um	

**d(0.1): 221.060 um      d(0.5): 402.868 um      d(0.9): 752.426 um**

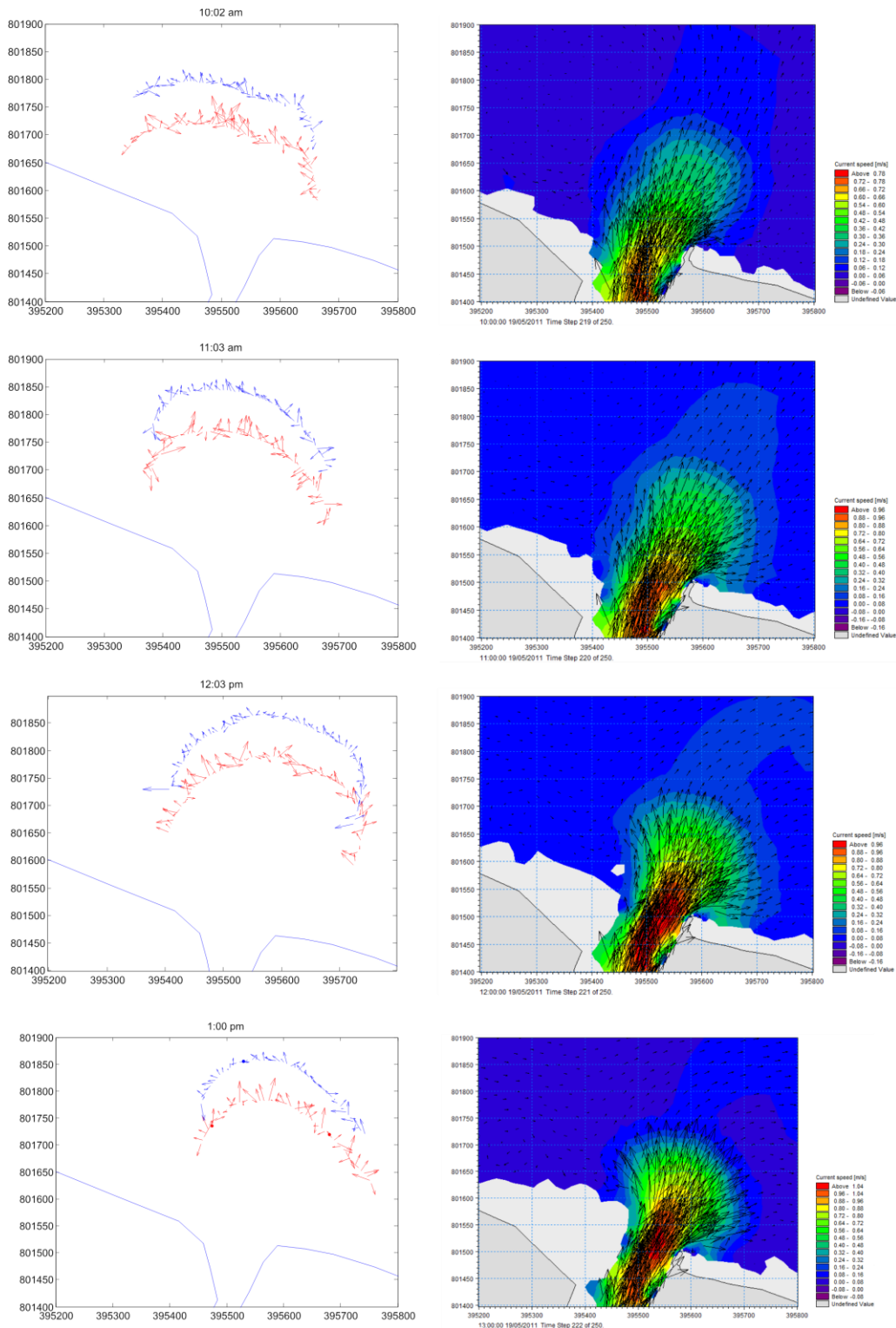


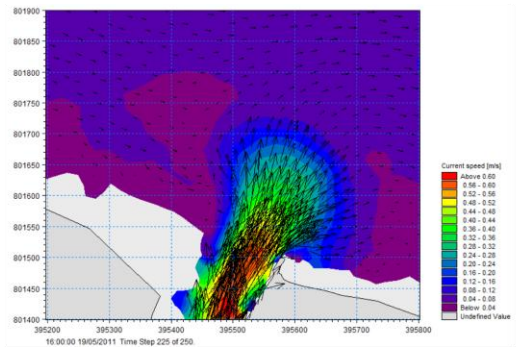
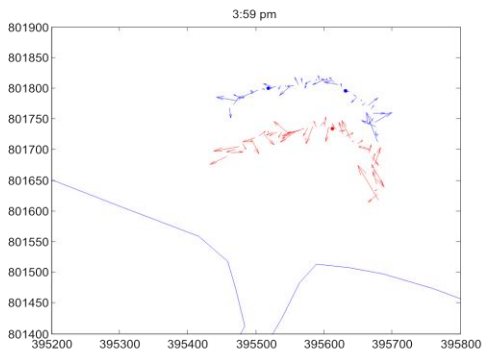
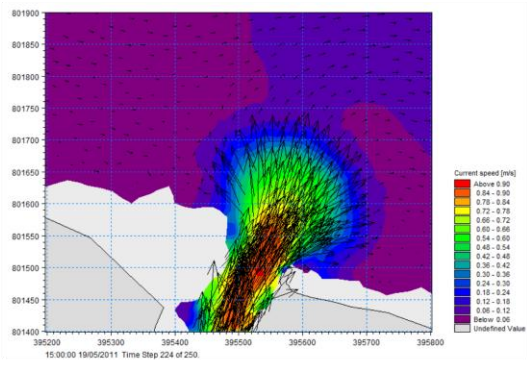
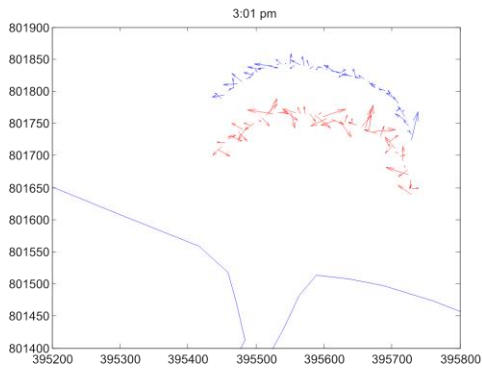
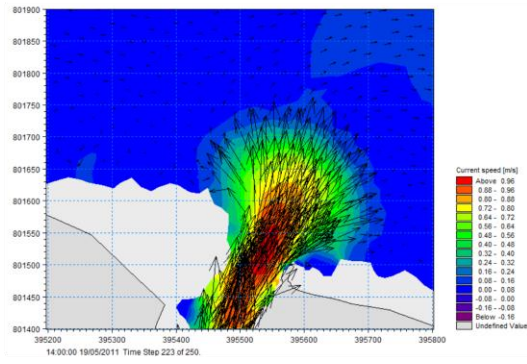
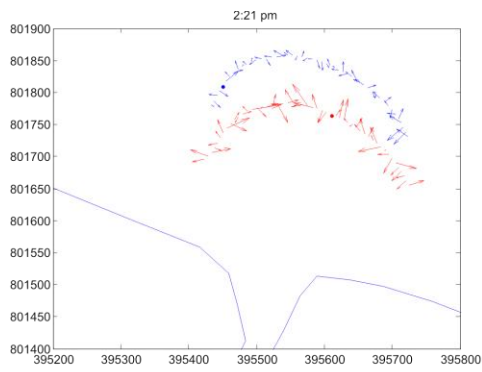
Size (µm)	Under %										
0.050	.00 0	0.980	.00 0	37.000	.00 0	105.000	.00 0	300.000	7.39 2	840.000	3.79 9
0.060	.00 0	2.000	.00 0	44.000	.00 0	125.000	.00 0	350.000	8.86 3	1000.000	7.72 9
0.120	.00 0	3.900	.00 0	53.000	.00 0	149.000	.61 0	420.000	3.31 5	2000.000	00.00 1
0.240	.00 0	7.800	.00 0	63.000	.00 0	177.000	.05 3	500.000	6.65 6		
0.490	.00 0	15.600	.00 0	74.000	.00 0	210.000	.96 7	590.000	7.76 7		
0.700	.00 0	31.000	.00 0	88.000	.00 0	250.000	5.96 1	710.000	7.57 8		

Operator notes:



## Appendix 2: ADCP and Modelled Current Vector Plots





### Appendix 3: Q3D ST Tables

**Table A3:** Settings used for Q3D Sediment Transport Table generation.

Parameters	Value		
<b>General Parameters</b>			
Tolerance in calc. of concentration	0.0001		
Max number of wave periods	100		
Steps per wave period	140		
Relative density of sediment	2.65		
Critical Shields parameter	0.05		
Water Temperature	14		
<b>Additional Parameters</b>			
Ripples	Include effects		
Bed slope	Include effects		
Bed concentration	Empirical		
Streaming	Include effects		
Density currents	Exclude		
Centrifugal Acceleration	Exclude		
<b>Wave Parameters</b>			
Wave theory	Stokes		
Order of solution	3		
<b>Breaking Wave Parameters</b>			
Gamma 1	1		
Gamma 2	0.8		
<b>Sediment Table Axis</b>	<b>First Value</b>	<b>Spacing</b>	<b>No. of points</b>
Current speed	0.05	0.3	7
Wave height	0.01	0.75	7
Wave period	1	3	7
Wave height / water depth	0.01	0.2	4
Angle current / waves	0	30	12
Grain size	0.2	2	4
Sediment grading	2.01	0.2	5
Bed slope, current direction	-0.01	0.01	3
Bed slope, normal to current	-0.02	0.02	3